INFORMATION TO USERS

This manuscript has been reproduced from the microfilm master. UMI films the text directly from the original or copy submitted. Thus, some thesis and dissertation copies are in typewriter face, while others may be from any type of computer printer.

The quality of this reproduction is dependent upon the quality of the copy submitted. Broken or indistinct print, colored or poor quality illustrations and photographs, print bleedthrough, substandard margins, and improper alignment can adversely affect reproduction.

In the unlikely event that the author did not send UMI a complete manuscript and there are missing pages, these will be noted. Also, if unauthorized copyright material had to be removed, a note will indicate the deletion.

Oversize materials (e.g., maps, drawings, charts) are reproduced by sectioning the original, beginning at the upper left-hand corner and continuing from left to right in equal sections with small overlaps.

Photographs included in the original manuscript have been reproduced xerographically in this copy. Higher quality 6" x 9" black and white photographic prints are available for any photographs or illustrations appearing in this copy for an additional charge. Contact UMI directly to order.

Bell & Howell Information and Learning
300 North Zeeb Road, Ann Arbor, MI 48106-1346 USA
800-521-0600

University of Alberta

Age-Related Morphological Changes in Fifth Cervical Vertebrae

by

Mark-Ulrich Knoefel 

A thesis submitted to the Faculty of Graduate Studies and Research in partial fulfillment of the requirements for the degree of Master of Science

in

Orthodontics

Department of Oral Health Sciences

Edmonton, Alberta

Fall 1999

National Library of Canada
Acquisitions and Bibliographic Services
395 Wellington Street
Ottawa ON K1A 0N4
Canada

Bibliothèque nationale du Canada
Acquisitions et services bibliographiques
395, rue Wellington
Ottawa ON K1A 0N4
Canada

Your file Votre référence

Our file Notre référence

The author has granted a non-exclusive licence allowing the National Library of Canada to reproduce, loan, distribute or sell copies of this thesis in microform, paper or electronic formats.

The author retains ownership of the copyright in this thesis. Neither the thesis nor substantial extracts from it may be printed or otherwise reproduced without the author's permission.

L'auteur a accordé une licence non exclusive permettant à la Bibliothèque nationale du Canada de reproduire, prêter, distribuer ou vendre des copies de cette thèse sous la forme de microfiche/film, de reproduction sur papier ou sur format électronique.

L'auteur conserve la propriété du droit d'auteur qui protège cette thèse. Ni la thèse ni des extraits substantiels de celle-ci ne doivent être imprimés ou autrement reproduits sans son autorisation.

0-612-47050-4

Canada

ABSTRACT

The purposes of this investigation were to determine the accuracy of a current software program (Sculptor™ by Acuscape, Inc.) in quantifying vertebral bodies three-dimensionally, and to develop a model correlating growth changes of the vertebral bodies with age.

For the first part of the study, two human cervical vertebrae of different sizes were selected to which eight radiopaque markers were attached. All inter-marker distances were measured both manually and by Sculptor™. There were no clinically significant differences between the two measurement methods.

For the second part of the study, 50 paediatric vertebrae (C5) were imaged radiographically from three views. Using Sculptor™, traces of the superior and inferior surfaces of each vertebral body were generated, and 3-D coordinates assigned to their constituent points. From these coordinates, various two- and three-dimensional variables were determined. Of these, body height and volumes of the superior and inferior surfaces proved most predictive of age.

TABLE OF CONTENTS

TABLE OF CONTENTS *(continued)*

LIST OF TABLES

CHAPTER TWO:

CHAPTER THREE:

LIST OF FIGURES

CHAPTER ONE:

CHAPTER TWO:

CHAPTER THREE:

CHAPTER ONE: GENERAL INTRODUCTION

INTRODUCTION

Skeletal age determination is an essential component of modern orthodontic treatment planning. A comprehensive understanding of the patient's developmental status influences the clinician's choice of biomechanical therapy as well as the likelihood of successful treatment results. Essentially, a patient's growth status will determine whether dentofacial orthopaedics still has the potential to correct the individual's skeletal malocclusion, or if other options, such as maxillofacial surgery, or dental "camouflage" treatment, are indicated.

In the last twenty-five years, the cervical spine, as seen on lateral cephalograms, has been examined as a potential tool in skeletal age assessment, as an alternative to hand-wrist radiography. Unfortunately, its growth and development have mostly been described qualitatively thus far. This literature review will begin by examining traditional skeletal age assessment methods, followed by an overview of growth and development of the cervical spine. Finally, recent attempts at quantifying various segments of the cervical spine will be presented.

I. TRADITIONAL SKELETAL AGE ASSESSMENT METHODS

Traditionally, orthodontists, as well as other health professionals concerned with paediatric growth and maturation, have employed hand-wrist radiographs to establish a patient's skeletal age. According to Grave[1], the hand-wrist radiograph permits recognition of early, average and late maturers. In clinical orthodontics it may be used as a means of growth prediction, as an estimation of the likely duration of retention, and the timing and efficiency of orthodontic treatment. The timing and utilisation of extraoral traction forces and of functional appliances, as well as the timing of orthognathic surgery are all based strongly on consideration of the growth of the craniofacial complex.

Various methods have been at the practitioner's disposal, the most well-known of which being the Greulich and Pyle (GP)[2] and the Tanner-Whitehouse (TW2)[3]. These have all been criticized, however, for demonstrating various weaknesses. Benso's group goes as far as questioning whether skeletal maturation can even be measured on a quantitative scale, whether its use is appropriate in computing, and what the 'numbers' used represent[4].

A. The Greulich and Pyle Atlas Method

The Greulich and Pyle Atlas consists of two series of standard plates obtained from hand-wrist radiographs of Caucasian, upper middle-class boys and girls of the Brush Foundation

Growth Study. When using the Greulich and Pyle method, the radiograph to be analysed is compared with the series of standard plates, and the age given to the standard plate that corresponds most closely is assigned as the skeletal age of the individual. For the sake of convenience, if the stage of osseous development falls between two standards, the assigned age is an interpolated value between the two[5]. Because of its apparent simplicity and speed, the Greulich and Pyle Atlas has become the most commonly used standard of reference for skeletal maturation worldwide[5]. According to Gilli[5], there are numerous problems with the GP method. The Atlas was constructed on the assumption that skeletal maturation is even, that all bones have an identical skeletal age, and that the appearance and subsequent development of bony centres follows a fixed pattern. Evidence from the literature suggests that a wide range of genetically determined variation exists in the pattern of ossification of bones in healthy children[5]. In the GP Atlas, the bones included vary considerably in their levels of maturity. Differences of up to 20 months exist between the least and most mature bones of a given standard. This fact reduces the replicability of assessments, unless they are made on a bone-by-bone basis. Gilli found that any method of bone-specific assessment is affected by the fact that, in two or more successive standards, bones may be assigned progressively older ages, even though they do not change in shape, or in size, during that period. Moreover, some bones may even appear less mature at older ages, due to poor selection of some standard plates.

Another weakness inherent to the GP method is the division of the maturity scale into skeletal age 'years'. These 'years' are not equivalent, since more maturation occurs during one year of skeletal age in girls than in boys, as girls reach the adult state of skeletal

maturity at a younger chronological age than boys. Furthermore, the concept of one skeletal year corresponding to one chronological year during the entire period of osseous development is not supported by any empirical evidence[5].

A further weakness of the GP Atlas is that no specific technique for its use has been recommended. It has been suggested that each bony centre be assigned a bone-specific bone age, and that the average of these should be calculated. However, the problem with averaging is that it makes no allowance for bones which ossify late.

Gilli felt that the Atlas method was highly subjective and hardly reproducible. He therefore suggested that it should be abandoned, particularly in clinical research. Nevertheless, the GP still continues to be used in these areas[6,7]. Jiménez-Castellanos and co-workers performed a study where, using the GP Atlas, skeletal maturation was studied in 239 Spanish boys and girls between birth and 14 years of age[7]. The literature review made no mention of more recent methods, such as the TW2 or the FELS (discussed in later sections). Individual bones were each assigned a bone age, based on the GP method as described by the authors. Realizing that the data obtained from the methodological process described by the atlas were "highly subjective", the authors suggested minimizing this problem by averaging readings from various different observers, or an average of various readings from the same observer. However, in their study, when cases demonstrated "significant discrepancies between observers", they were discussed until a consensus was reached.

B. The Tanner-Whitehouse Method

The Tanner-Whitehouse (TW2) method differs from the GP in two respects: it employs a bone-specific approach, and the results of the assessments are not always expressed as skeletal age years. Essentially, it assesses the maturity of twenty bones: radius, ulna, carpals (with the exception of the pisiform), and metacarpals and phalanges of the first, third, and fifth ray. Because they would provide redundant information, the second and fourth rays are excluded. The individual bones are compared with a series of written criteria describing eight or nine standard stages (A to H or I), through which a bone passes during its development. Each stage is defined by up to three criteria and is assigned a specific point score. The sum of these scores is termed the skeletal maturity score (SMS)[a]. Three different SMSs can be generated: all twenty bones may be involved (20B), only the carpals (CB), or only the radius, ulna and short bones (RUS). Of these, the RUS is the most popular. According to Gilli, the main weakness of the TW2 method lies in the fact that, in order to obtain enough information from each bone, the authors have consistently tried to identify in it eight or nine stages of maturation. As a consequence, ratios of the widths of epiphyses and diaphyses, or, in the case of the carpals, relationships between the diameters of a bone, or distances between bones, have been used. An additional problem is that the maturity scale is constructed in such a manner that, at the upper end, there may be a considerable change in the SMS simply by rating a single bone 'older' or 'younger' by

---

a. It can, for practical purposes, be transformed into a skeletal age, although this conversion has been criticized by Benso's group. The authors observe that the link-function between the degree of skeletal maturation and bone scores is not linear: an RUS score of 500, corresponding to a bone age of 14.3 years, is not halfway to complete maturity (RUS score = 1000; bone age = 18 years).

one stage. In other words, when translated to skeletal age, the difference can be up to 1.6 years. An example is given by Benso's group[4] to illustrate this point. A boy presents with radius and metacarpal 1 at stage F, and all the other short bones and the ulna at stage E. When the radius changes from stage F to stage G, the RUS score increases from 332 to 360 and bone age increases from 11 to 12 years, even if the other bones remain unchanged. Some stages may persist from a few months to years. Therefore, the persistence of stage G of the radius for 4 years may change the stage of skeletal maturation from advanced to delayed. Nonetheless, Gilli[5] reports that the standard errors of measurement within and between raters lie within the range of 0.2 to 0.5 years. Gilli appears pleased that almost all population surveys in the last 20 years have used the TW2 system.

C. The FELS Method

More recently, Roche and co-workers described another bone-specific approach, the Fels method[8]. As in the TW2, the second and fourth rays are omitted, but the pisiform and adductor sesamoid are included. The FELS method is based on 98 maturity indicators, 13 of which measure ratios between the widths of epiphyses and diaphyses. The number of indicators to be assessed varies according to age. Two or three grades are provided for each indicator. The grading of each pertinent indicator is assigned a score using a computer program that provides the bone age and the standard error for that assessment. When assigning scores, the method takes into account that a state, or grade, which normally lasts for a long period of time, provides less information about maturity than a

stage that is passed through quickly. Thus, in contrast to TW2, the biological weight of a particular bone does not apply to all its stages. To date (July 1999), no studies utilizing the FELS method have been published, since the publication of the method itself in 1988. Gilli pointed out that its major weakness appeared to be the fact that it provided bone-specific bone ages, and no skeletal maturity scores. He felt that, until more experience has been gained with this method, the TW2 would remain the method of choice.

D. Fishman's Skeletal Maturational Indicator Method

A unique method of determining skeletal maturation was devised by Fishman[9]. The system uses only four ossification stages (width of the epiphysis, capping of the epiphysis, ossification and fusion), all found at six anatomical sites located on the thumb, third finger, fifth finger and radius. Eleven discrete adolescent skeletal maturational indicators (SMIs), covering the period of adolescent development, are found on these six sites (Figure 1-1).

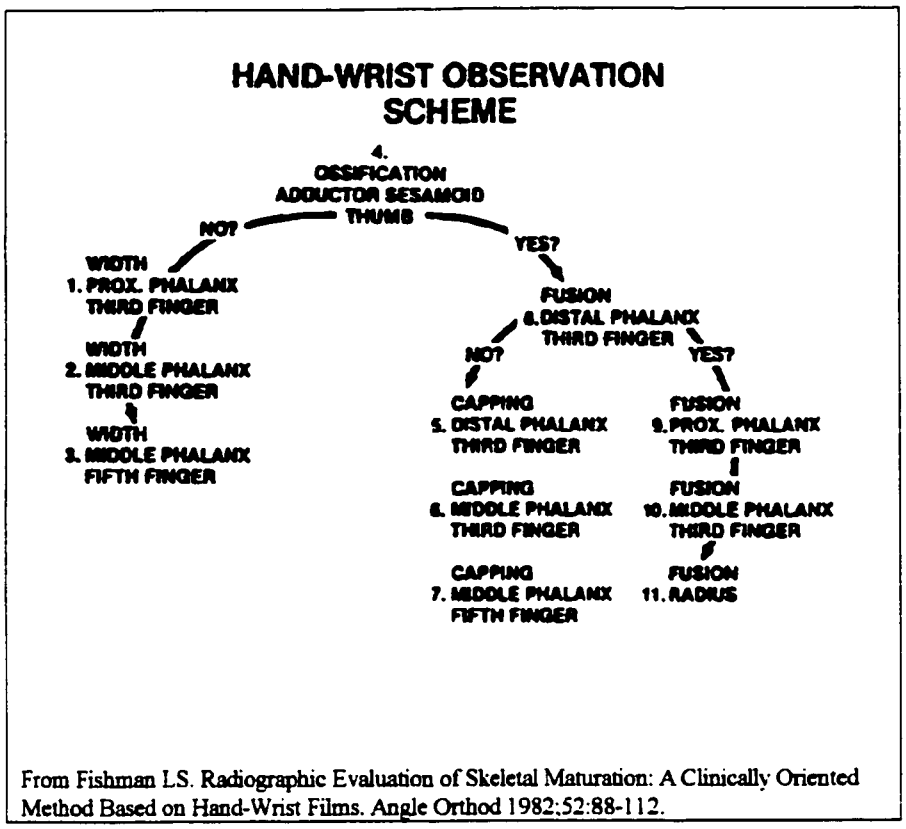

From Fishman LS. Radiographic Evaluation of Skeletal Maturation: A Clinically Oriented Method Based on Hand-Wrist Films. Angle Orthod 1982;52:88-112.

Figure 1-1: Fishman's SMI Method

Fishman stated that the sequence of occurrence of the eleven indicators was exceptionally stable, claiming that only three deviations had been detected in over two thousand observations. Unfortunately, no reference is made to that study, putting the validity of the statement, and of his skeletal age assessment method, into question. Studying both a longitudinal and a cross-sectional sample of growing children, Fishman examined relationships between his SMIs and statural height, and maxillary and mandibular growth. Although he used two measurements per jaw to assess their growth (Sella - A Point and Articulare - A Point for the maxilla, and Sella - Gnathion and Articulare - Gnathion), only one is graphed (S - A for the maxilla, and S - Gn for the mandible) and included in the data set. No explanation is given for this omission.

Fishman's skeletal maturity assessment technique does not appear to have gained widespread acceptance in the literature. A recent study[10] employed Fishman's SMI system to identify maturational stages in the cervical spine, and will be discussed later.

E. Proposed Solutions to Problems with Current Maturational Assessment Methods

The whole issue of being able to use skeletal maturation as a quantifiable variable similar to height or weight has been addressed by Benso and co-workers[4]. One of the problems the authors found with the TW2 was its discontinuity. To overcome some of TW2's weaknesses, Gilli[5] felt that the best solution would be a computer-assisted procedure. Citing works by Cox[12], and Hill and Pynsent[11] (reviewed below), Gilli hypothesized that the computerized system would allow interpolation between maturity indicator stages, thus providing a continuous maturity scale. Furthermore, computerization would eliminate subjective descriptions of shapes and shape changes. Difficulties in precisely describing the indicators, and correctly interpreting the descriptions, have been a major source of intra- and inter-observer variability.

Several authors have presented studies performed with a computerized TW2. Hill and Pynsent[11] described the Royal Orthopaedic Hospital Skeletal Ageing System (ROHSAS), which is able to examine a radiographic image and classify the features specified in the TW2 method. The system comprises an image capture device and a computer for image recognition and classification, report generation and the running of data storage software.

The digitized hand-wrist radiograph is analysed by the following steps:

1. The radiographic part of the image is extracted from the total scanned data
2. The outline of the hand is determined
3. The areas of relevance to the TW2 method are identified
4. The relevant bones within these areas are identified and classified
5. A report is generated and may be printed
6. The assessment results are entered into the database if so requested by the user.

The system has been developed to identify the bones and then classify their maturity according to shape. Once the bones are identified and classified, the computer calculates bone age by simple interpolation against the original scores of Tanner et al. Hill and Pynsent felt that their system eliminated intra-observer error and had the potential to eliminate inter-observer error. Four minutes are required to complete an ageing sequence. Cox evaluated the reproducibility of the system by examining a sample of 98 radiographs manually and by ROHSAS [12]. The results indicated that the computer system removed the variability and inconsistency seen in human assessments. Of the ratings made of the radius and ulna, 70% were identical and the rest were within one stage of one another. Similar results were obtained for the other bones, with some demonstrating a two-stage difference. The largest difference (three-stage) was seen in the assessment of the fifth proximal phalanx in one case, but this was attributed to poor positioning of the thumb on the radiograph, making the bone appear fused.

Drayer and Cox[13] utilized a computer-aided system to estimate bone age with the original radiographs used to produce the TW2 standards for the radius, ulna and short finger bones (RUS). Unlike the system of Hill and Pynsent, this system matched a template of each bone to the scanned image of the radiograph.

The set-up consisted of

1. software (version 3.5 of Discerning Systems Inc., Burnaby, B.C., Canada), running on a 386 computer operating under DOS 5.0
2. A view stand on which the radiographs were placed and on which a camera and lens were mounted
3. A video acquisition and display board which received the signal from the video camera[8,14].

The standard pictures of stages B to I of the bone were displayed around the edges of the screen as templates to guide positioning. Thus, the user could view the test image and select any stage to superimpose on the live test image. Using the zoom facility of the camera lens and moving the radiograph by hand to the correct position on the light box, the user selected image size, location and rotation to conform to the selected template. The authors stressed that the user-selected template did not influence the computer rating but was used only for placing the radiograph in a consistent orientation. The radiographic image was then enhanced and analysed by computer. Two models of this system were described: the thirteen-bone (RUS) and the six-bone (radius, ulna and the four bones of the third finger)[15]. The use of the six-bone (6b) model seemed preferable because it was less time-consuming than the rating of 13 bones[10]. Tanner and Gibbons[14] found that the computer-assisted skeletal age scores (CASAS) and manual scores both advanced with increasing age, but CASAS scores showed a relatively smooth curve. There were also fewer reversals (a situation where a lower bone rating is assigned to a specimen from an older individual). Whereas manual ratings demonstrated a 4% reversal rate of an entire (manual) stage, CASAS demonstrated only a 1% reversal rate, and of only half a stage[14]. In order to assess repeatability of the system, Tanner and Gibbons performed randomized

duplicate CASAS readings on 6 bones in each of 40 radiographs. The average absolute difference between duplicates was 0.25 stages. In only 3% of duplicates did a whole-stage difference occur. This stood in contrast to a 15% occurrence of whole-stage differences by the manual method. In another study by Tanner's group[16], differences between duplicates of individual bone ratings which exceeded 1 stage were 5% within observer and 8% between observers for CASAS, and 17 and 33%, respectively, for the unassisted manual method. The authors attributed virtually all of the increased reliability from the substitution of a continuous scale for a discrete-integer one. Drayer and Cox[13] found that the bone ages assessed by the computer system were no different from the original TW2 reference values in 85% of the ratings. Although only 64% of the computer-aided assessment and definitive ratings were the same, the total bone scores and the bone ages as assessed by the two methods were not significantly different.

Tanner and Gibbons[14] observed that the CASAS method was not without drawbacks. Although the computer was able to deal with over- and underexposed radiographs, it also required well-positioned hands and preferred radiographs with superior definition. A warning appeared in the system when more than one adjacent stage showed a relatively good match; the authors thus rejected 5-10% of ratings. Van Teunenbroek's group[15] observed that individual CASAS ratings sometimes varied considerably just by repositioning of the radiograph and without giving a warning to the user. For these and other reasons, there was a provision for inserting manual scores into the computer routine. However, the possibility of inserting a manual score with CASAS created the dilemma of when to make use of this feature. To what extent a difference between the expected and

determined rating would be accepted was likely to depend on the experience of the user and on the reliability of the computer rating of the individual bones[15]. In one study[15] the percentage of manual insertions ranged from 5 to 8%.

Frisch's group compared CASAS with GP and TW2 in three groups of children with Turner's syndrome (TS) , growth hormone deficiency (GHD) and familial short stature (FSS)[17]. With CASAS, individual bone assessments had to be repeated once in 7.3% and twice in 2.7% of all probands on request of the computer system because of doubtful results. Manual interventions by the investigator were necessary in 12.3% of evaluations in TS, 8.5% in GHD and 9.0% in FSS. Most of the external corrections for CASAS were necessary for assessments of the thumb and fifth finger. The authors concluded that CASAS represents a useful method for analysing skeletal age and, like Gilli[5], they found that it seems to increase reliability by rating on a continuous scale. On the other hand, difficulties with abnormally shaped bones restrict its use in some pathologic conditions. It should be noted that time spent on evaluating one radiograph, despite partial automation was 15 to 25 minutes, even though the analysis operation itself lasted 35 seconds per bone.

Another computer system for skeletal age assessment was presented by Sun and co-workers[18]. In contrast to the CASAS system, the hand-wrist radiographic image was taken directly by a CCD camera via a VFG board, and digitized into a 512 x 512 image with 256 gray levels. The system included four major stages: preprocessing, segmentation, parameter analysis, and skeletal age evaluation. The researchers unfortunately based their skeletal age assessment on the phalangeal bones only. Furthermore, all phalanges were

given equal weight by averaging to obtain a 'global' skeletal age. Perhaps even more surprising was that the authors tested the validity of their technique by demonstrating how closely the skeletal age estimated by the computer lay to the patient's chronological age. Rucci's group proposed yet another automated skeletal age assessment system[19], based on neural networks. According to the authors, due to their intrinsic operation mechanisms,

> neural networks are expected to provide an optimal use of acquired knowledge: for a given input stimulus, the output is usually obtained by an efficient integration of the data stored in the connection weights (which can be seen as a sort of knowledge base) with the actual input.

The results of the study suggested that the behaviour of the proposed system is similar to that of trained operators. System misclassification seemed to be related to the intrinsic 'fuzziness' of the TW2 categories.

II. THE CERVICAL VERTEBRAE

Lateral cephalometric radiographs have been examined as an alternative to hand-wrist radiographs in determining a patient's skeletal age[20]. Several attempts have been made at formulating an age determination system based on growth of the cervical vertebrae. Unfortunately, the distinguishing features of each age category have so far been described on a purely qualitative basis. The following discussion will begin by examining growth of the cervical spine from infancy to adulthood; it will then report the most recent advances in quantification of cervical vertebral anatomy.

A. Growth and Development of the Cervical Spine

In order to better understand growth and development of the cervical spine, the following discussion will begin with a brief anatomic description of the vertebrae, as presented by The Cervical Spine Research Society[21]. The cervical spine consists of the first seven vertebrae in the spinal column. The third through seventh vertebrae are similar in size and shape, whereas the atlas (C1) and axis (C2) have very different morphologies.

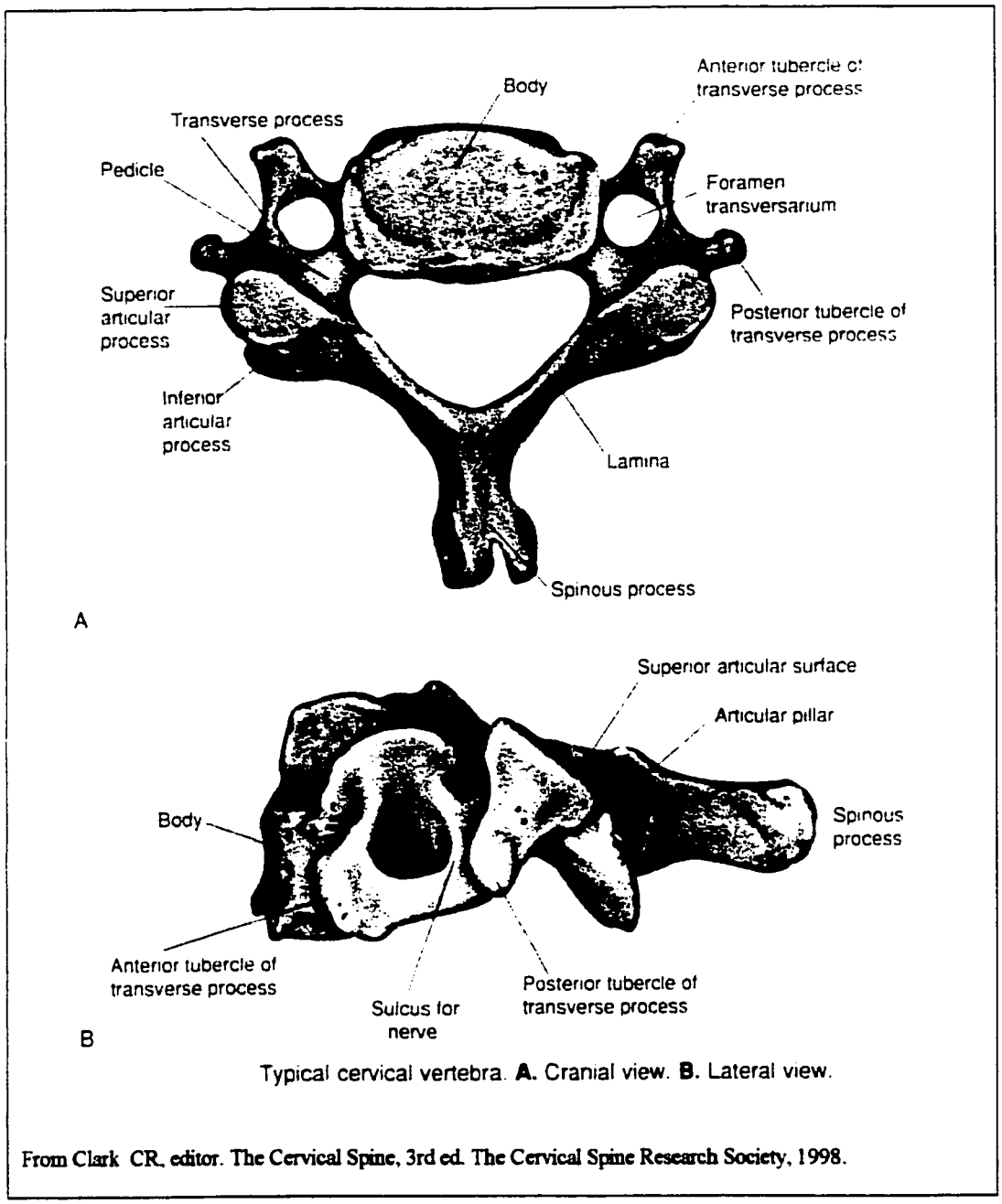

Typical cervical vertebra. **A.** Cranial view. **B.** Lateral view.

From Clark CR, editor. The Cervical Spine, 3rd ed. The Cervical Spine Research Society, 1998.

Figure 1-2: Typical Cervical Vertebra

A typical lower cervical vertebra (Figure 1-2) has a small vertebral body which is concave on its superior surface and lipped by a raised edge of bone on its margin. Correspondingly,

the inferior surface is convex. Projecting laterally from the body and roots of the pedicles on each side is a bar of bone which represents the rudimentary costal process (or rib). This bony structure fuses laterally to the transverse process through the costotransverse lamella. The costal process projects forward to end in the anterior tubercle of the transverse process. Posteriorly, the "true" transverse process ends in the posterior tubercle. The ventral ramus of each spinal nerve exits from the spinal column over the costotransverse lamella through a groove bounded posteriorly by the transverse process and posterior tubercle, and anteriorly by the vertebral artery and anterior tubercle. The groove is bounded by the vertebral body medially and by the facet joint and base of the lamina laterally. The floor and roof of the canal are made up of the superior and inferior pedicles, respectively. The spinous processes of the third, fourth, and fifth cervical vertebrae are usually bifid, whereas those of the sixth and seventh are longer and tapered. Viewed from above, the first cervical vertebra (atlas) is a ring-shaped structure with no centrum and no spinous process[22] (Figure 1-3). C1 is unique among vertebrae in that it has no centrum. It possesses a thick anterior arch that blends into the two bulky lateral masses. The atlas supports the occiput and articulates with the odontoid process of C2.

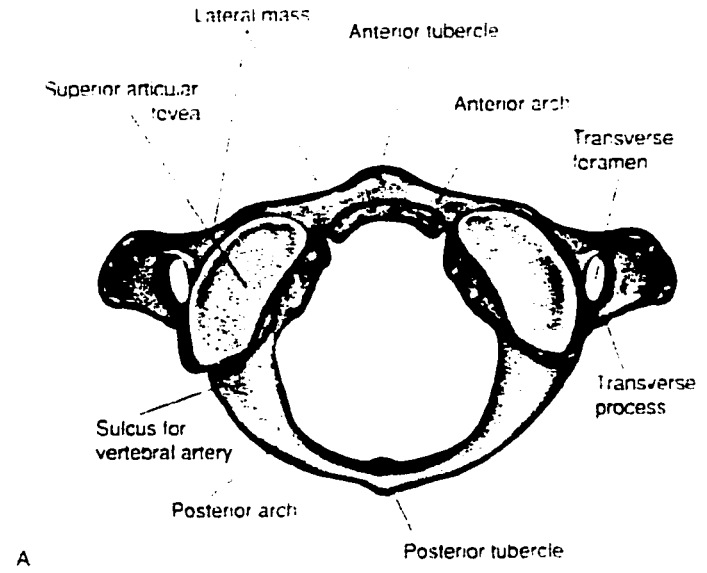

The atlas. **A.** Cranial view **B.** Caudal view of the atlas.

From Clark CR, editor. The Cervical Spine, 3rd ed. The Cervical Spine Research Society, 1998.

Figure 1-3: The Atlas

The vertebral body of C2 (axis) is fused with the embryological "vertebral body" of C1 (atlas) to form the odontoid process (dens) (Figure 1-4)[18]. The transverse process of C2 does not possess the costal element found in the lower cervical vertebrae. The odontoid

process extends upward to reach the anterior lip of the foramen magnum.

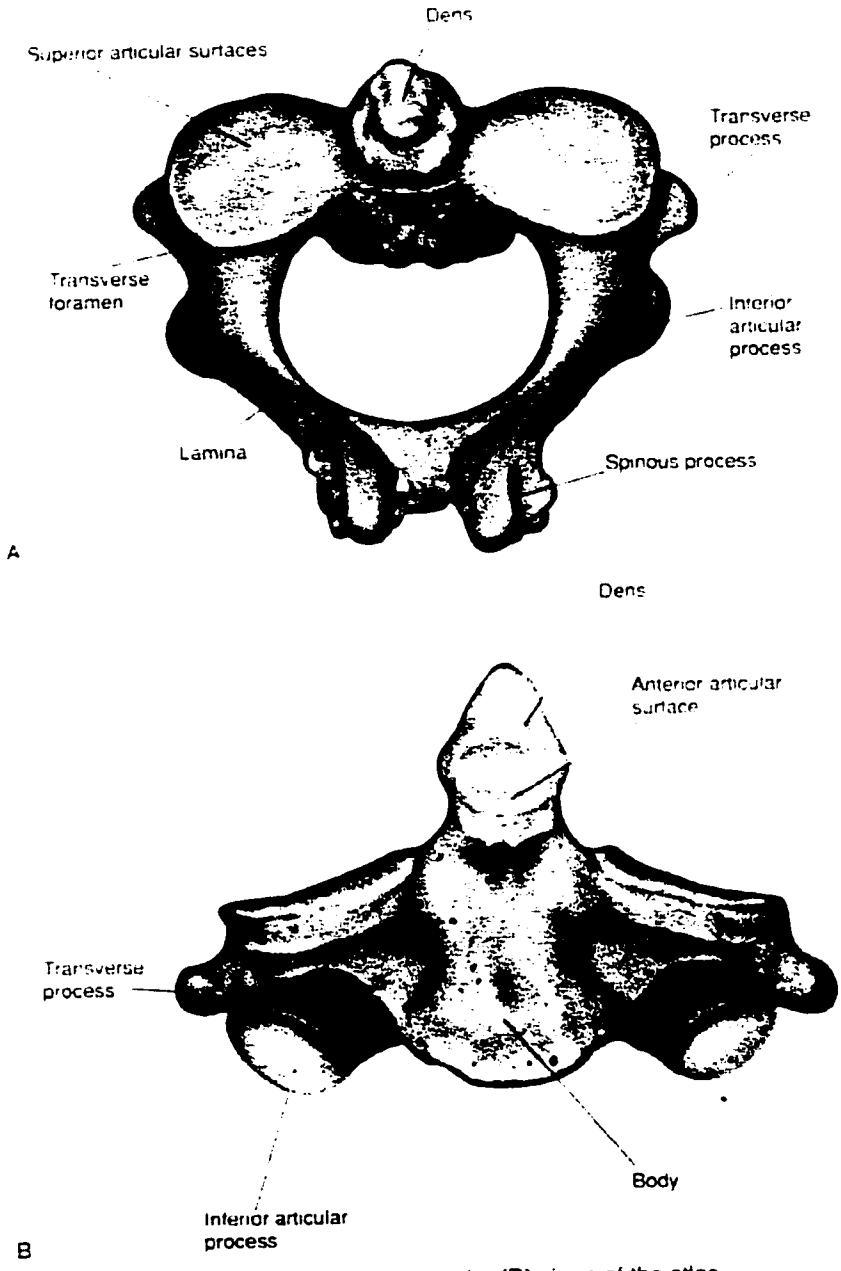

Cranial (**A**) and anterior (**B**) views of the atlas.

From Clark CR, editor. The Cervical Spine, 3rd ed. The Cervical Spine Research Society, 1998.

Figure 1-4: The Axis

As in most skeletal elements, the mesenchymal vertebrae, which develop at 4 weeks *in utero*, become cartilaginous. Chondrification of the vertebral column begins at 6 weeks. Ossification follows chondrification in the various components of the vertebrae, usually beginning around the 9th week[23]. The atlas is formed from three primary ossification centres - the body and two neural arches (Figure 1-5)[24].

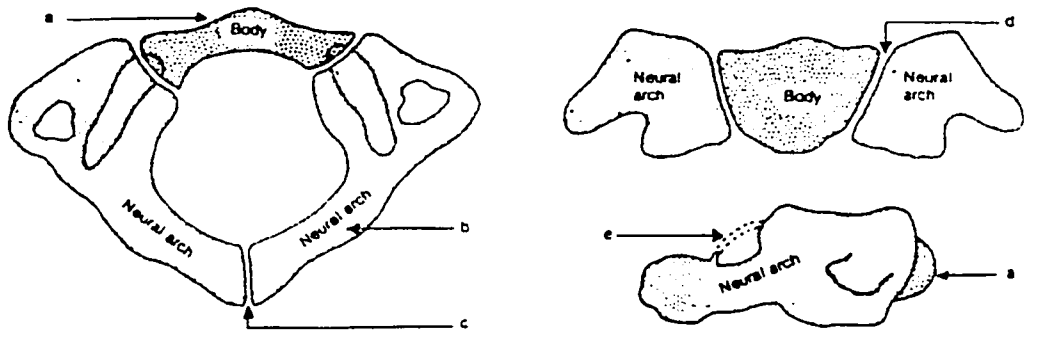

The first cervical vertebra (atlas). a. Body: ossification center becomes visible during the first year of life. b Neural arches: ossification center appears in utero at approximately the 7th fetal week. c. Synchondrosis of spinous process: fuses at approximately the third year of life. d. Synchondrosis about the body (neurocentral synchondrosis). fuses at approximately the seventh year of life. e. Ligament surrounding the superior vertebral notch: may ossify later in life. Reprinted with permission from Fielding JW Cervical spine injuries in children. In: The Cervical Spine Research Society (eds): The cervical spine. Philadelphia, PA. JB Lippincott; 1983:268-81.

From Fesmire FM, Luten RC. The Pediatric Cervical Spine: Developmental Anatomy and Clinical Aspects. J Emerg Med 1989;7:133-42.

Figure 1-5: Ossification of the Atlas

The body is not usually ossified at birth (although in less than 20% of neonates it is visible[25]), but appears as one or two ossification centres during the first year of life. The neural arches of the atlas appear *in utero* during the seventh week of life. The anterior ossification centre (body) expands laterally toward each posterior centre (neural arches), stopping when a cartilaginous gap of 3 to 4 mm exists. These gaps are the neurocentral synchondroses (which lie within the vertebral body in the other cervical vertebrae[20]). The synchondrosis of the spinous processes (situated posteriorly) fuses at approximately the

third year, whereas that of the body fuses at about seven years.

The second cervical vertebra (axis) possesses four ossification centres: odontoid, body and two neural arches (Figure 1-6).

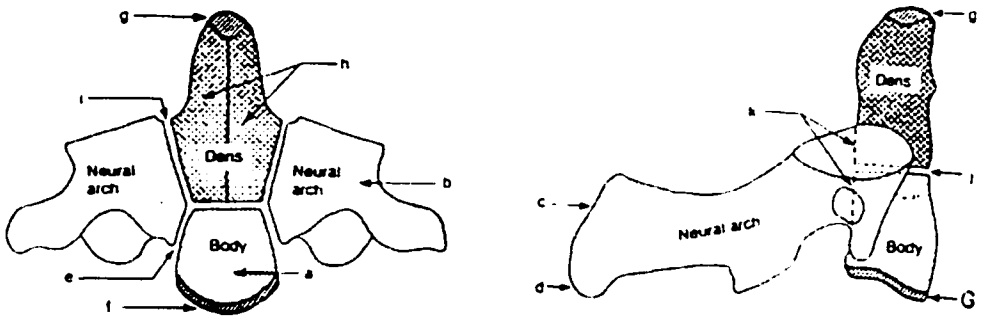

The second cervical vertebra (axis). a. Body: ossification center appears by the fifth fetal month. b. Neural arches: appear by the seventh fetal month. c. Synchondrosis of spinous process: fuses by the third to sixth year of life. e. and i. Neurocentral synchondrosis: fuses by the third to sixth year. f. and G. Inferior epiphyseal ring: appears at puberty and fuses to body at approximately twenty-five years of life. g. Summit ossification center for odontoid: appears at approximately the third to the sixth years and fuses with the odontoid by the twelfth year of life. h. Odontoid: develops from two ossification centers which fuse by the seventh fetal month. j. Synchondrosis between the odontoid and body: fuses at approximately the third to sixth year of life. Reprinted with permission from Fielding JW. Cervical spine injuries in children. In: The Cervical Spine Research Society (eds) The cervical spine. Philadelphia, PA: JB Lippincott, 1983:268-81.

From Fesmire FM, Luten RC. The Pediatric Cervical Spine: Developmental Anatomy and Clinical Aspects. J Emerg Med 1989;7:133-42.

Figure 1-6: Ossification of the Axis

The odontoid (or 'dens') forms *in utero* from two separate ossification centres that fuse in the midline by the third[26] to seventh fetal month. A secondary ossification centre appears at the odontoid's apex between 3 and 6 years and fuses with the odontoid itself by 12 years. The body of the axis develops usually from a single ossification centre which appears by the fifth month *in utero*. The synchondrosis between the body and the dens fuses by 3 to 6 years of age. The fusion line commonly remains visible until age 11 and, in one-third of individuals, it may remain so throughout life. The two neural arches of C2 appear bilaterally by the seventh fetal month and fuse posteriorly by 2 to 3 years. The

synchondroses between the neural arches and the dens-body complex fuse between 3 and 6 years. By nine to ten years, the synchondroses have all fused; variably evident remnants of each may appear on a radiograph[26].

The remaining cervical vertebrae (C3 to C7), due to their similar properties, will be described as a unit. The body arises from a single ossification centre (rarely two) by the fifth fetal month. Both neural arches appear by the 7th to 9th week *in utero* and fuse posteriorly by the 2nd to 3rd year. The anterior portion of the transverse process may develop from a separate ossification centre and fuse with the neural arch by the 6th year. The synchondrosis between the neural arches and body fuse between 3 and 6 years. A secondary ossification centre appears at the tips of these vertebrae at puberty and fuses with the spinous process at about age 25. Secondary ossification centres also appear at puberty along the superior and inferior aspects of the cervical bodies (superior and inferior epiphyseal rings). These ossification centres begin to fuse with the main body at age 15 to 16 years[21], a process which is usually completed by age 25; at this point, they consist of hard cortical bone. The central portion of the cartilaginous end plate remains unossified and is considered as one of the components of the intervertebral disk. Incomplete fusion of these centres to the vertebral body may be confused with chip fractures radiographically[27]. Roche[28] reports that Bick and Copel (1950) felt these epiphyses were not responsible for elongation, and thus differed fundamentally from long bone epiphyses. This opinion was based on the reality that the vertebral bodies elongate prior to ossification of these epiphyses, that they elongate in the central parts of the superior and inferior surfaces where the epiphyses do not develop and that elongation ceases at the same time in the

central and peripheral parts of the surfaces. However, as Roche determined, each of the above findings is true for long bone epiphyses as well. Thus, according to him, the vertebral bodies demonstrate growth typical of long bones[31]. Both the cranial and caudal growth layers participate to the same degree in the vertical expansion of the vertebral bodies. The chondroblasts of the ossification fronts between the primary vertebral epiphyses and the cartilaginous end plates demonstrate minimal columnization. As a result, the cervical spine has limited longitudinal growth potential, with each vertebral segment growing an average of only 0.7 mm per annum[21]. Macroscopically, at age 7 years, a typical cervical vertebral body will possess cribriform perforations, as well as groove-like radial irregularities (Figure 1-7). These become most pronounced between the ages of 8 and 10 and persist after the bony rims have formed; in fact, only after ages 21 to 25 do the remaining grooves become flattened[29].

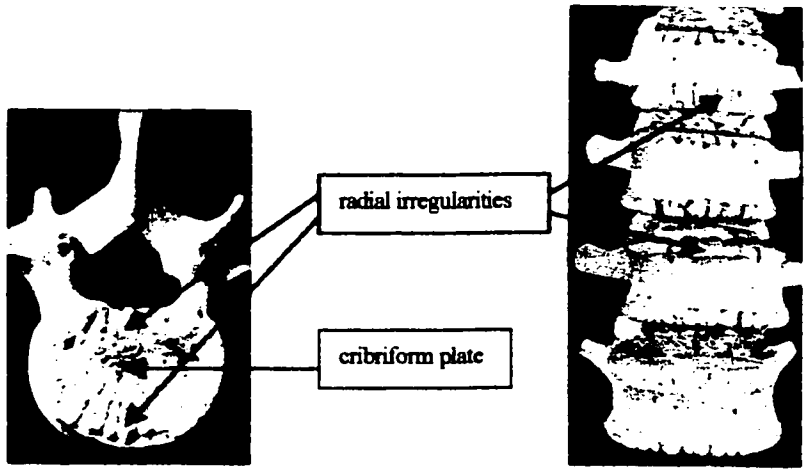

From Schmorl G, Junghanns H. The Human Spine in Health and Disease. Second Edition. Grune & Stratton, New York, 1971.

Figure 1-7: Cribriform Plate and Radial Irregularities

Cervical vertebrae 3 through 7 possess "uncinate" or "lunate" processes, the ridges of which are flat in the newborn (Figure 1-8). As they develop, they gradually give the superior surface of the body the appearance of a shovel or saddle. The depth of the shovel decreases caudad within a given vertebral column.

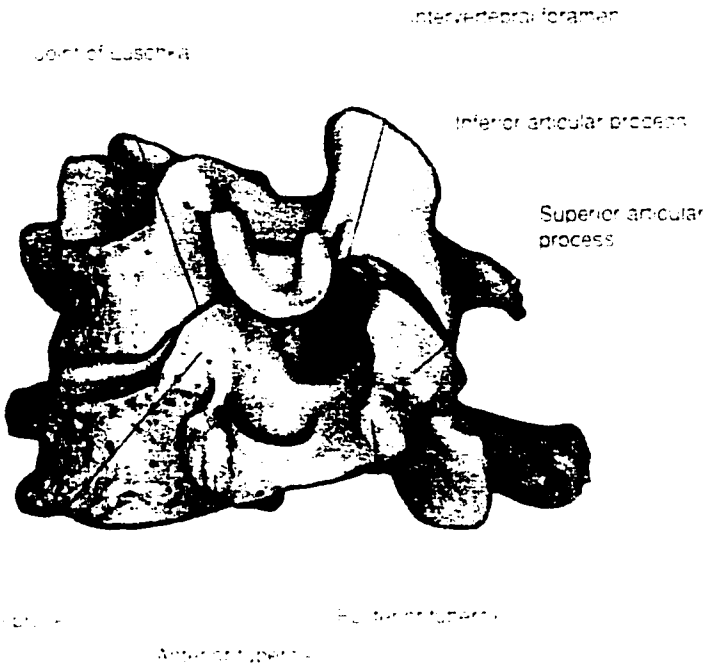

From Clark CR, editor. The Cervical Spine, 3rd edition. The Cervical Spine Research Society, 1998.

Figure 1-8: Two Articulated Vertebrae, Showing Uncinate Process

Vertical growth of the cervical spine has been examined by Roche[28], who studied serial lateral cephalograms of 16 Caucasian males and 16 Caucasian females living in Cleveland, Ohio, who were enrolled in the Brush Foundation Study of Child Growth and Development. The radiographs were taken at three-month intervals between birth and one year and at six-month intervals from then until five years, after which they were made annually until 17 years. The mean overall distance from the apex of the dens to the midpoint of the inferior margin of C4 increased rapidly with age in each sex until about 2 years. At later ages, the mean rate of elongation was less but spurts occurred at 12-13 years for boys, and 10-11 years for girls. Roche also found that the lateral silhouettes of

the vertebral bodies and discs tended to be reciprocal. Thus, at early ages, the mean intermediate height of a body was greater than the corresponding anterior or posterior height; during the same period, the mean intermediate height of a disc was less than the mean anterior or posterior height. At later ages (until about 15 years), the usual order of mean heights for each vertebral body was posterior > intermediate > anterior. The order of mean heights for each intervertebral disc was anterior > intermediate > posterior. After 15 years, the order of mean heights became posterior > anterior > intermediate for the vertebral bodies and intermediate > anterior > posterior for the intervertebral discs. Similar results, expressed slightly differently, were obtained by Kasai and co-workers[30]. They studied the lateral cephalograms of 180 boys and 180 girls regarding diameters and central heights of the cervical vertebrae, as well as other variables. Growth of the vertebral body diameters was accelerated between 1 and 3 years of age in both sexes, as well as between 10 and 13 for girls, and between 11 and 14 for boys. Corresponding periods of acceleration were found for vertebral body height; initial acceleration occurring between 1 and 5 years for both sexes, pubertal acceleration occurring between 10 and 12 years for girls, and between 12 and 14 years for boys. Thus, the vertebral developmental course showed the primary and secondary growth spurt and terminated a couple of years earlier in girls than boys. The mean body height index (BHI) for each vertebra was also determined, consisting of the ratio of the anterior height of each body to its posterior height. This ratio was observed to decrease until 9 years of age, and then demonstrated a rapid increase. This corresponds roughly to Lamparski's observations[20].

Tulsi[31] performed an osteological study of vertebral column growth on a sample of 20

juveniles and 112 adults from the skeletal collection in the South Australian Museum in Adelaide, and the Department of Anatomy of the University of Adelaide. He divided them into five groups as follows: group I (2-4 years), group II (6-7 years), group III (9-12 years), group IV (14-15 years) and group V (17-19 years). Examining the vertebral bodies in particular, Tulsi found that the height of all the vertebrae continues to increase until adulthood; there were periods of accelerated growth. The cervical vertebrae increased by 41% between 2-4 years (group I) and adulthood. The height of the vertebral column continued to increase until maturity and showed two periods of accelerated growth: first, between groups I and II (17%) and the second between groups III and IV (15%). According to Tulsi, the best method of studying overall rate of growth of the vertebral body was by volume determination. Thus, a maximum increase in the volume of the vertebral body occurred between early childhood and maturity in the lumbar region and least in the cervical region. However, volumetric measurements of the vertebral body were fairly crude. Essentially, volume was determined by multiplying the width of the vertebral body by its depth and by its height. Given that the body itself is by no means a cubical structure, any volumetric measurements taken by the above method must be treated with caution.

Dimensions of the cervical vertebral column were also examined by Hellsing, comparing them with statural height[32]. In her literature review, Hellsing describes the gradual enlargement of the vertebral bodies as staying in a central axis; thus, the vertebral column's increase in size would help maintain a constant dimension of the oral and laryngeal pharynx. Hellsing also observed from her own work that the spine straightened

with increasing age. In this particular study, Hellsing found that the height of the vertebral bodies was greater among the girls than the boys at each age. Among the 8- and 11-year-old children the height and length of the vertebral bodies showed significant correlations with statural height. However, among the 15-year-old children no correlation was found between vertebral size and body height; this finding was attributed to the decreasing velocity of growth after the pubertal peak.

Maturation of cervical vertebrae has been correlated to growth of the face directly[33]. Examining annual lateral cephalometric radiographs of thirteen Caucasian females from 9 to 15 years of age, O'Reilly and Yaniello were able to observe that statistically significant increases in various mandibular dimensions were associated with specific maturation stages in the cervical vertebrae. Lamparski's vertebral stages 1 through 3 occurred in the accelerative growth phase, with stages 2 and 3 occurring most frequently in the year preceding the maximum increment of mandibular growth. Stages 4 through 6 were observed to occur during the decelerative phase of growth after peak velocity. Significant increases were observed for mandibular length from stages 1 to 4, for corpus length from stages 1 to 3, and for ramus height between 1 and 2.

Examining the morphology of the first cervical vertebra (atlas) only, Huggare found a significant correlation between the initial height of its dorsal arch and horizontal growth of the mandible[34]. Two groups of subjects were examined. The first consisted of 18 children, 6 boys and 12 girls, for whom lateral cephalograms were taken at the ages of eight and ten years. All had Class I occlusion and none had received any orthodontic treatment. Growth of the mandible was measured as the difference in the position of prognathion in relation

to a vertical line drawn perpendicular to the sella-nasion line. For the second group, comprised of 12 children, 7 boys and 5 girls, all subjects had undergone orthodontic treatment and pre- and post-treatment cephalograms were available. Again, difference in the position of prognathion was measured, in order to determine if the patients' mandibles rotated forward or backward during treatment (either a decrease or an increase in the N-Pg-S angle, respectively). Huggare felt there was a clear association between the height of the dorsal arch of the first cervical vertebra and mandibular growth. In other words, a shorter arch implied backward rotation of the mandible, whereas a longer arch implied forward rotation. The researcher attributes this finding to a more raised head position in subjects with a low dorsal arch. As an additional finding, Huggare discovered that both forward and backward rotation of the mandible could be found among the subjects treated with cervical headgear.

Growth changes of the cervical spine have also been described qualitatively by Lamparski[20], who traced lateral cephalograms in order to develop 6 adolescent "vertebral" ages, from 10 to 15 years. These are illustrated in the following figures.

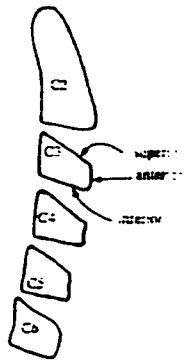

Characteristics of

VERTEBRAL AGE 10

1. All inferior borders of bodies are flat.
2. Greater posterior height than anterior
3. The superior border tapers from posterior to anterior (wedging of bodies C2 - C5).

Characteristics of

VERTEBRAL AGE 11

1. Development of a distinct concavity in the inferior border of the 2nd vertebrae
2. Increasing anterior vertical heights.

Characteristics of

VERTEBRAL AGE 12

1. A concavity has developed in the inferior border of the 3rd vertebral body
2. Anterior heights still increasing, with reduction in superior taper
3. All other inferior borders are still flat

Characteristics of

VERTEBRAL AGE 13

1. Distinct concavities on inferior border of bodies 2, 3, and 4
2. Development of concavities just initiated in bodies 5 and 6
3. Body shape approximates to a rectangle

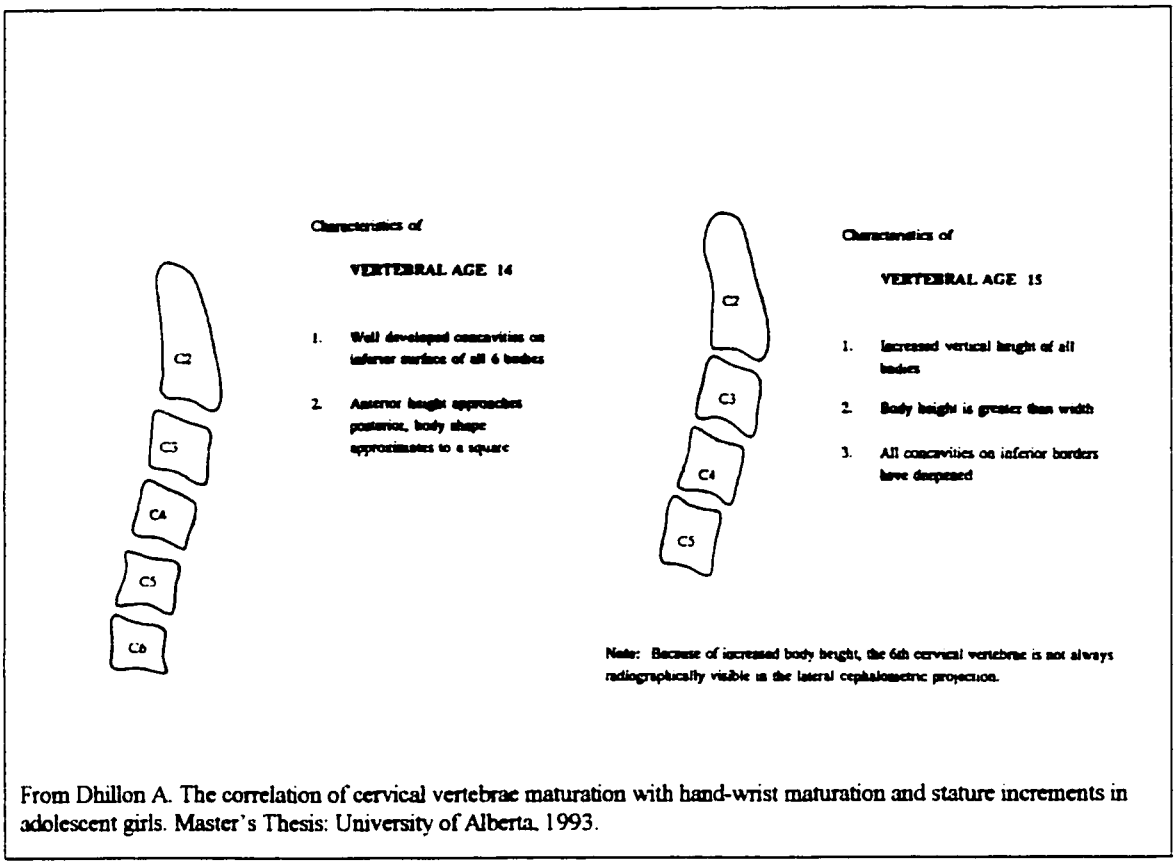

From Dhillon A. The correlation of cervical vertebrae maturation with hand-wrist maturation and stature increments in adolescent girls. Master's Thesis: University of Alberta, 1993.

Figure 1-9: Lamparski's Vertebral Age Categories

Dhillon[35], performing a study of adolescent female cervical vertebrae maturity, employed Lamparski's classification system in order to determine the validity of vertebral age as a maturity indicator. Unfortunately, she established its validity by comparing it to the Greulich and Pyle assessment, with its aforementioned inherent weaknesses. A similar study by Hassel and Farman[36] was performed in order to develop a cervical vertebrae maturation index (CVMI). Using Fishman's eleven skeletal maturation indicators (SMI), they assigned two of them to each of six cervical maturational stages (except for CVMI 6, which corresponded to SMI 11 only). The cervical vertebrae maturation indicators are described in the figure below.

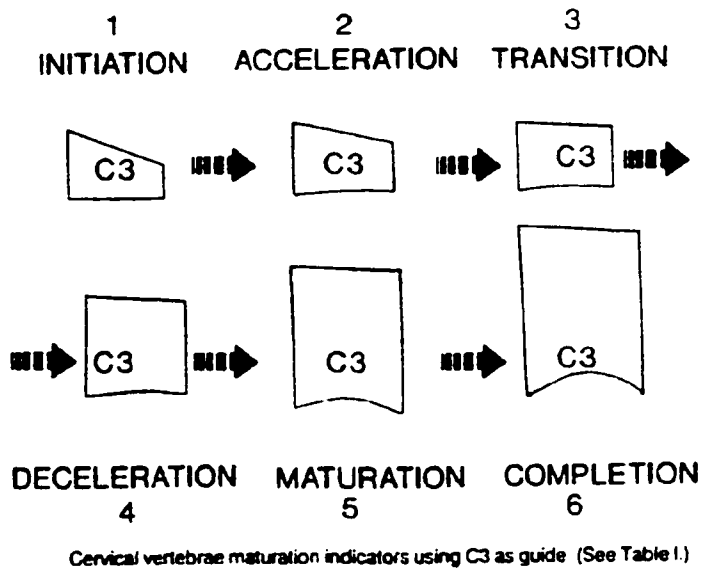

Cervical vertebrae maturation indicators using C3 as guide (See Table I.)

Table I. Cervical vertebrae maturation indicators

1. *Initiation*
   - Very significant amount of adolescent growth expected
   - C2, C3, and C4 inferior vertebral body borders are flat
   - Superior vertebral borders are tapered posterior to anterior
2. *Acceleration*
   - Significant amount of adolescent growth expected
   - Concavities developing in lower borders of C2 and C3
   - Lower border of C4 vertebral body is flat
   - C3 and C4 are more rectangular in shape
3. *Transition*
   - Moderate amount of adolescent growth expected
   - Distinct concavities in lower borders of C2 and C3
   - C4 developing concavity in lower border of body
   - C3 and C4 are rectangular in shape
4. *Deceleration*
   - Small amount of adolescent growth expected
   - Distinct concavities in lower borders of C2, C3, and C4
   - C3 and C4 are nearly square in shape
5. *Maturation*
   - Insignificant amount of adolescent growth expected
   - Accentuated concavities of inferior vertebral body borders of C2, C3, and C4
   - C3 and C4 are square in shape
6. *Completion*
   - Adolescent growth is completed
   - Deep concavities are present for inferior vertebral body borders of C2, C3, and C4
   - C3 and C4 heights are greater than widths

From Hassel B, Farman AG. Skeletal maturation evaluation using cervical vertebrae. Am J Orthod Dentofac Orthop 1995;107:58-66.

Figure 1-10: Cervical Vertebrae Maturation Indicators

B. Quantification of Cervical Vertebrae Anatomy

Accurate quantitative anatomic data have been rarely reported. Some quantitative studies of human cervical vertebral anatomy have been completed (such as the ones mentioned in previous sections), but most of these studies use relatively simplistic measurement techniques, and/or present anatomic data on a small portion of the total vertebral anatomy[37].

Recently, several attempts have been made to remedy these weaknesses. Efforts have concentrated on creating coordinates and reference points in order to obtain three-dimensional data and thus a more accurate assessment than can be established from two-dimensional radiographs.

The first model was proposed by Panjabi's group[37]. Using a specially designed morphometer, various marked points on the surfaces of the vertebrae were assigned three-dimensional coordinates. As a result, linear dimensions, angulations, and areas of surfaces and cross-sections of most vertebral components were calculated (Figure 1-11). The researchers secured two pointed threaded rods into each vertebral body. The two ends of one rod constituted two pin markers; the third pin marker was provided by the end of the second threaded rod. Then, A-P and lateral radiographs were taken to identify the pins in the vertebral body coordinate system with origin at the centre of the upper end plate.

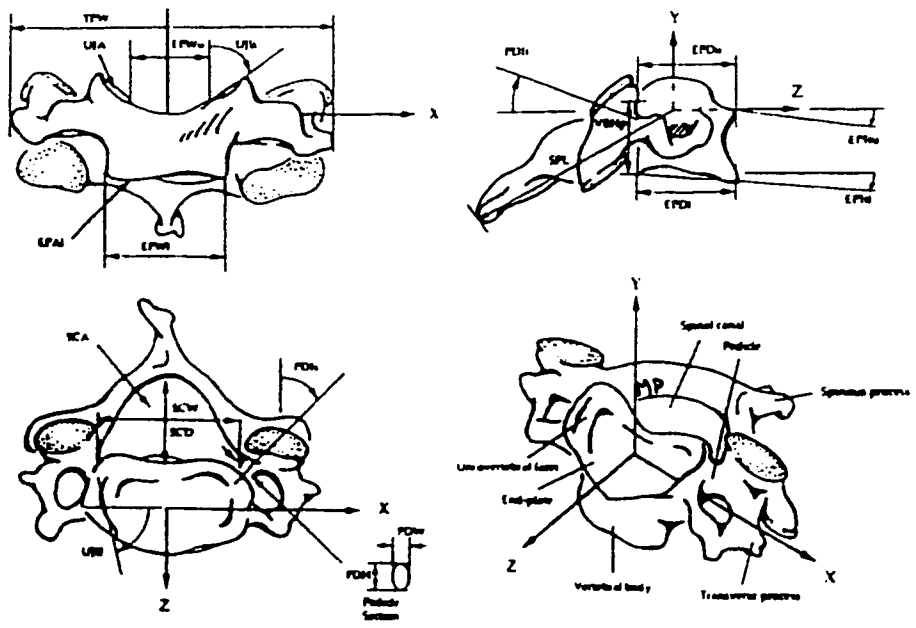

From Panjabi MM, Duranceau J, Goel V, Oxland T, Takata K. Cervical Human Vertebrae: Quantitative Three-Dimensional Anatomy of the Middle and Lower Regions. Spine 1991;16(8):861-9.

Figure 1-11: Variables examined by Panjabi's Group

Each vertebral part was defined in space by a series of points spanning or circumventing its surface. The number of points chosen was such that the geometry was well defined by straight lines joining the adjacent points. The morphometer consisted of one linear variable (LVDT) and two rotational variable (RVDT) displacement transducers arranged such that their axes meet at one point, thus establishing a spherical coordinate system. Thus, the location of any point, or series of points, with respect to the three pin markers, was determined by placing the tip of the morphometer at the point(s) in question and at the three pin markers. The three-dimensional coordinates were directly recorded into the computer.

Morphometric studies of the dens (odontoid process of the axis) were performed by

Schaffler and co-workers[38]. One hundred twenty second cervical vertebrae were examined from the Hamann-Todd Collection of the Cleveland Natural History Museum. However, no radiographs were taken, and measurements were made directly on the vertebrae themselves, using dial calipers. No mention was made of reference planes, so this study's applicability in an orthodontic, radiographic context remains questionable. The only finding of note was that anterior vertebral body height was consistently greater than posterior vertebral height in all specimens. Based on Lamparski's study, however, this is not surprising, since all bones in Schaffler's study were from individuals aged between 20 and 50 years; thus all would have completed their statural growth.

Panjabi's group performed another study similar to the first, in which the articular facets of the human spine were examined[39]. Using the same methods described previously, these researchers focused their investigation on providing a three-dimensional surface anatomy of the articular facets for the entire human vertebral column. Facet orientations were described as angles with respect to the sagittal and transverse planes and also as "card angles" (Figure 1-12). The authors found that this new concept was better at helping visualize the three-dimensional orientations of the facets.

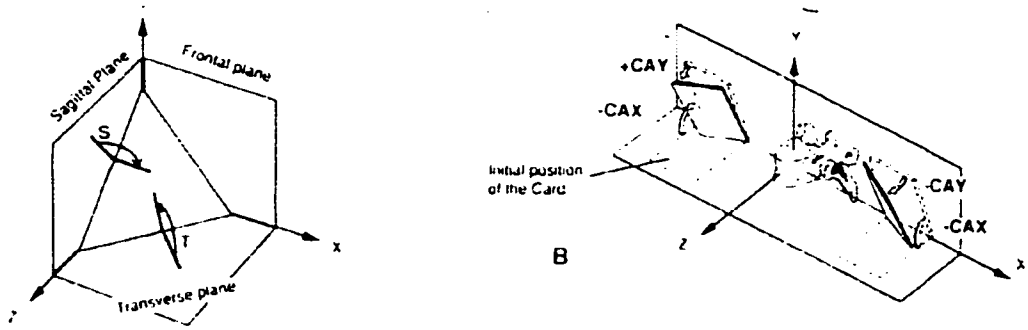

Facet surface was approximated by a plane. A, The orientation of the plane was defined by two angles made by the facet plane with the anatomic planes: sagittal (S) and transverse (T). B, Alternatively, the facet plane orientation was defined by two card angles: rotating a card, initially lying in the transverse plane, by angle CAX, followed by rotating the card around the Y-axis by angle CAY

From Panjabi MM, Oxland T, Takata K, Goel V, Duranceau J, Krag M. Articular Facets of the Human Spine: Quantitative Three-Dimensional Anatomy. Spine 1993;18(10):1298-310.

Figure 1-12: Facet Orientations

A different technique was employed by Xu and coworkers[40] in quantifying C2 through 18 linear and four angular parameters . The vertebral body of C2 was assessed for diameter, width, and anterior and posterior height. Unfortunately, no reference planes were given for these measurements, although such planes were defined for the angular data. As in other studies mentioned previously, Xu's group observed the consistent occurrence of a greater anterior vertebral body anterior height in comparison to the posterior.

In contrast to Xu and coworkers, Doherty and Heggeness defined reference planes when measuring C2[41]. Direct measurements were made using digital calipers and a goniometer on 51 dried human second cervical vertebrae. The reference plane for height measurements was defined by three anatomic landmarks: the anteroinferior-most point on

the endplate, in the mid-sagittal plane, the inferior-most point of the left interior facet joint surface, and the inferior-most point of the right inferior facet joint surface. To achieve consistency, the specimens were allowed to rest on these three points alone by using a milled plate.

Another three-dimensional quantification of the cervical spine was performed by Oh and co-workers[42]. In contrast to Panjabi's technique of employing radiographs, which is arguably more useful from an orthodontic viewpoint, Oh's group focussed on a video imaging analysis system, in order to eliminate the use of magnification factors. Measurements were made on human cervical vertebrae using a real-time video analysis of images transferred from a Zeiss microscope equipped with an image splitter and a Sony charge-coupled device (CCD) camera. Images were then transferred to an IBM personal computer-based image analysis system. Similar dimensions to those of aforementioned studies were measured. Whether or not the computer automatically used reference planes to ascertain dimensions was not clear. Neither was there any mention of how the vertebrae were orientated when being imaged by the CCD camera.

A recent study[43] evaluated the lower cervical pedicle and determined the correct location of the pedicle axis for transpedicular screw fixation (Figure 1-13). This procedure is performed by placing screws into the pedicles to treat an unstable cervical spine. Taking direct measurements on 40 whole spines, with an age range of 21-70 years, linear and angular data were collected. As in numerous previous studies, the orientation of the vertebrae was not stated. However, as well as using reference planes, Ebraheim's group employed horizontal and vertical reference lines.

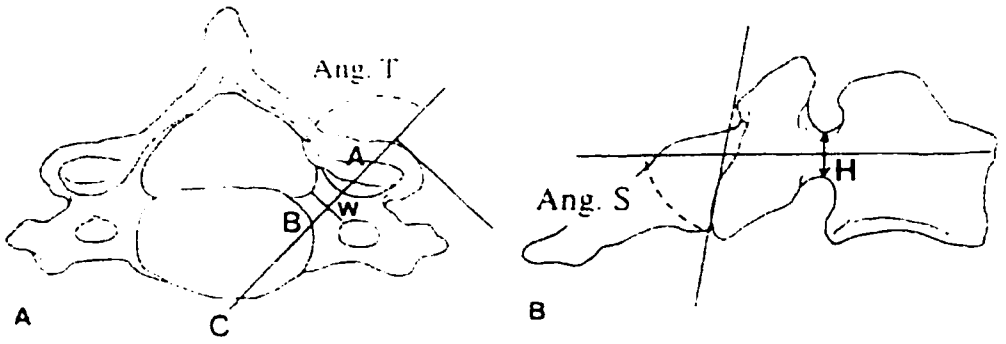

Illustration of linear and angular measurements of the pedicles of C3-C6 A. Superior view W = pedicle width AB = pedicle length BC = vertebral body length Ang T = pedicle transverse angle B. Lateral view H = pedicle height Ang S = pedicle sagittal angle

From Ebraheim NA. Xu R. Knight T. Yeasting RA. Morphometric Evaluation of Lower Cervical Pedicle and Its Projection. Spine 1997;22(1):1-6.

Figure 1-13 Linear and Angular Measurement of the Pedicles

Again, unfortunately, horizontal, transverse and sagittal planes were not defined in relation to anatomic landmarks on the vertebrae themselves.

Recently, various researchers have employed computer simulation to develop so-called finite element models of the cervical spine[44,45,46] (Figure 1-14). Although finite element analysis was introduced in 1956 to analyze structural mechanics problems in the aircraft industry, it soon found numerous medical applications[43,45], and became a valuable tool for biomechanical examination of the human spine. Advantages of simulation models lie in the fact that they are repeatable and that one can vary any parameter and quantify the effects of that change on the final outcome. Thus, they are a valuable complement to cadaver experimentation models and an adjunct to clinical studies. A finite element model is created using computed tomography to provide the necessary three-dimensional bony detail, and then generating an automatic mesh of the structure to be examined. The CT additionally provides accurate information about the material properties of the structure,

since quantitative CT is directly proportional to the apparent bone density[43]. Maurel's group examined 53 lower cervical vertebrae, determining the three-dimensional coordinates of 154 points spread over their surface using a spatial measuring machine[45]. An anatomical reference system was attached to each vertebra, allowing the investigators to determine parameters for the construction of a generic lower cervical vertebra. Using a specific pre-processor, the mesh of a three-dimensional finite element model of the lower cervical spine was created.

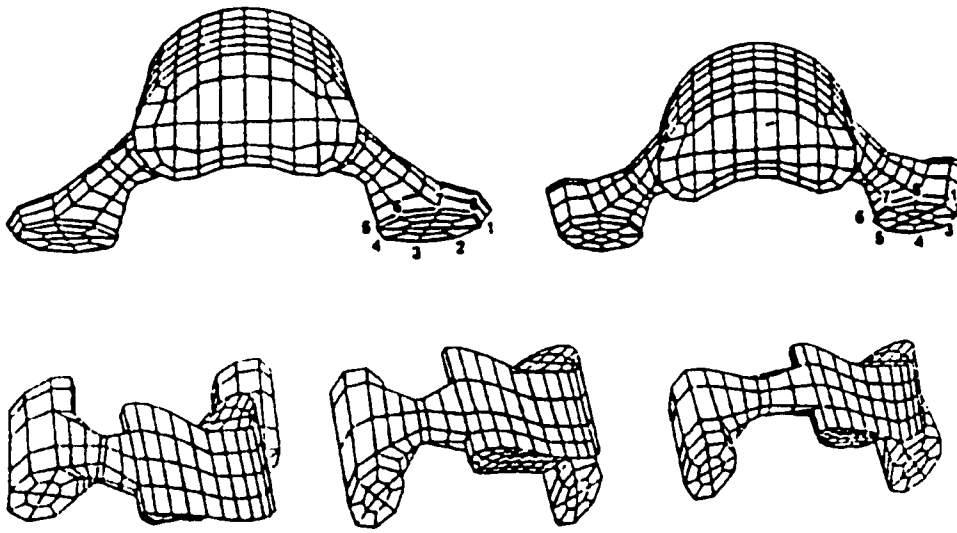

The finite element model can fit the different morphologies of vertebrae.

From Maurel N, Lavaste F, Skalli W. A Three-Dimensional Parameterized Finite Element Model of the Lower Cervical Spine. Study of the Influence of the Posterior Articular Facets. J Biomech 1997;30:921-31.

Figure 1-14: Finite Element Model of the Cervical Spine

Finite element analysis appears to be the technique of the future in three-dimensional quantitative anatomical analysis. Its applicability to current orthodontic practice is limited, however, due to its complexity and the lack of widespread use of computed tomography.

CONCLUSION

Traditionally, orthodontists and other health professionals involved in the care of paediatric patients have used the hand-wrist radiograph to assess an individual's developmental status.

Recently, the cervical spine, as seen on lateral cephalograms, has been found to be a reliable indicator of developmental status as well. However, so far, descriptions of the growth and development of the cervical vertebrae have been mostly limited to qualitative, or fairly crude, quantitative analyses.

Recent studies have achieved three-dimensional quantification of various vertebral structures. The application of this three-dimensional quantification to an analysis of growth and development of the cervical spine, as seen on lateral cephalograms, could provide an accurate, as well as reliable, skeletal age assessment method.

BIBLIOGRAPHY

1.Grave K. The use of the hand and wrist radiograph in skeletal age assessment; and why skeletal age assessment is important. Austral Orthod J 1994;13(3):196.

2.Greulich WW, Pyle SI: Radiographic atlas of skeletal development of the hand and wrist, ed 2. Palo Alto, CA, Stanford University Press, 1959.

3.Tanner JM, Whitehouse RH, Cameron N, Marshall WA, Healy M, Goldstein H: Assessment of skeletal maturity and prediction of adult height (TW2 Method), ed 2. London, Academic Press, 1983.

4.Benso L, Vannelli S, Pastorin L, Angius P, Milani S. Main Problems Associated with Bone Age and Maturity Evaluation. Horm Res 1996;45(suppl 2):42-8.

5.Gilli G. The Assessment of Skeletal Maturation. Horm Res 1996;45(suppl 2):49-52.

6.Carpenter CT, Lester EL. Skeletal Age Determination in Young Children: Analysis of Three Regions of the Hand/Wrist Film. J Pediatr Orthop 1993;13:76-9.

7.Jiménez-Castellanos J, Carmona A, Catalina-Herrera CJ, Viñuales M. Skeletal Maturation of Wrist and Hand Ossification Centers in Normal Spanish Boys and Girls: A Study Using the Greulich-Pyle Method. Acta Anat 1996;155:206-11.

8.Roche AF, Chumlea WC, Thissen D. Assessing the skeletal maturity of the hand-wrist: Fels method. Springfield, Illinois, Charles C. Thomas, 1988.

9.Fishman LS. Radiographic Evaluation of Skeletal Maturation: A Clinically Oriented Method Based on Hand-Wrist Films. Angle Orthod 1982;52:88-112.

10.Hassel B, Farman AG. Skeletal maturation evaluation using cervical vertebrae. Am J Orthod Dentofac Orthop 1995;107:58-66.

11.Hill K, Pynsent PB. A fully automated bone-ageing system. Acta Paediatr Suppl 1994; 406:81-3.

12.Cox LA. Preliminary report on the validation of a grammar-based computer system for assessing skeletal maturity with the Tanner-Whitehouse 2 method. Acta Paediatr Suppl 1994;406:84-5.

13.Drayer NM, Cox LA. Assessment of bone ages by the Tanner-Whitehouse method using a computer-aided system. Acta Paediatr Suppl 1994;406:77-80.

14.Tanner JM, Gibbons RD. A Computerized Image Analysis System for Estimating Tanner-Whitehouse 2 Bone Age. Horm Res 1994;42:282-7.

15.Van Teunenbroek A, De Waal W, Roks A, Chinafo P, Fokker M, Mulder P, De Muinck Keizer-Schrama S, Drop S. Computer-Aided Skeletal Age Scores in Healthy Children, Girls with Turner Syndrome, and in Children with Constitutionally Tall Stature. Pediatr Res 1996;39:360-7.

16.Tanner JM, Oshman D, Lindgren G, Grunbaum JA, Elsouki R, Labarthe D. Reliability and Validity of Computer-Assisted Estimates of Tanner-Whitehouse Skeletal Maturity (CASAS): Comparison with the Manual Method. Horm Res 1994;42:288-94.

17.Frisch H, Riedl S, Waldhör T. Computer-aided estimation of skeletal age and comparison with bone age evaluations by the method of Greulich-Pyle and Tanner-Whitehouse. Pediatr Radiol 1996;26:226-31.

18.Sun YN, Ko CC, Mao CW, Lin CJ. A Computer System for Skeletal Growth Measurement. Comp Biomed Res 1994;27: 2-12.

19.Rucci M, Coppini G, Nicoletti I, Cheli D, Valli G. Automatic Analysis of Hand Radiographs for the Assessment of Skeletal Age: A Subsymbolic Approach. Comp Biomed Res 1995;
28:239-56.

20.Lamparski DG. Skeletal age assessment utilizing cervical vertebrae. Master of Science Thesis, University of Pittsburgh, 1972.

21.Sherk HH, editor. The Cervical Spine, 2nd ed. The Cervical Spine Research Society, 1989.

22.Farman AG, Escobar V. Radiographic Appearance of the Cervical Vertebrae in Normal and Abnormal Development. Br J Oral Surg 1982;20:264-74.

23.Bradford DS, Hensinger RM. The Pediatric Spine. Georg Thieme Verlag, New York, 1985.

24.Fesmire FM, Luten RC. The Pediatric Cervical Spine: Developmental Anatomy and Clinical Aspects. J Emerg Med 1989;7:133-42.

25.Ogden JA. Radiology of Postnatal Skeletal Development: XI. The First Cervical Vertebra. Skeletal Radiol 1984;12:12-20.

26.Ogden JA. Radiology of Postnatal Skeletal Development: XII. The Second Cervical Vertebra. Skeletal Radiol 1984;12:169-77.

27.Swischuk LE. The Cervical Spine in Childhood. Curr Prob Diag Radiol 1984;13(5):1-26 (Sept-Oct).

28.Roche AF. The Elongation of the Human Cervical Vertebral Column. Am J Phys Anthrop 1972;36(2):221-8.

29. Schmorl G, Junghanns H. The Human Spine in Health and Disease, Second Edition. Grune & Stratton, New York, 1971.

30. Kasai T, Ikata T, Katoh S, Miyake R, Tsubo M. Growth of the Cervical Spine With Special Reference to Its Lordosis and Mobility. Spine 1996;21(18):2067-73.

31. Tulsi RS. Growth of the human vertebral column: An osteological study. Acta anat 1971;79:570-80.

32. Hellsing E. Cervical vertebral dimensions in 8-, 11-, and 15-year-old children. Acta Odontol Scand 1991;49:207-13.

33. O'Reilly MT, Yaniello GJ. Mandibular Growth Changes and Maturation of Cervical Vertebrae -- A Longitudinal Cephalometric Study. Angle Orthod 1988;58(2):179-84.

34. Huggare J. The first cervical vertebra as an indicator of mandibular growth. Eur J Orthod 1989;11:10-6.

35. Dhillon A. The correlation of cervical vertebrae maturation with hand-wrist maturation and stature increments in adolescent girls. Master of Science Thesis, University of Alberta, 1993.

36. Hassel B, Farman AG. Skeletal maturation evaluation using cervical vertebrae. Am J Orthod Dentofac Orthop 1995;107:58-66.

37. Panjabi MM, Duranceau J, Goel V, Oxland T, Takata K. Cervical Human Vertebrae: Quantitative Three-Dimensional Anatomy of the Middle and Lower Regions. Spine 1991;16(8):861-9.

38. Schaffler MB, Alson MD, Heller JG, Garfin SR. Morphology of the Dens: A Quantitative Study. Spine 1992;17(7):738-43.

39.Panjabi MM, Oxland T, Takata K, Goel V, Duranceau J, Krag M. Articular Facets of the Human Spine: Quantitative Three-Dimensional Anatomy. Spine 1993;18(10):1298-310.

40.Xu R, Nadaud MC, Ebraheim NA, Yeasting RA. Morphology of the Second Cervical Vertebra and the Posterior Projection of the C2 Pedicle Axis. Spine 1995;20(3):259-63.

41.Doherty BJ, Heggeness MH. Quantitative Anatomy of the Second Cervical Vertebra. Spine 1995;20(5):513-7.

42.Oh SH, Perin NI, Cooper PR. Quantitative Three-dimensional Anatomy of the Subaxial Cervical Spine: Implication for Anterior Spinal Surgery. Neurosurg 1996;38(6):1139-44.

43.Ebraheim NA, Xu R, Knight T, Yeasting RA. Morphometric Evaluation of Lower Cervical Pedicle and Its Projection. Spine 1997;22(1):1-6.

44.Yoganandan N, Kumaresan S, Voo L, Pintar F. Finite Element Applications in Human Cervical Spine Modeling. Spine 1996;21:1824-34.

45. Maurel N, Lavaste F, Skalli W. A Three-Dimensional Parameterized Finite Element Model of the Lower Cervical Spine. Study of the Influence of the Posterior Articular Facets. J Biomechanics 1997;30:921-31.

46. Yoganandan N, Kumaresan SC, Voo L, Pintar FA, Larson SJ. Finite element modeling of the C4-C6 cervical spine unit Spine 1996;18:569-74.

CHAPTER TWO:

Accuracy of Sculptor™ Software in Making Three-Dimensional Measurements on Cervical Vertebrae from Three Plane Film Radiographs Taken at Different Angulations

A version of this chapter has been submitted for publication. Knoefel et al. Spine.

INTRODUCTION

The ability to obtain three-dimensional data from two-dimensional plane film radiographic images could find widespread use in medicine, dentistry and related health professions. The advent of computed tomography (CT) and nuclear magnetic resonance imaging (MRI) in recent years has provided the health practitioner with the ability to obtain three-dimensional depictions of anatomical entities. However, these techniques are not sufficiently practical to demonstrate widespread usefulness. MRI's are very expensive, whereas CT's are not readily available and subject the patients to relatively high levels of radiation. Plane films are readily available for the general medical or dental practitioner, are relatively inexpensive, and submit subjects to less radiation.

The potential uses of three-dimensional description of anatomical objects are manifold. By examining the changes occurring in structures over time, degenerative processes can be studied and quantified. In the case of the human spine, diseases such as scoliosis, ankylosing spondylitis and arthritis could be better understood and represented three-dimensionally. A more thorough comprehension of growth changes in the vertebrae could lead to a growth prediction tool or a new skeletal age assessment method.

In recent years, attempts have been made to more accurately quantify human vertebral anatomy. Efforts have concentrated on creating coordinates and reference points in order to obtain three-dimensional data. Panjabi's group presented a model that utilized a specially designed morphometer[1,2] which assigned three-dimensional coordinates to various marked points on the vertebral surfaces. As a result, linear dimensions, angulations, and areas of surfaces and cross-sections of most vertebral components were calculated. Several groups[3-6] performed manual morphometric studies of the cervical

vertebrae, using digital calipers for linear distances and a goniometer for angular measurements. An indirect quantification technique was developed by Oh and coworkers[7]. Vertebrae were examined via a surgical microscope, equipped with an image-splitter and a CCD camera. Recently, numerous finite element models of the cervical spine have been proposed[8-10]. The cervical anatomy is replicated by using information from CT and cryomicrotome anatomic sections.

The purpose of this study was to determine the accuracy of a current three-dimensional measuring tool (Sculptor™ by Acuscape, Inc.), which utilizes information from radiographs to quantify three-dimensional anatomical structures. Sculptor™ was originally developed for cephalometric use, but the software can be easily adapted to other uses. For this study, it was modified in order to quantify vertebrae.

Sculptor™ utilizes photogrammetry as part of its image analysis method. In photogrammetry[11-14], selected anatomic points are "triangulated". The result of the triangulation process is a three-dimensional "swarm" of points. This swarm can be examined from any point of view. Sculptor™ allows the user to create the three-dimensional swarm of points from plane film radiographs.

Sculptor™ was developed as part of a diagnostic software system (Acuscape™ Medical Imaging System) for orthodontists. It is a digital image-processing program that sculpts a dimensionally accurate digital patient model, called a .Profile™, from standard orthodontic cephalograms. The program's accuracy is a result of the cross-calibration of images from multiple sources (e.g. radiographs and photographs). Utilizing close-range photogrammetry[11-14] and calibration techniques, Sculptor™ fuses multiple, correlated image sets into a common three-dimensional database and then creates a dimensionally accurate digital patient model (.Profile). The cross-calibration is made possible by the use of a calibration frame containing radiopaque markers, which the patient wears during both the photographic and radiographic imaging processes.

Since this study examined vertebrae, and not skulls, it was necessary to construct a different calibration frame. The frame was built entirely of leucite, to ensure its radiolucency. It consisted of four pillars held together by transverse plates (Figure 2-1). Embedded throughout the frame were sixteen 2.5-mm spherical metal pellets (beebees), which acted as radiopaque calibration markers. Parallel to the frame's long axis were two leucite rods, stabilized by a perpendicular leucite plate positioned near the centre of the frame. The rods passed through the right and left transverse foramina of each vertebra, holding it stable within the calibration frame during an imaging session.

For statistical purposes, a smaller (C3) and a larger vertebra (C6) were chosen, since it was anticipated that the significance of the measurement error would depend on the size of the specimen. Eight 1.57-mm spherical steel bearings were glued to each vertebral

body, four on the superior, and four on the inferior surface. They were distributed in such a way as to avoid superimposition of the bearings on any given radiographic view. The setup of the two vertebrae, with the bearings, is illustrated in Figure 2-1.

Figure 2- 1 Calibration Frame Containing Two Marked Vertebrae

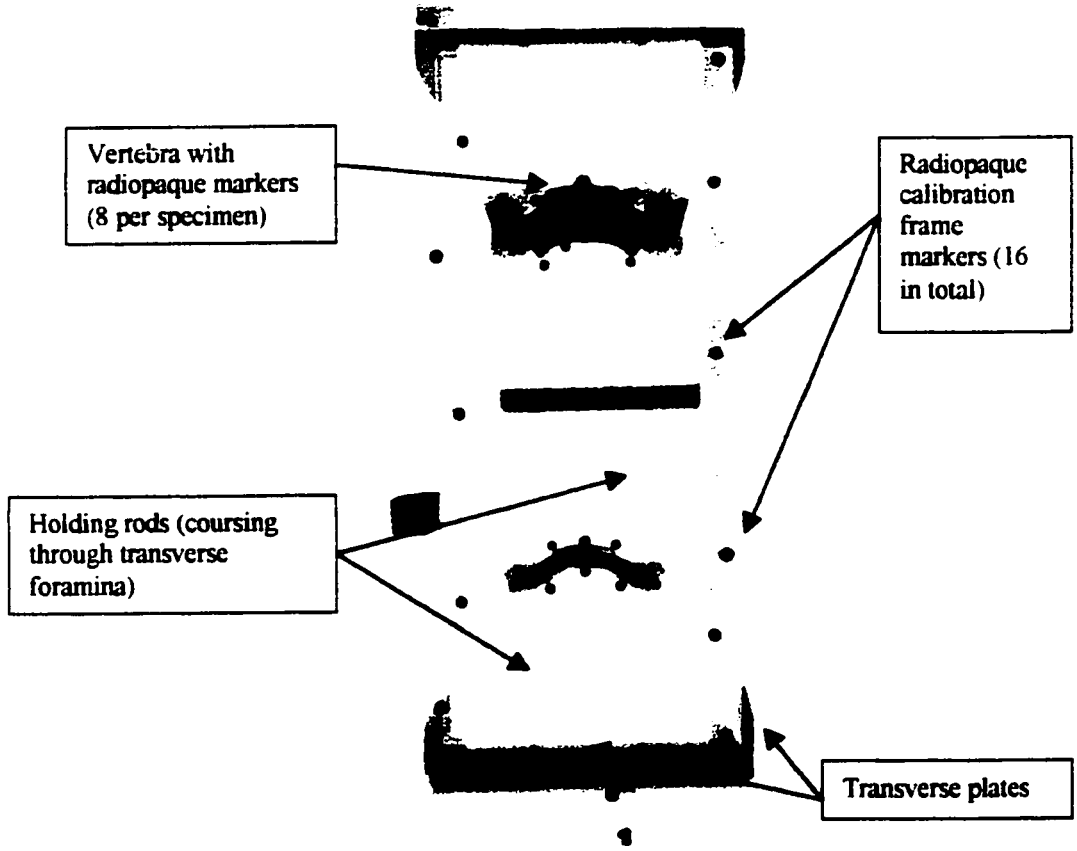

Three views of the vertebral setup were imaged, using 8" x 10" Fuji Super HR S30 film. Exposure factors were 100mA, 40 kVp and 1/60 sec. The first two views were taken at exactly 90 degrees to each other, with the calibration frame laying flat on the tabletop. The third view was taken at 180 degrees to the second view, but the frame was raised

approximately 10 degrees. The cant was achieved by attaching a leucite rod to the frame's underside, thus generating an "off-angle" effect. All three views were required by Sculptor™ to complete the image analysis process (see Figure 2-2 below).

Figure 2-2 Three Radiographic Views of Vertebra Setup

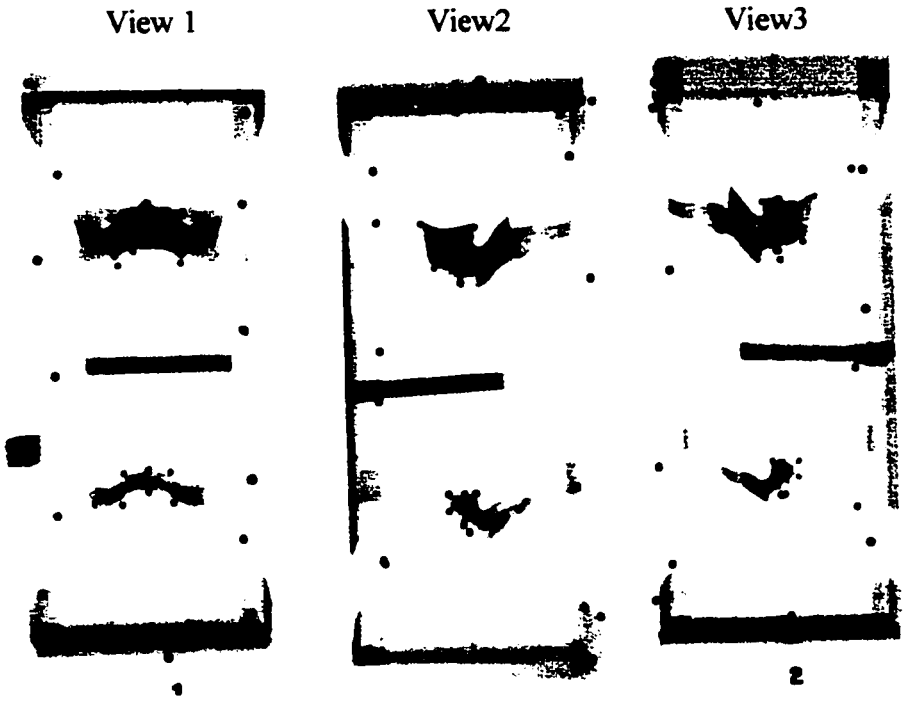

Using the target-film distance of the imaging unit (Hewlett-Packard Faxitron, Model 43855A), Sculptor™ was modified in order to take into account the magnification error of the radiographic images.

The radiographs were scanned into an IBM-compatible personal computer, using a Hewlett-Packard ScanJet scanner (resolution 150 dpi, approximately 5.9 pixels/mm) with a transparency adapter. The images were saved as JPEG's (.jpg), with a compression ratio of 15. The scanner was also calibrated to determine the precise number of pixels per millimeter in the x and y directions.

Description of Calibration and Reference Frame Setting

The ultimate goal of the Sculptor™ software is to assign a true x, y, z reference system to a patient or specimen. At the beginning of an imaging session, a reference system has been assigned to the calibration frame. Furthermore, the spatial orientation of the calibration markers (beebees) is also known. The unknowns include the patient (or specimen) and x-ray unit reference systems.

Before the calibration process begins, the reference system associated with the x-ray unit and the one associated with the calibration frame are not linked. To overcome this hurdle, the x-ray source needs to be located with 7 degrees of freedom (7 DOF) - x, y, z, yaw, pitch, roll and focal length - relative to the calibration frame. Imaging the specimen within the calibration frame, and then calibrating the image, achieves this goal. When the virtual calibration frame (i.e. the known geometry of calibration markers) is fitted to the image of the actual calibration frame, a geometric transformation of the virtual frame occurs. This transformation is the key to mathematically locating the x-ray source with 7 DOF.

The procedure is repeated for all images (i.e. all three views). At the completion of this calibration process all images have been placed into the same 3D matrix (calibration frame reference).

The reference system can then be adjusted and set to the specimen's anatomy, thus becoming specific to the latter. It will apply to all anatomical structures contained in the 3-D space that is represented. When an anatomical landmark is then located on the calibrated images from two different points of view, triangulation mathematics can be used to locate and record the landmark in x, y and z space.

Measuring Inter-Landmark Distances on the Vertebrae

Following the calibration process, Sculptor™ assigned x-, y- and z-coordinates to each of the eight radiopaque markers on the vertebrae (Figure 2-1). In order to perform the accuracy study, the distances between the centres of every possible combination of two bearings were calculated from these coordinates. Since there was a total of eight markers, and two were selected for any given distance measurement, the total number of distances was expressed by "8 choose 2", or

$$\frac{8!}{(8-2)!} = \frac{8!}{6!} = 28$$

The following formula was employed to calculate the 28 distances, where (x1, y1, z1) and (x2, y2, z2) were the coordinates of the centres of any two bearings:

$$\text{Distance} = \text{SQRT}\left[(x2-x1)^2 + (y2-y1)^2 + (z2-z1)^2\right]$$

The two vertebrae were then removed from the calibration frame, and the measurements repeated manually. Using a digital caliper accurate to one one-hundredth of a millimeter, the principal investigator repeated the 28 measurements five times for each vertebra. Since the caliper could only measure the distance from the outside of one beebee to the outside of the second beebee, the distance measured was greater than that measured by the software. In order to determine the true distance from the centre of one beebee to the centre of the other, the diameter of one beebee (1.57 mm) was subtracted from the total distance, as measured manually with the calipers (see Figure 2-3).

Figure 2-3 Determination of Inter-Beebee Distance

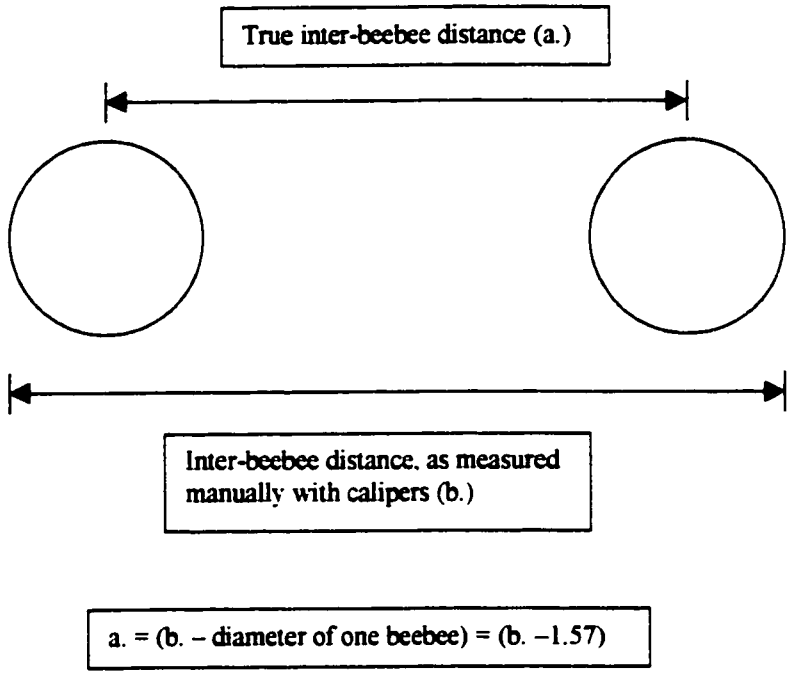

A second investigator, not involved with the study, repeated the same measurements three times. The investigators did not have access to each other's data nor to that generated by Sculptor™ when they obtained their respective measurements. Intra- and inter-investigator reliabilities were determined, and Sculptor's™ measurements compared to the manual measurements. Correlations between variables, as well as the results of paired t-tests, were obtained.

RESULTS

The caliper measurements for the five trials of investigator 1 and the three trials of investigator 2 are presented in Appendix A.

Reliability analysis results for investigator 1, for the small vertebra, are presented in Table 2-1.

Table 2-1

Intra-Rater Reliability, Investigator 1 – Small Vertebra

Trial	Corrected Item-Total Correlation	Alpha if Item Deleted
1	.9998	1.0000
2	.9999	.9999
3	.9999	.9999
4	.9999	.9999
5	.9999	.9999

Number of Measurements = 28
Number of Trials = 5

Reliability coefficient (Alpha) = 1.0000

The overall alpha reliability coefficient was 1.0000. The alpha values, if any given trial was removed, ranged from 0.9999 to 1.0000. These latter values provide a different perspective of intra-rater reliability, by verifying consistency between trials and determining if any one trial demonstrated greater error than the others.

Table 2-2 presents the mean, standard deviation, minimum, maximum and range values for all of investigator 1's measurements of the small vertebra.

Table 2-2

Investigator 1 – Caliper Measurements of Small Vertebra

Measurement	Mean	Standard Deviation	Minimum	Maximum	Range
1	11.08	.05	11.01	11.13	.12
2	16.13	.05	16.08	16.18	.10
3	8.23	.03	8.20	8.27	.07
4	11.74	.03	11.71	11.77	.06
5	12.32	.03	12.28	12.37	.09
6	19.86	.04	19.81	19.91	.10
7	11.94	.02	11.91	11.97	.06
8	9.46	.07	9.38	9.55	.17
9	10.82	.05	10.77	10.89	.12
10	19.58	.07	19.46	19.62	.16
11	12.20	.01	12.19	12.22	.03
12	18.86	.06	18.77	18.92	.15
13	17.37	.03	17.33	17.41	.08
14	12.63	.07	12.53	12.71	.18
15	20.71	.07	20.66	20.82	.16
16	11.29	.01	11.28	11.31	.03
17	12.45	.04	12.40	12.51	.11
18	15.24	.03	15.22	15.28	.06
19	16.80	.09	16.63	16.85	.22
20	14.79	.03	14.74	14.82	.08
21	18.98	.10	18.86	19.12	.26
22	12.09	.05	12.02	12.14	.12
23	11.30	.07	11.22	11.42	.20
24	16.36	.11	16.28	16.54	.26
25	8.74	.02	8.71	8.77	.06
26	9.53	.01	9.51	9.54	.03
27	10.38	.01	10.36	10.40	.04
28	11.72	.05	11.67	11.80	.13

Units: millimeters

The smallest range between measurements was 0.03 mm, the greatest was 0.26 mm. In other words, investigator 1's error ranged from 0.03 to 0.26 mm.

Table 2-3 presents the reliability results for the large vertebra, for the same investigator.

Table 2-3

Intra-Rater Reliability, Investigator 1 – Large Vertebra

Trial	Corrected Trial-Total Correlation	Alpha if Item Deleted
1	.9999	1.0000
2	.9999	1.0000
3	.9999	1.0000
4	.9999	1.0000
5	.9999	1.0000

Number of Measurements = 28
Number of Trials = 5

Reliability coefficient (Alpha) = 1.0000

The overall alpha reliability coefficient was 1.0000. The alpha coefficient if any trial was deleted remained at 1.0000.

Table 2-4 summarizes the standard deviation and range values for investigator 1's measurements of the large vertebra.

Table 2-4

Statistics for Investigator 1's Measurements, Large Vertebra

	From	To
Standard Deviations	.01	.11
Range	.02	.27

Units: millimeters

As is evident from Table 2-4, investigator 1's measurement error ranged from 0.02 mm to 0.27 mm.

Reliability analysis results for investigator 2, for both vertebrae, were very similar to those of investigator 1. The overall correlation coefficients for the small and large vertebrae were 0.9999 and 1.0000, respectively.

Table 2-5 summarizes the standard deviation and range values for investigator 2's measurements.

Table 2-5

Statistics for Investigator 2's Measurements, Both Vertebrae

	From	To
Standard Deviations, Small Vertebra	.01	.11
Standard Deviations, Large Vertebra	.01	.10
Range, Small Vertebra	.01	.19
Range, Large Vertebra	.01	.20

Units: millimeters

As is evident from Table 2-5, investigator 2's overall measurement error ranged from 0.01 mm to 0.20 mm.

Table 2-6 summarizes the descriptive statistics (mean, standard deviation, minimum and maximum difference) for absolute differences and actual differences between the two investigators' measurements. (Note: sm12dif is the absolute difference, sm_1_2 is the actual difference for the small vertebra. The equivalent variables for the large vertebra are lg12dif and lg_1_2.)

To obtain the absolute mean difference, the absolute differences for each measurement were added together, and the average determined. Results are given for the small vertebra first, followed by the large vertebra. The maximum absolute differences for the small and large vertebrae were 0.18 mm and 0.20 mm, respectively.

Table 2-6

Descriptive Statistics, Differences Between Investigators

	Mean	Standard Deviation	Minimum	Maximum
sm12dif	.0490	.0388	.0047	.1767
sm_1_2	.0359	.0516	-.0733	.1767
lg12dif	.0578	.0510	.0007	.2033
lg_1_2	.0376	.0678	-.0987	.2033

Units: millimeters

Correlations between the two investigators' measurements were very high, with values of 1.0000 for both vertebrae. The results of paired t-tests comparing the means of the two investigators' measurements are presented in Table 2-7.

Table 2-7 – Paired t-tests, Investigators 1 and 2

Pair	Paired Differences					t	Df	Sig. (2-tailed)
	Mean	Std. Dev.	Std. Error Mean	95% Confidence Interval of the Difference				
				Lower	Upper			
Av_sm_1 & Av_sm_2	.03590	.05158	.009747	.01591	.05590	3.684	27	.001
Av_lg_1 & Av_lg_2	.03757	.06784	.01282	.01127	.06388	2.931	27	.007

Units: millimeters

Although the correlation between the two investigators' data was high, the differences between their measurements were significant at the 0.05 level, for both vertebrae, due to the fact that the value "0" was not contained in the 95% confidence intervals. However, the difference was not considered to be significant clinically, since it was less than 0.1 mm on average.

The manual measurements were compared with those of the software, in order to validate the software. Since it had been established that there was no significant clinical difference between the two investigators' measurements, the Sculptor™ values were only compared with those of investigator 1. Table 2-8 summarizes the descriptive statistics (mean, standard deviation, minimum and maximum difference) for the absolute difference and the actual difference between investigator 1's measurements and the software's. (Note: sm1scdif is the absolute difference, sm_1_sc is the actual difference for the small vertebra. The equivalent variables for the large vertebra are lg1scdif and lg_1_sc.)

Table 2-8

Descriptive Statistics, Differences Between Investigator 1 and Software

	Mean	Standard Deviation	Minimum	Maximum
sm1scdif	.1170	.0828	.0069	.3023
sm_1_sc	.0587	.1322	-.3023	.2134
lg1scdif	.1451	.0891	.0032	.3327
lg_1_sc	.0845	.1496	-.3061	.3327

Units: millimeters

Correlations between the two measurement sets were very high, with values of 0.999 for both vertebrae.

The results of the paired t-tests comparing the means of investigator 1's measurements to those of the software are presented in Table 2-9.

Table 2-9 – Paired t-tests, Investigator 1 and Software

Pair	Paired Differences					t	Df	Sig. (2-tailed)
	Mean	Std. Dev.	Std. Error Mean	95% Confidence Interval of the Difference				
				Lower	Upper			
Av_sm_1 & Sc_sm	.05874	.1322	.02499	.007463	.1100	2.350	27	.026
Av_lg_1 & Sc_lg	.08450	.1496	.02827	.02650	.1425	2.989	27	.006

Units: millimeters

Although the correlation coefficients for both vertebrae were very high (0.999), the differences between their measurements were significant at the 0.05 level, for both vertebrae, due in part to the fact that the value "0" was not contained in the 95% confidence intervals. However, the difference was not considered to be significant clinically, since it was less than 0.1 mm on average.

DISCUSSION

The purpose of this study was to determine the accuracy of a current three-dimensional measuring tool, Sculptor™, by Acuscape, Inc., in its ability to quantify human vertebrae. It was originally developed for cephalometrics, but the software can be quite easily adapted to other uses. Sculptor™ utilizes photogrammetry[11-14] as part of its image analysis method, a technique which is well documented in the dental and medical literature. By definition, photogrammetry is the science of generating exact measurements by accurately mapping surface contours through the use of photographic images. Various points on an anatomical structure are plotted and connected to create three-dimensional mesh diagrams. These meshes can then be examined from any perspective. Sculptor™ allows the user to create such mesh diagrams from plane film radiographs, allowing the researcher to accurately measure and trace inner anatomic entities.

Both investigators demonstrated very high reliability in measuring the vertebrae. The measurement error of both investigators was also comparable. Whereas the error ranged from 0.02 mm to 0.27 mm for investigator 1, the range was from 0.01 to 0.20 mm for investigator 2. Inter-rater reliability was also very good, with measurements between investigators being within one-tenth of a millimeter of each other, on average. However, although the differences were minute, they still achieved statistical significance at the 0.05 level, since the value of "0" was not contained in the 95% confidence interval. Some of the observed variability between measurements could be attributed to difficulty in achieving consistent positioning of the digital calipers. Depending on the location of the beebees on the vertebra, there was a tendency for bony structures to interfere with

positioning of the calipers. Similarly, since the beebees were spherical, there was some subjectivity involved in determining whether or not the calipers were contacting the true outermost points of each pair. Any excessive amount of finger pressure would result in sliding of the calipers, and a change in the measured distance.

Errors could also have occurred during any of the stages of the image analysis process: surveying the calibration frame, determination of scanner calibration, manual calibration of the images, and mathematical calculation of image source coordinates.

The software's measurements were compared only with those of the principal investigator. Since it had already been determined that there was no significant difference between the two investigators' measurements, it was not necessary to compare the software measurements with those of investigator 2. However, strictly speaking, this simplification of the statistical analysis increased the risk of committing Type I error. In fact, by utilizing this method to determine if the null hypothesis is true (i.e. that the mean of investigator 1's measurements is equal to investigator 2's mean, which in turn is equal to that of the software), the risk of committing Type I error could theoretically be as high as threefold.

The difference between the principal investigator's and the software's measurements achieved statistical significance, since the value "0" was not contained in the 95% confidence interval. However, when the actual value of the difference was examined (0.05874 mm), it became evident that it was clinically insignificant. Table 2-6 compared absolute and average values of the differences between the two investigators' measurements. Although the means of the absolute differences were higher than the means of the average differences, as expected, they were still less than 0.1 mm, and

insignificant clinically. Table 2-8 compared the absolute and average values of the differences between investigator 1's measurements and those of the software. Again, the means of the absolute differences were higher than the means of the average differences, with values ranging between 0.1 and 0.15 mm. Still, these differences were not considered clinically significant.

The accuracy of the software, as determined in this study, is particularly astounding when one interprets it in relation to the limitations of the instruments used. Other systems, such as CT scans, require that a pixel or voxel be chosen to represent a landmark location. For example, a high quality CT scan with an 8 inch x 8 inch field of view using a 512 x 512 matrix and 1 mm slice thickness will have a voxel size of 0.4 mm x 0.4 mm x 1.0 mm. Although the actual landmark may fall inside this voxel, there is no ability to locate it with an accuracy better than one voxel. In our study, since the radiographs were scanned at approximately 5.9 pixels/mm, a typical pixel size was about 0.17 mm. Because Sculptor™ possessed an average measurement error of less than 0.1 mm, it essentially demonstrated sub-pixel accuracy. Such precision can be achieved only when measurement is based on a 3-D coordinate system, and not on image resolution.

Few quantitative accuracy studies have been performed with other modern imaging techniques, such as computed tomography and magnetic resonance imaging. In one study[15], radiologists determined tumor size measurements from CT scans, and compared them to manual measurements of the actual specimens. For tumors greater than 2 and less than 5 cm in diameter, correlation between manual and CT measurements was excellent. However, for 4 specimens less than 2 cm in diameter, all were measured by the radiologists as being at least 1.5 cm larger than the actual dimension. Other specimens

demonstrated errors up to 2.5 cm. The error was likely a consequence of the slice thickness selected in generating the CT scans. In the smaller specimens, a relatively wide slice would entail greater error in volume estimation.

The question remains whether or not Sculptor™ would demonstrate the same accuracy in analyzing curved, continuous structures, as it does for discrete points. Assuming that the curve can be clearly identified on the radiographs, the resultant trace should be as precise as individual points. However, should the outlines of the curve be ill defined, the error envelope for the software would be expected to increase proportionally.

The potential uses of accurate three-dimensional description of anatomical objects are manifold. By examining the time-related pathologic changes occurring in diseased tissues, degenerative processes can be studied and quantified. Similarly, morphological evolution of tumors and other expanding lesions could be analyzed. In the case of the human spine, diseases such as scoliosis, ankylosing spondylitis and arthritis could be better understood and represented three-dimensionally. A more thorough comprehension of growth changes in the vertebrae could potentially lead to a growth prediction tool or a new skeletal age assessment method.

CONCLUSIONS

This study has demonstrated conclusively that Sculptor™ is a precise three-dimensional measuring tool. It is able to reliably combine two-dimensional quantitative data from radiographic images of vertebrae into accurate three-dimensional information.

BIBLIOGRAPHY

1. Panjabi MM, Duranceau J, Goel V, Oxland T, Takata K. Cervical Human Vertebrae: Quantitative Three-Dimensional Anatomy of the Middle and Lower Regions. Spine 1991;16(8):861-9.

2. Panjabi MM, Oxland T, Takata K, Goel V, Duranceau J, Krag M. Articular Facets of the Human Spine: Quantitative Three-Dimensional Anatomy. Spine 1993;18(10):1298-310.

3. Schaffler MB, Alson MD, Heller JG, Garfin SR. Morphology of the Dens: A Quantitative Study. Spine 1992;17(7):738-43.

4. Doherty BJ, Heggeness MH. Quantitative Anatomy of the Second Cervical Vertebra. Spine 1995;20(5):513-7.

5. Xu R, Nadaud MC, Ebraheim NA, Yeasting RA. Morphology of the Second Cervical Vertebra and the Posterior Projection of the C2 Pedicle Axis. Spine 1995;20(3):259-63.

6. Ebraheim NA, Xu R, Knight T, Yeasting RA. Morphometric Evaluation of Lower Cervical Pedicle and Its Projection. Spine 1997;22(1):1-6.

7. Oh SH, Perin NI, Cooper PR. Quantitative Three-dimensional Anatomy of the Subaxial Cervical Spine: Implication for Anterior Spinal Surgery. Neurosurg 1996;38(6):1139-44.

8. Yoganandan N, Kumaresan S, Voo L, Pintar F. Finite Element Applications in Human Cervical Spine Modeling. Spine 1996;21:1824-34.

9. Maurel N, Lavaste F, Skalli W. A Three-Dimensional Parameterized Finite Element Model of the Lower Cervical Spine. Study of the Influence of the Posterior Articular Facets. J Biomechanics 1997;30:921-31.

10. Yoganandan N, Kumaresan SC, Voo L, Pintar FA, Larson SJ. Finite element modeling of the C4-C6 cervical spine unit Spine 1996;18:569-74.

11. Ayoub AF, Wray D, Moos KF, Siebert P, Jin J, Niblett TB, Urquhart C, Mowforth R. Three-dimensional modeling for modern diagnostic and planning in maxillofacial surgery. Int J Adult Orthod Orthog Surg 1996;11:225-33.

12. Ferrario VF, Sforza C, Puleo A, Poggio CE, Schmitz JH. Three-dimensional facial morphometry and conventional cephalometrics: a correlation study. Int J Adult Orthod Orthog Surg 1996;11:329-38.

13. Stevens WP. Reconstruction of three-dimensional anatomical landmark coordinates using video-based stereophotogrammetry. J Anat 1997;191:277-84.

14. Kakoschke D, Gabel H, Schettler D. Three-dimensional photogrammetry assessment of facial contours [German]. Mund-, Kiefer- und Gesichtschirurgie 1997;1:61-4.

15. Ballard RB, Hoffman JP, Guttman MC, Barber L, Litwin S. How accurate is size measurement of pancreas cancer masses by computed axial tomography (CT) scanning? Am Surgeon 1995;61:686-91.

CHAPTER THREE:

Age-Related Changes in C5 Vertebra Morphology in a 5 to 19 year-old sample

A version of this chapter has been submitted for publication. Knoefel et al. Spine.

INTRODUCTION

In the past two decades, attention has been focussed on the bones of the cervical spine, as seen on lateral cephalograms, to evaluate their usefulness in skeletal age prediction. Several attempts have been made at formulating a system based on which age determination can be ascertained from the cervical vertebrae. Unfortunately, the distinguishing features of each age category have so far been described on a mostly qualitative basis.

Vertical and horizontal growth of the cervical spine is such that it accelerates until approximately age 2, and then decelerates until the pubertal growth spurt, for both girls and boys. The longitudinal growth of the vertebral body takes place by means of true epiphyseal cartilage plates, similar to the longitudinal growth of long bones. The inferior surfaces of the vertebral bodies become increasingly concave with time, with a cephalocaudal progression. In addition, the bodies, as seen in profile, gradually change their morphology from an essentially trapezoidal form to an increasingly square and finally, rectangular, form[1-17].

In the 1990's, groups of researchers have examined methods of quantifying various cervical vertebrae three-dimensionally. However, all measurements were made either on actual bone material, or from radiographs of bones with their inherent magnification and distortion factors[18-24].

Recently, some authors have described the use of computer simulation to develop so-called finite element models of the cervical spine. Advantages of such simulation models lie in the fact that they are repeatable and that one can vary any parameter and quantify

the effects of that change on the final outcome. They are created using computed tomography to provide the necessary three-dimensional bony detail, and then generating an automatic mesh of the structure to be examined. The CT additionally provides accurate information about the material properties of the structure[25-27]. However, the major disadvantages of CT are that it is still not readily available and that it subjects the patient to relatively high doses of radiation. Magnetic resonance imaging (MRI) can be used for three-dimensional imaging as well, but it is even less readily available than CT and it is expensive.

The ability to obtain three-dimensional data from two-dimensional plane film radiographic images could find widespread use in medicine, dentistry and related health professions. Plane films are readily available for the general medical or dental practitioner, are relatively inexpensive, and submit subjects to minimal radiation. The decreased dose is due in part to the use of intensifying screens. The potential uses of three-dimensional description of anatomical objects are manifold. By examining the changes occurring in structures over time, degenerative processes can be studied and quantified. In the case of the human spine, diseases such as scoliosis, ankylosing spondylitis and arthritis could be better understood and represented three-dimensionally. A more thorough comprehension of growth changes in the vertebrae could potentially lead to a growth prediction tool or a new skeletal age assessment method.

The purpose of this study was to determine which morphologic characteristics of cervical vertebrae vary with growth. Using a contemporary three-dimensional imaging software program, Acuscape Sculptor™, these changes were quantified in a small sample of

human paediatric specimens, and a linear regression model was developed with the variables that demonstrated the clearest age-related changes.

Sculptor™ was originally developed for cephalometrics, but the software can be quite easily adapted to other uses. It utilizes photogrammetry[28-31] as part of its image analysis method, a technique which is well documented in the dental and medical literature. By definition, photogrammetry is the science of generating exact measurements by accurately mapping surface contours through the use of photographic images. Various points on an anatomical structure are plotted and connected to create three-dimensional mesh diagrams. These meshes can then be examined from any perspective. Sculptor™ allows the user to create such mesh diagrams from plane film radiographs, allowing the researcher to accurately measure and trace inner anatomic structures.

In this study, the software was modified in order to measure vertebrae instead of skulls. Consequently, the meshes to describe facial contours were replaced by three-dimensional traces of the superior and inferior outlines of the vertebral bodies.

MATERIALS AND METHODS

Fifty spines representing the age range of a "typical" orthodontic population were selected from the Hamann-Todd Collection at the Cleveland Museum of Natural History (One Wade Oval Drive, Cleveland, Ohio). Since it is highly unlikely that any significant orthodontic treatment will be attempted before the age of 5 years, this age was selected as the minimum. For all practical purposes, it can be assumed that the age of 19 represents the virtual completion of statural growth for both males and females.

Only the fifth cervical vertebra of each spine was examined. Since vertebrae C3 to C7 are considered to be virtually identical[33], and would therefore provide redundant data, it would only be necessary to examine one of these. The decision to choose C5 was based on the reality that often only this vertebra is clearly visible on a typical human posteroanterior cephalogram. Significant overlap from the mandible rostrally, as well as the image of the lead apron caudally, prevent adequate viewing of the remaining cervical vertebrae. Furthermore, C5 was particularly convenient since it is located exactly in the middle of the C3-C7 segment.

The Hamann-Todd Collection contained fifty specimens in the selected age bracket. There was an equal distribution of males and females. Thirty-seven of the individuals were black, and 13 white. Of the black individuals, 20 were male, and 17 were female. There were 5 white males and 8 white females. Table 3-1 summarizes the demographics of the specimens. The mean age was 14.84 years, with a standard deviation of 4.40 years. Figure 3-1 represents the age distribution graphically.

Table 3-1 – Summary of Demographic Data

	Female	Male	Total
White	8	5	13
Black	17	20	37
Total	25	25	50

Figure 3-1 – Bar Graph of Age Distribution

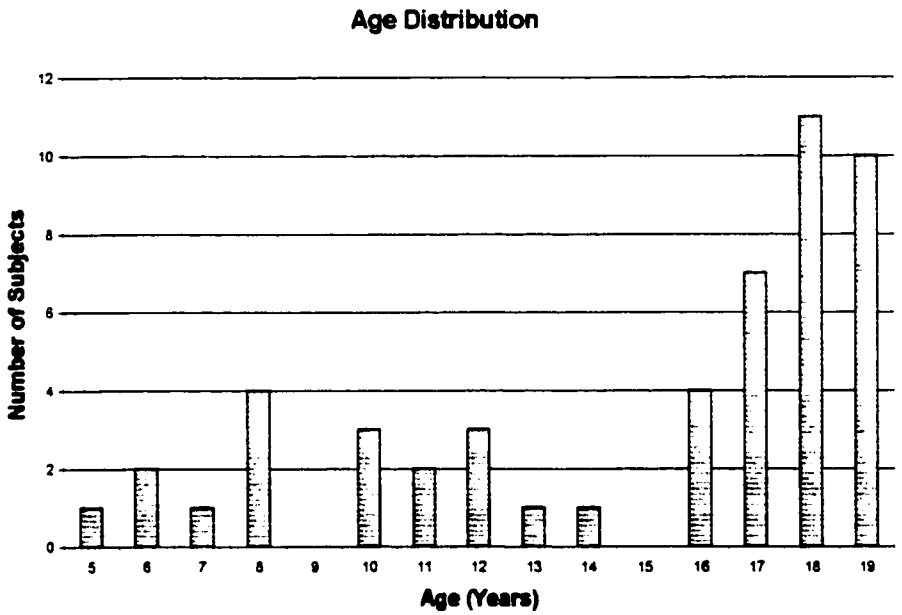

The fifth vertebra (C5) was removed from each cervical spine. Using beeswax, 0.009" stainless steel orthodontic ligature wire segments were affixed to the superior and inferior surfaces of each vertebral body. The ligature wire followed, as precisely as possible, the outline and curvature of these surfaces (Figure 3-2).

Figure 3-2 – Sample Vertebra with Wires

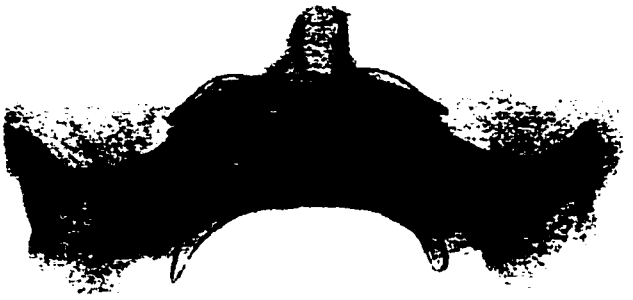

Sculptor™ was the three-dimensional software utilized in this project. Essentially, it creates the ability to generate three-dimensional outlines of anatomical structures from two-dimensional radiographs. Since it utilizes a calibration frame to remove radiographic magnification and distortion factors, it enables the user to orient all points on the outline of a specimen in 3-D space. Its accuracy in measuring distances between discrete points on vertebral bodies was established in a previous study

The radiographic calibration frame used in this study was described in detail in Chapter 2. Since four vertebrae fit into the calibration frame at any given time, twelve set-ups of four vertebrae were imaged, followed by one set-up of two (Figure 3-3).

Figure 3-3 – Calibration Frame with Two-Vertebra Setup

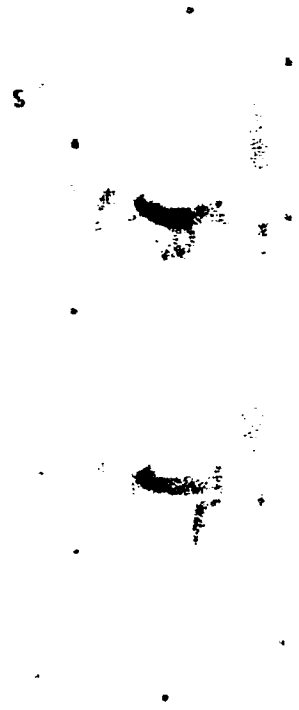

Three views of each set of four vertebrae were imaged. The first two views were taken at exactly 90 degrees to each other, with the calibration frame laying flat on the tabletop. The third view was taken at 180 degrees to the second view, but the frame was raised approximately 10 degrees. The cant was achieved by attaching a leucite rod to the frame's underside, thus generating an "off-angle" effect. All three views were required by Sculptor™ to complete the image analysis process (Figure 3-4 below).

Figure 3-4 Three Radiographic Views of Vertebral Setup

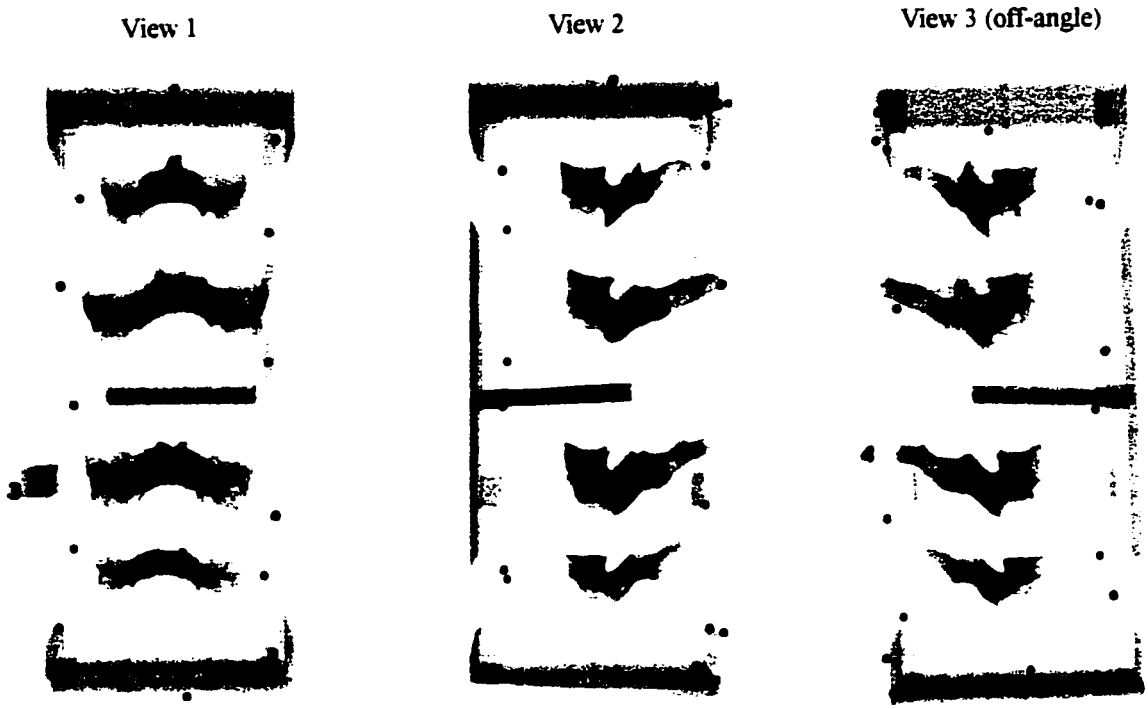

Data Generation and Analysis

The radiographs were saved as JPEGs, after having been scanned (Hewlett-Packard ScanJet, equipped with a transparency adapter) into an IBM-compatible personal computer. The images were calibrated in the same manner as those in the previous study (Chapter 2). The software was then used to generate three-dimensional traces of the superior and inferior vertebral body surfaces, as determined by the stainless steel wires (which appeared as radiopaque curves on the films) (Figure 3-5).

Figure 3-5 Sample Traces

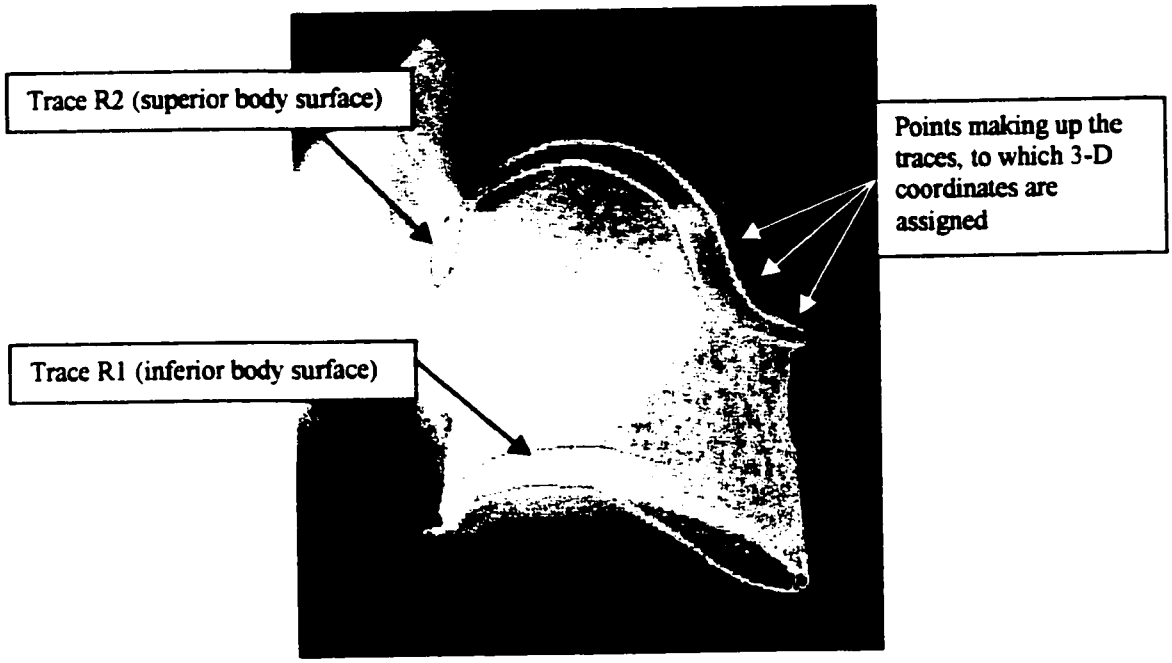

Beginning with one of the three views, the principal investigator traced the image of each stainless steel wire by clicking the left mouse button to generate successive points (30 to 60 per trace). The quantity of points generated for each trace was determined subjectively as being that which would adequately define the contour of the wire. Selecting a second view, perpendicular to the first, the same points of the first trace were matched to the new image with the help of the software. By then choosing the "triangulation" feature, all points were automatically projected onto the third view. Some manual adjustment of any point was performed as necessary to ensure that the traces closely followed the actual wires in all three views.

Once the triangulation process was completed, Sculptor™ assigned x-, y- and z-coordinates to each plotted point. For any given trace, between 30 and 60 sets of three-

dimensional coordinates were generated. The inferior and superior traces of each vertebra were labelled R1 and R2, respectively. The x-, y- and z-axes corresponded to the width, length and height of each vertebra, respectively. The origin (0,0,0) was consistently located on each calibration frame, near the centre of one of its sides.

Dimension variables were constructed from combinations of the above. The z-average difference variable (z_av_dif), corresponding to vertebral body height, was constructed by taking the absolute difference between the mean z values of traces R1 and R2 for each vertebra (Figure 3-6). The z-average difference variable squared (z_av_di2) and cubed (z_av_di3) corresponded to the square and to the cube of z_av_dif, respectively. Since many of the vertebrae were significantly tilted, either forward or backward, in the sagittal plane, the z-maximum and z-minimum values demonstrated an inaccurate representation of reality. Therefore, four "new" z values were determined for each trace: two corresponding to the greatest and least x-values (to obtain an average z-maximum value) and two corresponding to the greatest and least y values (to obtain an average z-minimum value). The z-minimum average difference (z_minav_dif) and z-maximum average difference (z_max_df) variables were calculated by subtracting the average R1 and R2 z-minimum values (z_minav2 - z_minav1) and the average R1 and R2 z-maximum values (z_maxav2 - zmaxav1) for a given vertebral body. Maximum height (max_height) was determined by subtracting the z-minimum average of trace 1 from the z-maximum average of trace 2 (z_maxav2 – zminav1). Conversely, minimum height (min_height) was determined by subtracting the z-maximum average of trace 1 from the z-minimum average of trace 2 (z_minav2 – zminav1). Width (width1 and width2) and length (length1 and length2) variables were generated by subtracting x-minimum (x_min) values from x-

maximum values (x_max), and y-minimum (y_min) from y-maximum (y_max) values, respectively (Figure 3-6).

Figure 3-6 Length, Width and Height Measurements[a]

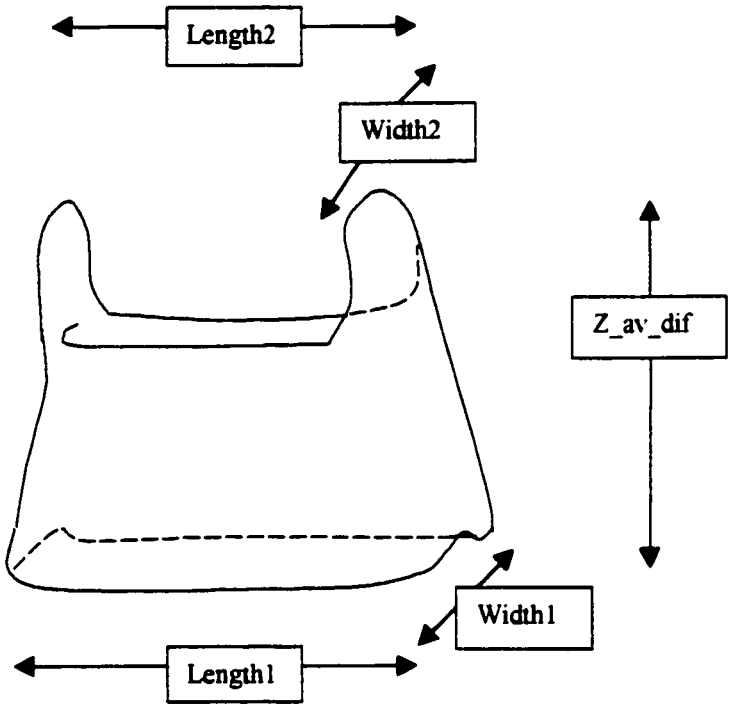

[a]For the sake of clarity, only one height variable was included in this figure. Z_av_dif was selected because it proved to be the most powerful predictor of age in the linear regression model.

Various slope values were calculated for both frontal and lateral aspects of each trace, in order to quantify the increasing depth of the superior and inferior vertebral surfaces. As seen in the following diagram, a total of six slope variables were examined.

Figure 3-7 Slope Measurements

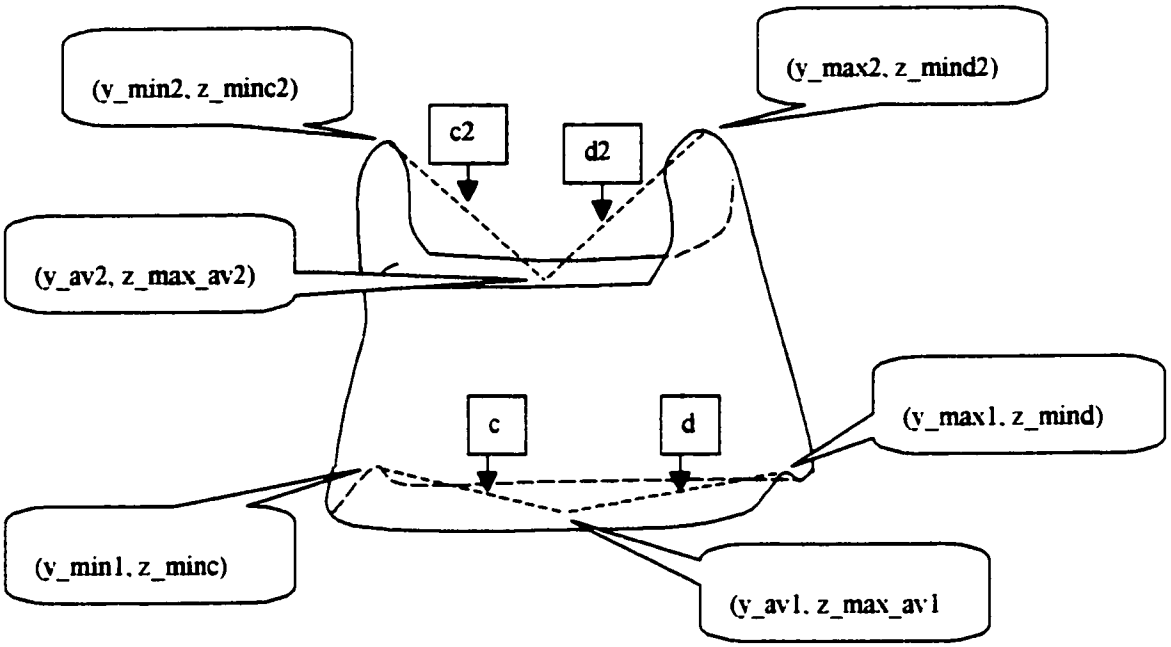

FRONTAL VIEW

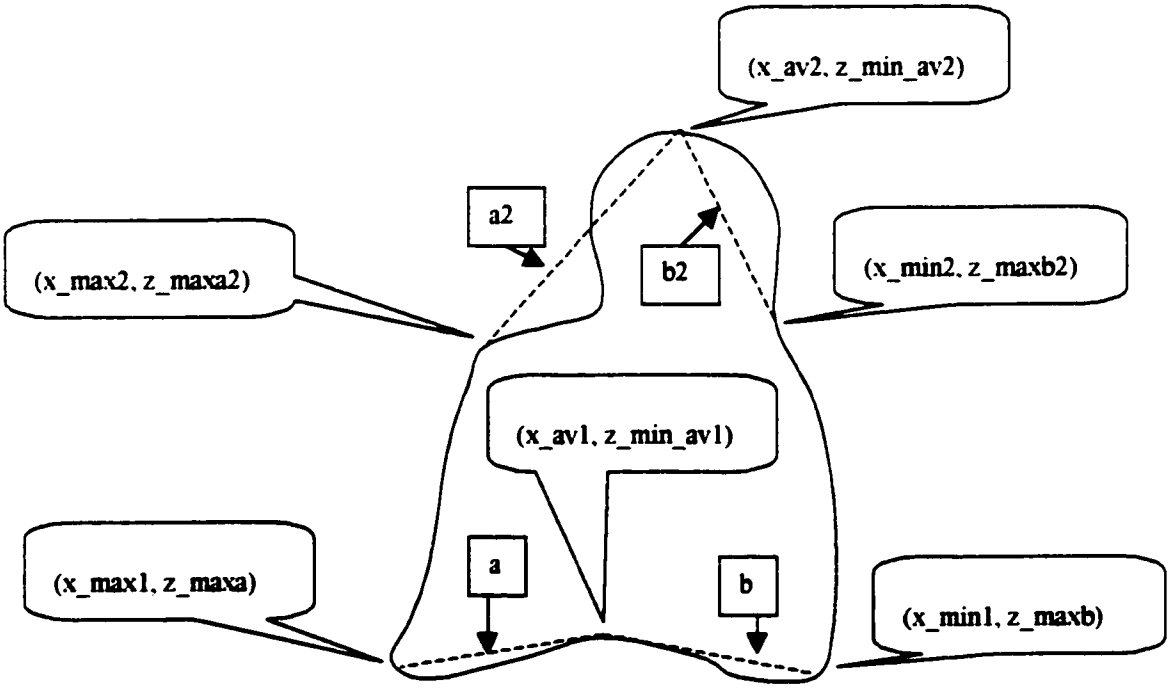

LATERAL VIEW

The four slope variables generated for R1 were labelled as slope_a, slope_b, slope_c and slope_d. The two additional slope variables, slope_ab and slope_cd, represented the averages of slope_a and slope_b, and of slope_c and slope_d, respectively. The variables slope_a2, slope_b2, slope_c2, slope_d2, slope_ab2 and slope_cd2 were the R2 equivalents of the aforementioned variables. The slope values were determined by the following formula:

$$Slope = \frac{Y2 - Y1}{X2 - X1}$$

where the coordinates of the two points are (*X1, Y1*) and (*X2, Y2*). The actual coordinates of the points generating the slope values are included in Figure 3-7 above. For example, to calculate slope_a, the following variables were substituted in the above formula:

$$slope\_a = \frac{(z\_min\_av1 - z\_max\_a)}{(x\_av1 - x\_max1)}$$

Volume variables (volume1 and volume2) were calculated as well. To quantify changes within the superior and inferior surfaces of the vertebral body, both surfaces were described as consisting of symmetric wedges. For the inferior surface, the following model was proposed (Figure 3-8).

Figure 3-8 Volume1 Wedge Model

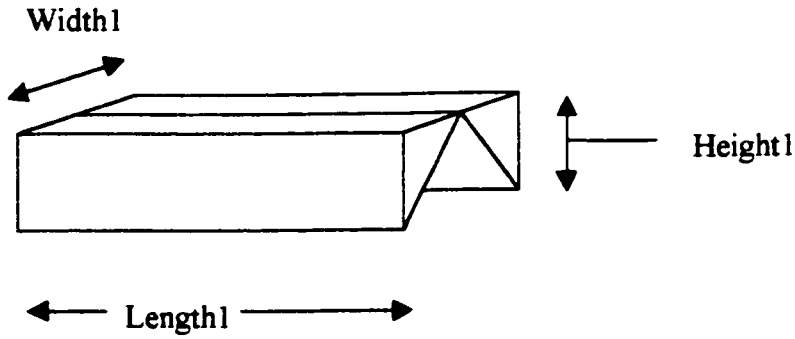

The base of one wedge corresponded to one-half the anteroposterior width of the vertebral body (width1), whereas the length corresponded to the full left to right length of the body (length1). Height was determined by taking the average z-coordinate at the base of the wedge (z_min_av1), and subtracting it from the average z-coordinate at the tip (z_max_av1). Knowing the length, width and height of each wedge, the volume was calculated.

In a similar manner to the inferior surface, the superior surface was also described as two mutually opposed wedges (Figure 3-9). However, this time, the base of each wedge was one-half the vertebral body length (length2), with the depth corresponding to the body width (width2). The height was determined in a similar manner to that of the inferior surface, by subtracting the average z-coordinate at the base of the wedge (z_max_av2) from that at the tip (z_min_av2).

Figure 3-9 Volume2 Wedge Model

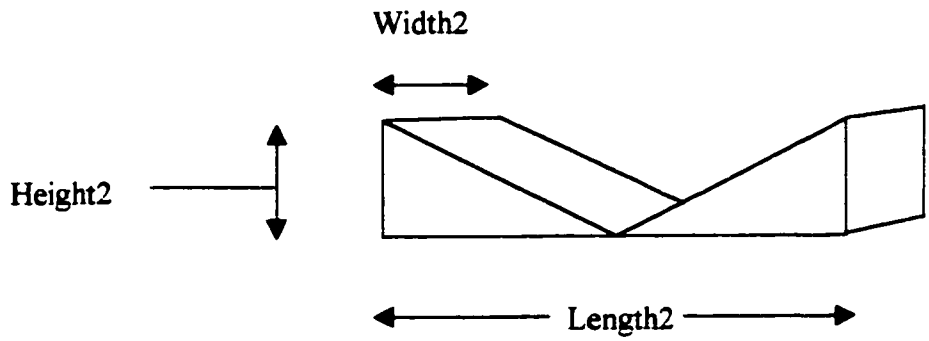

Linear regressions were performed with all of the above variables after the sample was separated into males and females. Dependent variables were age of the patient in years, and age-log, corresponding to the natural logarithm of the age. This latter variable was chosen for statistical purposes to create a somewhat more continuous scale. Since specimen age was only available to the nearest year, this variable would otherwise have been non-continuous. R-squared values were determined, and several age prediction models tested. Actual and predicted chronological age values were compared for each patient and the standard errors of prediction determined.

An example of the actual x-, y- and z-coordinates for the points in a sample trace (R1), as generated by the software, is illustrated in Appendix C.

The values of the vertical dimension ("height") variables for each vertebral body [z-average difference (z_av_dif), z-average difference squared (z_av_di2), z-average difference cubed (z_av_di3), z-minimum average difference (zminavdf), z-maximum average difference (zmaxavdf), maximum height (max_hght) and minimum height (min_hght)] are contained in Appendix D.

The values of the horizontal dimension variables for traces R1 (length1 and width1) and R2 (length2 and width2) of each vertebral body are contained in Appendix E.

The various slope values that were calculated for traces 1 and 2 of each specimen are contained in Appendix F.

A summary of the volume values for the superior and inferior vertebral surfaces (volume1 and volume2, respectively) is contained in Appendix G.

Table 3-2 presents the variables most predictive of age, with their corresponding adjusted R-squared values. The R-squared values are those obtained from individual linear regressions between the variables and age_log. Data will not be presented for other variables which, although expected to significantly contribute to age prediction, did in fact not.

Table 3-2 – Most Predictive Variables

Variable	R-sq, Females	R-sq, Males
Z_av_dif	**0.833**	**0.648**
Z_av_di2	**0.785**	**0.573**
Volume1	**0.600**	**0.544**
Vol1_sq	**0.367**	**0.326**
Volume2	**0.542**	**0.400**
Vol2_sq	**0.435**	**0.182**

The most predictive variables were height (in the form of z_av_dif), volume1 and volume2, along with the squares of their values.

Linear regressions were performed with all of the preceding variables (vertical dimensions, horizontal dimensions, slopes and volumes) using age_log as the dependent variable, to create an age prediction model.

The model was described mathematically as follows:

$$\textit{Log [predicted age (female)]} = \underset{(0.665)}{-0.909} + \underset{(0.182)}{0.737}(z\_av\_dif) - \underset{(0.010)}{0.03236}(z\_av\_di2) + \underset{(0.002)}{0.001103}(volume1)$$

$$\underset{(0.000)}{-2.807 \times 10^{-7}}(vol1\_sq) - \underset{(0.002)}{0.003338}(volume2) + \underset{(0.000)}{4.089 \times 10^{-6}}(vol2\_sq)$$

$$\textit{Log [predicted age (male)]} = \underset{(0.920)}{-0.315} + \underset{(0.212)}{0.353}(z\_av\_dif) - \underset{(0.009)}{0.01651}(z\_av\_di2) + \underset{(0.003)}{0.003450}(volume1)$$

$$\underset{(0.000)}{-5.280 \times 10^{-6}}(vol1\_sq) + \underset{(0.001)}{0.002572}(volume2) - \underset{(0.000)}{1.703 \times 10^{-6}}(vol2\_sq)$$

To obtain actual age, the above equations were rewritten:

$$\textit{Predicted age (female)} = [-0.909 + 0.737(z\_av\_dif) - 0.03236(z\_av\_di2) + 0.001103(volume1) - 2.807 \times 10^{-7}(vol1\_sq) - 0.003338(volume2) + 4.089 \times 10^{-6}(vol2\_sq)]^e$$

$$\textit{Predicted age (male)} = [-0.315 + 0.353(z\_av\_dif) - 0.01651(z\_av\_di2) + 0.003450(volume1) - 5.280 \times 10^{-6}(vol1\_sq) + 0.002572(volume2) - 1.703 \times 10^{-6}(vol2\_sq)]^e$$

For the sake of clarity, only those variables that contributed significantly to age prediction were included. Neither the slope variables nor the length and width variables contributed significantly. The results of regression with these rejected variables are contained in Appendix H.

Table 3-3 presents the R-squared values for the overall model.

Table 3-3 – "Enter" Linear Regression Model

Model Summary[c]

SEX	Model	R	R Square	Adjusted R Square	Std. Error of the Estimate
f	1	.953[a]	.908	.877	.1418
m	1	.954[b]	.909	.879	.1115

a. Predictors: (Constant), VOL2_SQ, VOL1_SQ, Z_AV_DIF, VOLUME1, VOLUME2, Z_AV_DI2

b. Predictors: (Constant), VOL2_SQ, Z_AV_DIF, VOL1_SQ, VOLUME2, VOLUME1, Z_AV_DI2

c. Dependent Variable: AGE_LOG

For the female model, the variables z_av_dif and z_av_di2 were the most predictive of age, and demonstrated the highest significance ($p = 0.001$ and $p=0.005$, respectively). At the 10% level, volume2 and vol2_sq also demonstrated significance. For the male model, however, no variables demonstrated significance at the 5% level, and only z_av_di2 and volume2 were significant at the 10% level. Nonetheless, all six variables were kept for the male and female regression models.

The linear regression model was then used to predict specimen age. Tables 3-4a and 3-4b list the true and calculated ages (trueage and calcage, resp.) followed by the age difference (age_diff). The average difference between predicted and true age was 1.22 years (S.D. = 0.86 years) for females, and 0.81 years (S.D.= 1.09) for males. The minimum differences were 0 years for both sexes, but the maximum difference was 3 years for females, and 4 years for males.

Tables 3-4a and 3-4b

True and Predicted Age Comparison

		TRUEAGE	CALCAGE	AGE_DIFF
1		18	17	1
2		16	16	0
3		11	10	1
4		16	17	1
5		6	7	1
6		12	12	0
7		8	10	2
8		17	15	2
9		5	6	1
10		8	7	1
11		16	17	1
12		19	18	1
13		12	14	2
14		19	20	1
15		18	16	2
16		17	18	1
17		12	14	2
18		19	18	1
19		7	7	0
20		19	16	3
21		8	8	0
22		13	10	3
23		14	17	3
24		19	18	1
25		17	16	1
Total	Mean	13.84	13.76	1.22
	Std. Deviation	4.65	4.42	.86
	Minimum	5	6	0
	Maximum	19	20	3

a. SEX = f

True and Predicted Age Comparison[a]

		TRUEAGE	CALCAGE	AGE_DIFF
1		19	18	1
2		18	18	0
3		19	19	0
4		11	11	0
5		18	19	1
6		17	18	1
7		19	19	0
8		18	18	0
9		18	18	0
10		10	13	3
11		18	18	0
12		19	18	1
13		18	18	0
14		18	20	2
15		10	10	0
16		17	13	4
17		10	10	0
18		17	17	0
19		6	6	0
20		8	9	1
21		18	18	0
22		19	17	2
23		16	17	1
24		18	17	1
25		17	17	0
Total	Mean	15.84	15.79	.81
	Std. Deviation	3.99	3.85	1.09
	Minimum	6	6	0
	Maximum	19	20	4

a. SEX = m

Although the mean difference between predicted age and actual age was slightly less for the male specimens, the overall greatest error (4 years) occurred for a male vertebra.

Since the length and width values were used to calculate volume1 and volume2, they are highly correlated with the latter (see Tables 3-5a and 3-5b). Consequently, they were omitted from the age prediction model. The length and width variables are also correlated with each other (see Tables 3-5a and 3-5b).

Table 3-5a – Pearson Correlations Between Length, Width and Volume Variables

Trace 1

	Width 1	Volume 1
Length 1	.650	.669
Volume1	.840	

Table 3-5b – Pearson Correlations Between Length, Width and Volume Variables

Trace 2

	Width 2	Volume 2
Length 2	.597	.699
Volume 2	.864	

DISCUSSION

The sample size was limited by the number of specimens available. Thus, fifty C5s were examined, representing the age range from 5 to 19 years. The racial distribution was uneven, with a majority (74%) of the specimens being of blacks, and the rest (26%) being of whites. According to Schaffler's group[19], it is unlikely that the mix of racial origins would have significantly affected the data analysis. Examining the second cervical vertebrae of 120 cadavers from the Hamann-Todd collection, they found that other than for dens height (11% greater in whites than blacks), there were no racial differences for any other dimensions. As a result of this observation, Schaffler combined the black and white specimens, choosing only to pool the data into male and female groups.

The majority of the specimens in this study succumbed to tuberculosis and other pulmonary diseases (Appendix A). Most of the causes of death were not expected to have significantly altered the vertebral growth of the individuals. Although tuberculosis has been found to affect skeletal growth, its effect on the cervical spine is minimal[10]. Less than 2% of cases involve the cervical spine, with the vast majority affecting the lower thoracic, lumbar and sacral vertebrae. One of the individuals died of juvenile rheumatoid arthritis (JRA), a disease that may affect the cervical spine. Occasionally, subluxation of the atlantoaxial joint will occur, but the effect of JRA on actual vertebral growth appears to be minimal[33].

Precise, descriptive, quantitative studies of human vertebrae have so far mostly been produced by direct manual measurement of specimens[21,22,24]. Exceptions were investigations led by Panjabi[18,20]. Having obtained vertebrae from adult autopsy

specimens, these investigators placed two pointed metal rods into each vertebral body to establish a local three-dimensional coordinate system. Using a specially designed morphometer, various points on each vertebra were marked and assigned x, y and z coordinates. In a similar fashion to our investigation, the superior and inferior vertebral body surfaces were traced by connecting marked points. The number of points was chosen such that the surface geometry was defined reasonably well by the straight lines joining the adjacent points. Numerous linear, angular, and area dimensions were calculated, and the measurement technique validated. Although the establishment of a coordinate system was a similarity between this study and ours, a significant difference occurred in that it required the insertion of metal rods into the vertebrae to create the coordinate system. Thus, this model could only be utilized on dead specimens. In our study, the coordinate system was exterior, being determined by the externally located calibration frame. This system could, therefore, be potentially used in live studies.

No previous publication has combined information from lateral and frontal radiographs to generate three-dimensional vertebral data. Some radiographic studies [1,6,7,9,10,13-17] have been performed, but these have examined only two-dimensional views. Although some were quantitative, the measurement techniques employed were not validated.

Oh's group performed a non-invasive, indirect measurement study, using real-time video analysis[23]. Fifty disarticulated vertebrae were imaged using a Zeiss microscope equipped with an image splitter and a Sony CCD camera. Information was transferred to an IBM personal computer-based image analysis system. The images were calibrated using horizontally and vertically oriented rulers, placed at the focal depth. No validation study was performed to confirm the precision of the calibrated measurements. The software

employed in our study to quantify the radiographic images (Sculptor™, by Acuscape, Inc.) was validated in a previous investigation (Chapter 2), and was found to be accurate within 0.1 mm. In Oh's study, precise orientation of the specimens in relation to the camera was not described. Such information is vital, since vertical and anteroposterior measurements are both affected by forward or backward tilting of the specimens. This difficulty was also encountered in our study, since it was not possible to orient all vertebrae identically within the calibration frame. For the vertical measurements, however, the data were interpreted in such a way as to minimize the effect of tilt. Specifically, instead of measuring the difference between the maximum or minimum z-coordinates of trace 1 and trace 2 to determine vertebral body height (both of which would be a function of tilt), the difference between the average z-coordinate values was taken (z_av_dif, or z_av from trace 2 subtracted from z_av from trace 1). Thus the effect of the tilting was minimized, since average, not absolute, z values were taken.

Lamparski[1] was the first investigator to evaluate the reliability of cervical vertebrae as maturation indicators, using the Greulich and Pyle atlas method as the gold standard. Dhillon[16] repeated his study on a sample of adolescent females, correlating statural height with the GP and vertebral methods. Both found that there was a high correlation between hand-wrist and vertebral ages. However, in both studies, analysis of the cervical vertebrae was based solely on information from lateral radiographs. No dimensions of the vertebrae were actually measured. Rather, cervical age was determined subjectively by inspection of vertebral body shape changes. In particular, Lamparski observed the increasing concavity of the inferior surfaces with time, and the gradual increase in vertical dimension of the body. Our study attempted to quantify these changes. To illustrate the

concavity of the inferior surface of the vertebrae, the surface itself was described as two identical, mutually opposed wedges (Figure 3-8). Thus, as the "concavity" of the inferior vertebral body would increase with time, the volume of the wedge would increase accordingly. This increase in concavity was confirmed by our data, as we demonstrated a steady increase in volume over time.

In addition to Dhillon's observations of increasing inferior surface concavity, there was a similar increase in concavity of the superior surface. The superior surface of each vertebral body was virtually flat at birth, but its lateral margins became raised with time to give it a shovel or saddle-shaped appearance. This growth change was quantified using volume2 (Figure 3-9). In a similar manner to volume1, the surface was described as two mutually opposed wedges. Again, our data confirmed the increase in saddle depth quantitatively, by demonstrating high correlation between the volume variables and the logarithm of age.

As an alternative to volume measurements, slope values were also examined. Specifically, it was expected that the slope of the hypotenuse in the "wedge model" would increase with age as well, a reflection of the increased curvature of both the superior and inferior vertebral surfaces. However, given the small sample size and the cross-sectional nature of the sample, such a trend could not be clearly demonstrated. An added complication was the reality that slope is dependent both on height and width measurements. Consequently, two vertebral body surfaces of different sizes could possess the same slope values, if the ratio of the "rise" over the "run" of the two surfaces was the same. These factors combined resulted in the low adjusted R-squared values (Appendix H). It is anticipated that a longitudinal sample would have demonstrated clear increases in

slope values over time, since the continuously increasing curvature of the surfaces would not have been masked by differently sized vertebrae from multiple individuals.

Dhillon[16] also observed the height increase of the vertebrae with age. As explained previously, the height variable used in this study was z-average difference (z_av_dif). There was an age-related change in z_av_dif, demonstrated statistically by the high adjusted R-squared values of 0.648 for males, and 0.833 for females, respectively. Similarly high values (0.573 and 0.785, respectively) were obtained for z_av_di2, the square of z_av_div. In fact, of all the variables tested, z_av_dif was the most predictive of age. A longitudinal study would have been able to demonstrate whether or not an adolescent growth spurt in vertebral height occurs. This study was not able to demonstrate such a spurt, likely due to its cross-sectional nature and its limited sample size. Width and length were omitted from the actual growth model as discrete variables, since their information is contained *de facto* within the volume variables. However, taken individually, these variables were quite strong in predicting age. Appendix H illustrates the adjusted R-squared values for length1, length2, width1 and width2. Evidently, there appeared to be a fairly strong relationship between vertebral body length, width and age, an observation not previously noted in the literature.

The age prediction model developed in the present study consisted of 6 variables (z_av_dif, z_av_di2, volume1, vol1_sq, volume2 and vol2sq) and a constant. Although z_av_dif, volume1 and volume2 were the most predictive variables of age, the linear regression model would have been incomplete without using the squares of the above variables as well, namely z_av_di2, vol1_sq and vol2_sq. An exclusively linear model would have implied incorrectly that all variables increased indefinitely with age. In order

to ensure that the variables gradually plateaud at adulthood, the squares of the variables were included as well. Given the high R-squared values of 0.877 for females and 0.879 for males, the regression model proved quite powerful in predicting age_log.

All six variables were utilized in the linear regression model, even though there were significant gender differences in R-squared values for some of them. Since there would be no sound biological reason to justify these differences, the variables were kept. It was assumed, again, that a longitudinal sample would not demonstrate such significant gender differences.

Tables 3-4a and 3-4b compare the actual and predicted patient ages. The mean difference between the two variables was approximately one year for both sexes (1.22 years for females, S.D. = 0.86 years; 0.81 years for males, S.D. = 1.09 years). Thus, it can be concluded that, in general, the proposed model was fair to good in predicting age. The maximum difference between actual and predicted age occurred for a male specimen. Whereas the predicted age of the specimen was 13 years, the actual age was 17. The origin of the error may not have resided in the regression model itself, but in specific dimensional characteristics of the specimen. For example, a vertebra from a small individual would be erroneously interpreted as belonging to a younger one. It can be argued that the value of comparing predicted age with chronological age is purely academic, since chronological age is not necessarily a reflection of skeletal age. A longitudinal study comparing cervical vertebra size and shape to craniofacial development is necessary to produce a valid assessment of the predictive value of this model. The results of this study were very promising and justify a longitudinal prospective one.

CONCLUSIONS

The purpose of this study was to correlate growth changes of the fifth cervical vertebra body with age. The variables most predictive of age were average vertebral body height, volume of the superior surface curvature, and volume of the inferior surface curvature. An age prediction model was proposed, employing the above variables. It was tested, and actual and predicted specimen ages compared. In general, the proposed model appears promising in predicting growth staging.

BIBLIOGRAPHY

1. Lamparski DG. Skeletal age assessment utilizing cervical vertebrae. Master of Science Thesis, University of Pittsburgh, 1972.

2. Sherk HH, editor. The Cervical Spine, 2nd ed. The Cervical Spine Research Society, 1989.

3. Farman AG, Escobar V. Radiographic Appearance of the Cervical Vertebrae in Normal and Abnormal Development. Br J Oral Surg 1982;20:264-74.

4. Bradford DS, Hensinger RM. The Pediatric Spine. Georg Thieme Verlag, New York, 1985.

5. Fesmire FM, Luten RC. The Pediatric Cervical Spine: Developmental Anatomy and Clinical Aspects. J Emerg Med 1989;7:133-42.

6. Ogden JA. Radiology of Postnatal Skeletal Development: XI. The First Cervical Vertebra. Skeletal Radiol 1984;12:12-20.

7. Ogden JA. Radiology of Postnatal Skeletal Development: XII. The Second Cervical Vertebra. Skeletal Radiol 1984;12:169-77.

8. Swischuk LE. The Cervical Spine in Childhood. Curr Prob Diag Radiol 1984;13(5):1-26 (Sept-Oct).

9. Roche AF. The Elongation of the Human Cervical Vertebral Column. Am J Phys Anthrop 1972;36(2):221-8.

10. Schmorl G, Junghanns H. The Human Spine in Health and Disease, Second Edition. Grune & Stratton, New York, 1971.

11. Kasai T, Ikata T, Katoh S, Miyake R, Tsubo M. Growth of the Cervical Spine With Special Reference to Its Lordosis and Mobility. Spine 1996;21(18):2067-73.

12. Tulsi RS. Growth of the human vertebral column: An osteological study. Acta anat 1971;79:570-80.

13. Hellsing E. Cervical vertebral dimensions in 8-, 11-, and 15-year-old children. Acta Odontol Scand 1991;49:207-13.

14. O'Reilly MT, Yaniello GJ. Mandibular Growth Changes and Maturation of Cervical Vertebrae -- A Longitudinal Cephalometric Study. Angle Orthod 1988;58(2):179-84.

15. Huggare J. The first cervical vertebra as an indicator of mandibular growth. Eur J Orthod 1989;11:10-6.

16. Dhillon A. The correlation of cervical vertebrae maturation with hand-wrist maturation and stature increments in adolescent girls. Master of Science Thesis, University of Alberta, 1993.

17. Hassel B, Farman AG. Skeletal maturation evaluation using cervical vertebrae. Am J Orthod Dentofac Orthop 1995;107:58-66.

18. Panjabi MM, Duranceau J, Goel V, Oxland T, Takata K. Cervical Human Vertebrae: Quantitative Three-Dimensional Anatomy of the Middle and Lower Regions. Spine 1991;16(8):861-9.

19. Schaffler MB, Alson MD, Heller JG, Garfin SR. Morphology of the Dens: A Quantitative Study. Spine 1992;17(7):738-43.

20. Panjabi MM, Oxland T, Takata K, Goel V, Duranceau J, Krag M. Articular Facets of the Human Spine: Quantitative Three-Dimensional Anatomy. Spine 1993;18(10):1298-310.

21. Xu R, Nadaud MC, Ebraheim NA, Yeasting RA. Morphology of the Second Cervical Vertebra and the Posterior Projection of the C2 Pedicle Axis. Spine 1995;20(3):259-63.

22. Doherty BJ, Heggeness MH. Quantitative Anatomy of the Second Cervical Vertebra. Spine 1995;20(5):513-7.

23. Oh SH, Perin NI, Cooper PR. Quantitative Three-dimensional Anatomy of the Subaxial Cervical Spine: Implication for Anterior Spinal Surgery. Neurosurg 1996;38(6):1139-44.

24. Ebraheim NA, Xu R, Knight T, Yeasting RA. Morphometric Evaluation of Lower Cervical Pedicle and Its Projection. Spine 1997;22(1):1-6.

25. Yoganandan N, Kumaresan S, Voo L, Pintar F. Finite Element Applications in Human Cervical Spine Modeling. Spine 1996;21:1824-34.

26. Maurel N, Lavaste F, Skalli W. A Three-Dimensional Parameterized Finite Element Model of the Lower Cervical Spine. Study of the Influence of the Posterior Articular Facets. J Biomechanics 1997;30:921-31.

27. Yoganandan N, Kumaresan SC, Voo L, Pintar FA, Larson SJ. Finite element modeling of the C4-C6 cervical spine unit Spine 1996;18:569-74.

28. Ayoub AF, Wray D, Moos KF, Siebert P, Jin J, Niblett TB, Urquhart C, Mowforth R. Three-dimensional modeling for modern diagnostic and planning in maxillofacial surgery. Int J Adult Orthod Orthog Surg 1996;11:225-33.

29. Ferrario VF, Sforza C, Puleo A, Poggio CE, Schmitz JH. Three-dimensional facial morphometry and conventional cephalometrics: a correlation study. Int J Adult Orthod Orthog Surg 1996;11:329-38.

30. Stevens WP. Reconstruction of three-dimensional anatomical landmark coordinates using video-based stereophotogrammetry. J Anat 1997;191:277-84.

31. Kakoschke D, Gabel H, Schettler D. Three-dimensional photogrammetry assessment of facial contours [German]. Mund-, Kiefer- und Gesichtschirurgie 1997;1:61-4.

32. Sherk HH, editor. The Cervical Spine, 2nd ed. The Cervical Spine Research Society, 1989.

33. Rose LF, Kaye D. Internal Medicine for Dentistry, 2nd Edition. Mosby, 1990, 37-41.

CHAPTER FOUR: GENERAL DISCUSSION AND CONCLUSIONS

The first part of this investigation concerned itself with the accuracy of a three-dimensional measuring tool, Sculptor™, from Acuscape, Inc. The second part correlated growth features of human fifth cervical vertebrae with age, utilizing the validated tool. Acuscape, Inc. originally developed Sculptor™ as a three-dimensional cephalometric measuring tool[1]. A calibration frame, containing radiopaque markers, was placed onto the subject's head. Lateral, frontal and off-angle photographs were taken, as well as lateral, posteroanterior (PA) and off-angle cephalograms. Using the radiopaque markers, the photographs and radiographs were calibrated. As a result, accurate three-dimensional measurements of facial dimensions could be obtained from photographs as well as from radiographs.

The fact that accurate measurements could be made from radiographs suggested that, perhaps, Sculptor™ could be useful in quantifying cervical vertebrae as well. In orthodontics, the diagnostic records of a typical patient contain at least a lateral cephalogram (lateral ceph) and a panoramic radiograph. Often a PA cephalogram (PA ceph) is included as well. Not only does the head appear on these images, but most of the cervical vertebrae as well. From inspection of several patient PA cephs at the University of Alberta Graduate Orthodontic Clinic, it was determined subjectively by the principal investigator that superimposition of the chin made visualization of the first 3 to 4 vertebrae difficult. Only C5 (and C6, if actually present on the film) was clearly visible most of the time.

In the past 30 years, researchers have been examining the cervical vertebrae as potential maturational indicators. Lamparski performed the first study of this kind, where he attempted to determine if maturational changes of the cervical vertebrae could be used to assess the skeletal age of an individual[2]. Using lateral cephalograms of orthodontic patients at the University of Pittsburgh, Lamparski developed standards to describe "vertebral ages" 10 to 15. He found a significant correlation between skeletal age, as determined by the Greulich and Pyle hand-wrist method, and vertebral age. However, his description of the vertebrae was purely qualitative. No measurements were made, and the vertebral age scale was discontinuous, using only discrete integers. Especially during the adolescent growth spurt, such a discontinuous scale would likely mask some of the significant maturational changes occurring in a given 12-month time period. Other studies[3-5] have since employed the Lamparski standards, correlating them to stature and other maturity indicators.

The drive to find alternate skeletal maturation indicators has arisen in part from dissatisfaction with the hand-wrist radiographic method. Studies[6,7] have demonstrated numerous weaknesses inherent to both the Greulich and Pyle (GP) and Tanner-Whitehouse (TW2) methods. The GP atlas was constructed on the assumption that skeletal maturation is even, that all bones have an identical skeletal age, and that the appearance and subsequent development of bony centres follows a fixed pattern. However, in the atlas, the bones included differ considerably in their levels of maturity, with differences of up to 20 months existing between the least and most mature bones of a given standard[7]. Furthermore, it was found that some bones in the atlas even appeared less mature at older ages, due to poor selection of some standard plates. Problems with

the TW2 method centre around consistently trying to identify in each bone eight or nine stages of maturation, thus resorting to measuring ratios of bone sizes and distances between them. Other problems revolve around the fact that there may be a significant change in the skeletal maturation score (SMS) simply by rating a single bone as 'older' or 'younger' by one stage. When translated to skeletal age, the difference could be up to 1.6 years.

Other skeletal age assessment methods utilizing the hand-wrist radiograph have been proposed, but these have not yet gained widespread acceptance[8,9].

Solutions to problems with the GP and TW2 methods have concentrated mainly on the use of computers, to decrease subjectivity and, therefore, intra- and inter-observer variability[10-18].

For the field of orthodontics, a skeletal age assessment method should ultimately serve the purpose of predicting the amount of maxillary and mandibular growth remaining in a given individual. Since the success of Class II and Class III skeletal corrections is a direct consequence of maxillary and mandibular growth, lower jaw growth prediction would be of particular interest to the orthodontist. It is in this regard that cervical vertebral age determination would be especially useful. Given the cephalocaudal gradient of growth[19], one would expect the more proximally located cervical vertebrae to be more predictive of mandibular growth than the hand or wrist. Direct comparisons between cervical vertebral and mandibular growth have been made[20,21]. These studies demonstrated that statistically significant increases in mandibular length, corpus length and ramus height were associated with specific Lamparski maturation stages in the cervical vertebrae.

As an initial step toward the eventual development of an alternative skeletal age assessment method, the purpose of this investigation was to correlate growth changes of C5 with age. A sample of juvenile and adolescent C5's was chosen from the Hamann-Todd Collection at the Cleveland Museum of Natural History. Unfortunately, only 50 vertebrae were available. Thirty-seven of the specimens were of African American individuals, with the remainder being of Caucasians. The sample was over-represented in the 17 to 19 year category, with 56% of all specimens belonging to this group. Ages 9 and 15 were not represented at all. Thus, from a statistical perspective, caution needed to be exercised when making conclusions regarding the growth from ages 5 to 16, since only 22 vertebrae were available for this entire period. In this type of study, a longitudinal study would have naturally been far more powerful.

Several investigators have performed quantitative studies on human vertebrae, or images thereof[6,22-27]. From a clinical perspective, it is not possible to examine vertebral specimens directly, and some form of imaging becomes necessary to analyze these bones. Thus, those studies which performed direct measurements on vertebrae themselves, although highly accurate, demonstrated limited use in a clinical context. The radiographic studies, although clinically useful, suffered from the errors associated with superimposition, magnification and distortion. Thus, an ideal study would have been one in which highly accurate measurements were made from radiographs of vertebrae.

To meet these objectives, this study was executed in two parts. Firstly, two vertebrae were selected and 8 radiopaque markers (beebees) glued to each of them. Every possible distance between any two markers (28 in all) was then measured with digital calipers by two investigators. The vertebrae were imaged radiographically from three sides (lateral,

PA, and off-angle) in a calibration frame. The films were scanned, imported into Sculptor™ and calibrated. Utilizing the software, the same 28 distances were remeasured. Intra- and inter-investigator reliability were confirmed for both investigators, and their measurements compared with those of Sculptor™. Average differences between manual and image-based results were less than 0.1 mm, and attained neither statistical nor clinical significance. Thus, Sculptor™ was established as an accurate three-dimensional measuring tool for vertebrae.

Once the software was proven to be accurate, its use for the second part of the study became justified. Fine stainless steel ligature wire was attached to the superior and inferior surfaces of each of the fifty C5s, to delineate the periphery of these structures. The wire, being radiopaque, was clearly visible on the radiographs of the specimens. Using Sculptor™, the images of the wires were recreated in three dimensions. Each trace consisted of between 30 and 60 points, all of which were assigned x, y and z coordinates. Thus, with the coordinates of these points, various dimensions of the vertebral body could be calculated.

Using linear regression, a model was set up using height and volume variables to predict individual age. Thus, actual and predicted ages could be compared. Unfortunately, actual patient age was only given to the nearest year, making it a discontinuous variable. No birth and death records were available to obtain more precise values. Therefore, the natural logarithm of the age was used, to "create" a somewhat continuous variable. The use of chronological age was also questionable, since for many individuals, chronological and skeletal age can be significantly different. It is perhaps no wonder, therefore, that the actual and predicted ages were quite different for many specimens. For

example, in one instance a specimen of small proportions was assigned a "vertebral" age of only 13, even though the individual was 17 at time of death. Actual predicted age values in this study, however, were not as important as understanding which dimensions of the vertebrae changed significantly with time.

This study was the first to quantify changes in the curvature of the superior and inferior vertebral surfaces. Using the model of two mutually opposed wedges to approximate each surface, a gradual increase in volume could be demonstrated. In the case of the superior vertebral surface, this increase in volume meant that the edges of this surface rose with time, taking it from a fairly flat, oval structure, to a saddle-shaped one[28]. Lamparski[2] also observed the increasing concavity of the inferior vertebral surface with time. Again, the wedge model quantified these changes. As the anterior and posterior borders of the inferior surface grew downward, the depth of curvature increased, thus increasing the volume of the wedge.

It could be argued that the clinical applicability of this study was questionable. Even though the software was capable of recreating three-dimensional structures from radiographs, it was only able to do so with the help of the stainless steel wires. One would not have the ability to place such wires on living human subjects. To see if the same three-dimensional traces of the body surfaces could be generated on C5s without wires, 5 vertebrae were taken from the University of Alberta's Dental Hygiene collection and their superior and inferior surfaces delineated by 0.009" stainless steel wires. They were imaged in the same three views used in Cleveland. The wires were then removed, and the vertebrae re-imaged. After all of the films were scanned and calibrated by Sculptor™, tracings of the "wired" vertebrae were completed. However, it was not

possible to trace the surfaces of the "unwired" C5s. There was too much superimposition from other vertebral structures, and the outlines of the curved surfaces were not sufficiently radiopaque to be distinguishable from the normal trabeculation pattern of the vertebral body.

Another aspect of this study which questioned its clinical applicability was the dependency on a calibration frame. Although a calibration frame could be worn by the patient, its orientation relative to the vertebrae would need to remain consistent throughout imaging procedures. Any movement of the frame could potentially affect measurements.

Scanning and calibration of each radiograph, followed by tracing of the surfaces, was very time consuming and labour intensive. In a clinical context, such a procedure would need to be performed quickly in order to be practical. Improvements in the software to avoid repetitive tasks would help to achieve this goal.

With the ultimate goal of developing an alternative skeletal age assessment model to predict and describe mandibular growth, there are numerous methods for future studies to improve upon this one. If a cross-sectional study was planned, attempts should be made to determine the skeletal age of the studied specimens, such as by the hand-wrist method. Although the hand-wrist methods available[8,9,29,30] possess significant weaknesses, they would represent a more accurate assessment of skeletal maturation than chronological age. Ideally, in order to provide more conclusive data, the studies would need to be longitudinal. Annual cephalograms should be taken on a large sample of growing children, and the vertebrae analyzed. Perhaps different imaging techniques could be utilized to distinguish the vertebral surfaces more clearly, such as tomosynthesis, or

computed tomography. Using the same calibration frame as the one for the cephalometric studies, it may be useful to image and quantify the mandible directly. Thus a three-dimensional database for mandibular growth would be generated, and its information employed to predict changes in jaw dimensions with time. If a longitudinal study is not feasible, a cross-sectional one could be performed similar to this one, but examining mandibles instead of vertebrae. Various consistently identifiable points could be followed over time, using geometric techniques, such as Euclidean distance matrix analysis[31], in order to describe growth patterns of the mandible. This technique, proposed by Richtsmeier and Lele, could not be applied in our study, since no landmarks on the superior and inferior vertebral body surfaces could be consistently identified.

This investigation achieved two goals: the first was to determine the accuracy of a three-dimensional measuring tool, Sculptor™, in its ability to quantify vertebrae. The second was to correlate growth of the fifth cervical vertebra with age, in order to examine which dimensions were most predictive. Height of the vertebral body, as described by the variable "z-average difference", and the volumes of the superior and inferior curvatures were the strongest predictors.

BIBLIOGRAPHY

1. Hatcher D. Personal communication. June, 1997.

2. Dhillon A. The correlation of cervical vertebrae maturation with hand-wrist maturation and stature increments in adolescent girls. Master of Science Thesis, University of Alberta, 1993.

3. Hassel B, Farman AG. Skeletal maturation evaluation using cervical vertebrae. Am J Orthod Dentofac Orthop 1995;107:58-66.

4. Benso L, Vannelli S, Pastorin L, Angius P, Milani S. Main Problems Associated with Bone Age and Maturity Evaluation. Horm Res 1996;45(suppl 2):42-8.

5. Gilli G. The Assessment of Skeletal Maturation. Horm Res 1996;45(suppl 2):49-52.

6. Roche AF, Chumlea WC, Thissen D. Assessing the skeletal maturity of the hand-wrist: Fels method. Springfield, Illinois, Charles C. Thomas, 1988.

7. Fishman LS. Radiographic Evaluation of Skeletal Maturation: A Clinically Oriented Method Based on Hand-Wrist Films. Angle Orthod 1982;52:88-112.

8. Hill K, Pynsent PB. A fully automated bone-ageing system. Acta Paediatr Suppl 1994; 406:81-3.

9. Cox LA. Preliminary report on the validation of a grammar-based computer system for assessing skeletal maturity with the Tanner-Whitehouse 2 method. Acta Paediatr Suppl 1994;406:84-5.

10. Drayer NM, Cox LA. Assessment of bone ages by the Tanner-Whitehouse method using a computer-aided system. Acta Paediatr Suppl 1994;406:77-80.

11. Tanner JM, Gibbons RD. A Computerized Image Analysis System for Estimating Tanner-Whitehouse 2 Bone Age. Horm Res 1994;42:282-7.

12. Van Teunenbroek A, De Waal W, Roks A, Chinafo P, Fokker M, Mulder P, De Muinck Keizer-Schrama S, Drop S. Computer-Aided Skeletal Age Scores in Healthy Children, Girls with Turner Syndrome, and in Children with Constitutionally Tall Stature. Pediatr Res 1996;39:360-7.

13. Tanner JM, Oshman D, Lindgren G, Grunbaum JA, Elsouki R, Labarthe D. Reliability and Validity of Computer-Assisted Estimates of Tanner-Whitehouse Skeletal Maturity (CASAS): Comparison with the Manual Method. Horm Res 1994;42:288-94.

14. Frisch H, Riedl S, Waldhör T. Computer-aided estimation of skeletal age and comparison with bone age evaluations by the method of Greulich-Pyle and Tanner-Whitehouse. Pediatr Radiol 1996;26:226-31.

15. Sun YN, Ko CC, Mao CW, Lin CJ. A Computer System for Skeletal Growth Measurement. Comp Biomed Res 1994;27: 2-12.

16. Rucci M, Coppini G, Nicoletti I, Cheli D, Valli G. Automatic Analysis of Hand Radiographs for the Assessment of Skeletal Age: A Subsymbolic Approach. Comp Biomed Res 1995;28:239-56.

17. Proffit WR. Contemporary Orthodontics, Second Edition. Mosby Yearbook, 1993.

18. O'Reilly MT, Yaniello GJ. Mandibular Growth Changes and Maturation of Cervical Vertebrae -- A Longitudinal Cephalometric Study. Angle Orthod 1988;58(2):179-84.

19. Huggare J. The first cervical vertebra as an indicator of mandibular growth. Eur J Orthod 1989;11:10-6.

20. Panjabi MM, Duranceau J, Goel V, Oxland T, Takata K. Cervical Human Vertebrae: Quantitative Three-Dimensional Anatomy of the Middle and Lower Regions. Spine 1991;16(8):861-9.

21. Schaffler MB, Alson MD, Heller JG, Garfin SR. Morphology of the Dens: A Quantitative Study. Spine 1992;17(7):738-43.

22. Panjabi MM, Oxland T, Takata K, Goel V, Duranceau J, Krag M. Articular Facets of the Human Spine: Quantitative Three-Dimensional Anatomy. Spine 1993;18(10):1298-310.

23. Xu R, Nadaud MC, Ebraheim NA, Yeasting RA. Morphology of the Second Cervical Vertebra and the Posterior Projection of the C2 Pedicle Axis. Spine 1995;20(3):259-63.

24. Doherty BJ, Heggeness MH. Quantitative Anatomy of the Second Cervical Vertebra. Spine 1995;20(5):513-7.

25. Oh SH, Perin NI, Cooper PR. Quantitative Three-dimensional Anatomy of the Subaxial Cervical Spine: Implication for Anterior Spinal Surgery. Neurosurg 1996;38(6):1139-44.

26. Ebraheim NA, Xu R, Knight T, Yeasting RA. Morphometric Evaluation of Lower Cervical Pedicle and Its Projection. Spine 1997;22(1):1-6.

27. Schmorl G, Junghanns H. The Human Spine in Health and Disease, Second Edition. Grune & Stratton, New York, 1971.

28. Lamparski DG. Skeletal age assessment utilizing cervical vertebrae. Master of Science Thesis, University of Pittsburgh, 1972.

29. Richstmeier JT, Lele S. A Coordinate-Free Approach to the Analysis of Growth Patterns: Models and Theoretical Considerations. Biol Rev 1993;68:381-411.

30. Greulich WW, Pyle SI: Radiographic atlas of skeletal development of the hand and wrist, ed 2. Palo Alto, CA, Stanford University Press, 1959.

31. Tanner JM, Whitehouse RH, Cameron N, Marshall WA, Healy M, Goldstein H: Assessment of skeletal maturity and prediction of adult height (TW2 Method), ed 2. London, Academic Press, 1983.

APPENDIX A

RAW DATA, CALIBRATION STUDY

Investigator 1

Investigator 1, Small Vertebra

		TRIAL1	TRIAL2	TRIAL3	TRIAL4	TRIAL5
1		11.01	11.08	11.12	11.05	11.13
2		16.18	16.18	16.10	16.10	16.08
3		8.27	8.20	8.22	8.22	8.24
4		11.72	11.71	11.77	11.76	11.75
5		12.33	12.28	12.37	12.30	12.32
6		19.84	19.91	19.88	19.81	19.85
7		11.91	11.94	11.94	11.97	11.94
8		9.55	9.50	9.45	9.42	9.38
9		10.81	10.79	10.83	10.77	10.89
10		19.58	19.46	19.62	19.61	19.61
11		12.20	12.19	12.21	12.20	12.22
12		18.77	18.91	18.92	18.85	18.85
13		17.36	17.37	17.33	17.38	17.41
14		12.63	12.60	12.69	12.53	12.71
15		20.75	20.82	20.67	20.67	20.66
16		11.29	11.31	11.28	11.28	11.28
17		12.51	12.46	12.43	12.40	12.47
18		15.22	15.26	15.23	15.28	15.23
19		16.63	16.82	16.85	16.85	16.84
20		14.79	14.74	14.81	14.81	14.82
21		18.99	18.86	18.91	19.12	19.01
22		12.07	12.11	12.02	12.11	12.14
23		11.29	11.22	11.42	11.28	11.31
24		16.54	16.37	16.29	16.28	16.32
25		8.75	8.75	8.73	8.71	8.77
26		9.53	9.54	9.51	9.52	9.54
27		10.38	10.37	10.40	10.36	10.38
28		11.80	11.70	11.73	11.67	11.72
Total	Mean	13.6679	13.6589	13.6689	13.6539	13.6739
	Std. Deviation	3.6628	3.6756	3.6650	3.6826	3.6649
	Minimum	8.27	8.20	8.22	8.22	8.24
	Maximum	20.75	20.82	20.67	20.67	20.66

Units: mm

Investigator 1, Large Vertebra

		TRIAL1	TRIAL2	TRIAL3	TRIAL4	TRIAL5
1		10.58	10.53	10.69	10.68	10.69
2		18.28	18.22	18.14	18.12	18.24
3		9.69	9.63	9.61	9.66	9.67
4		16.50	16.53	16.47	16.51	16.49
5		18.48	18.49	18.44	18.38	18.39
6		22.42	22.49	22.47	22.43	22.42
7		14.23	14.36	14.25	14.34	14.29
8		12.93	12.87	12.92	12.88	12.89
9		15.10	15.03	15.04	15.03	15.01
10		20.89	20.95	20.99	21.09	20.85
11		15.02	15.01	15.02	15.01	15.00
12		22.22	22.26	22.25	22.11	22.10
13		19.40	19.42	19.31	19.39	19.39
14		14.61	14.64	14.53	14.68	14.68
15		25.44	25.46	25.57	25.48	25.61
16		13.55	13.50	13.51	13.50	13.50
17		16.74	16.70	16.65	16.65	16.67
18		19.11	19.08	19.09	19.07	19.02
19		20.44	20.37	20.17	20.21	20.27
20		18.91	18.94	18.95	18.94	18.95
21		19.33	19.28	19.28	19.21	19.38
22		12.38	12.33	12.53	12.57	12.38
23		15.68	15.71	15.70	15.61	15.74
24		17.47	17.46	17.49	17.55	17.53
25		10.85	10.96	10.84	10.92	10.85
26		9.60	9.53	9.56	9.50	9.49
27		13.78	13.81	13.83	13.76	13.77
28		11.47	11.49	11.50	11.40	11.46
Total	Mean	16.2536	16.2518	16.2429	16.2386	16.2404
	Std. Deviation	4.1434	4.1553	4.1433	4.1309	4.1451
	Minimum	9.60	9.53	9.56	9.50	9.49
	Maximum	25.44	25.46	25.57	25.48	25.61

Units: mm

Investigator 2

Investigator 2, Small Vertebra

		TRIAL1	TRIAL2	TRIAL3
1		10.97	11.08	11.04
2		16.04	16.01	16.08
3		8.15	8.11	8.21
4		11.72	11.72	11.71
5		12.33	12.24	12.30
6		19.94	19.75	19.76
7		11.91	11.98	11.88
8		9.25	9.27	9.33
9		10.69	10.81	10.77
10		19.55	19.48	19.59
11		12.12	12.13	12.14
12		18.85	18.80	18.77
13		17.29	17.32	17.41
14		12.62	12.66	12.63
15		20.64	20.61	20.56
16		11.26	11.25	11.23
17		12.51	12.42	12.36
18		15.25	15.14	15.31
19		16.89	16.86	16.85
20		14.71	14.78	14.78
21		19.08	18.96	18.91
22		12.13	12.23	12.13
23		11.27	11.29	11.29
24		16.37	16.40	16.38
25		8.65	8.65	8.66
26		9.50	9.46	9.59
27		10.44	10.37	10.35
28		11.75	11.57	11.57
Total	Mean	13.6386	13.6196	13.6282
	Std. Deviation	3.6962	3.6696	3.6687
	Minimum	8.15	8.11	8.21
	Maximum	20.64	20.61	20.56

Units: mm

Investigator 2, Large Vertebra

		TRIAL1	TRIAL2	TRIAL3
1		10.50	10.61	10.47
2		18.17	18.24	18.20
3		9.62	9.55	9.56
4		16.60	16.51	16.50
5		18.52	18.44	18.47
6		22.52	22.42	22.40
7		14.41	14.34	14.33
8		12.96	12.76	12.82
9		15.07	15.04	15.12
10		20.92	20.94	20.89
11		15.02	14.97	15.01
12		22.22	22.19	22.10
13		19.40	19.32	19.39
14		14.72	14.73	14.73
15		25.33	25.34	25.39
16		13.48	13.49	13.45
17		16.60	16.66	16.59
18		19.00	19.00	19.05
19		20.28	20.32	20.26
20		18.90	18.95	18.97
21		19.21	19.30	19.17
22		12.36	12.37	12.44
23		15.61	15.60	15.65
24		17.30	17.33	17.26
25		10.66	10.77	10.71
26		9.52	9.47	9.41
27		13.79	13.78	13.72
28		11.36	11.47	11.44
Total	Mean	16.2161	16.2111	16.1964
	Std. Deviation	4.1503	4.1465	4.1506
	Minimum	9.52	9.47	9.41
	Maximum	25.33	25.34	25.39

Units: mm

APPENDIX B

CAUSES OF DEATH FOR STUDY SPECIMENS

Specimen	Cause of Death
HTH 0017	Unknown
HTH 0098	Gunshot Wound
HTH 0233	Drowning
HTH 0404	Tuberculous Meningitis
HTH 0410	Lobar Pneumonia
HTH 0437	Pulmonary Tuberculosis
HTH 0485	Sepsis
HTH 0526	Measles
HTH 0548	Myocarditis
HTH 0576	Pulmonary Tuberculosis
HTH 0588	Pneumonia
HTH 0624	Influenza
HTH 0645	Influenza
HTH 0695	Influenza
HTH 0696	Gunshot Wound - Suicide
HTH 0710	Acute Nephritis
HTH 0721	Tuberculosis
HTH 0854	Lobar Pneumonia
HTH 0872	Tuberculous Meningitis
HTH 1041	Pulmonary Tuberculosis
HTH 1097	Tetanus
HTH 1098	Accidental Burns
HTH 1140	Pulmonary Tuberculosis
HTH 1156	Tuberculous Peritonitis
HTH 1232	Active Pulmonary Tuberculosis
HTH 1238	Suicide
HTH 1240	Pulmonary Tuberculosis
HTH 1328	Pulmonary Tuberculosis
HTH 1441	Pericarditis
HTH 1589	Pulmonary Tuberculosis
HTH 1590	Pulmonary Tuberculosis
HTH 1606	Periarteritis Nodosa
HTH 1688	Diphtheria
HTH 1711	Pulmonary Tuberculosis
HTH 1772	Pulmonary Tuberculosis
HTH 1784	Splenomegaly
HTH 1834	Tuberculous Peritonitis
HTH 1949	Pulmonary Tuberculosis
HTH 1974	Pulmonary Tuberculosis
HTH 2036	Juvenile Rheumatoid Arthritis

HTH 2065	Pulmonary Tuberculosis
HTH 2074	Pulmonary Tuberculosis
HTH 2118	Pericarditis
HTH 2135	Tuberculous Meningitis
HTH 2558	Lobar Pneumonia
HTH 3112	Brain Abscess
HTH 3455	Pulmonary Tuberculosis
HTH 3470	Pulmonary Tuberculosis
HTH 3699	No Data
HTH 4056	Rheumatic Endocarditis

APPENDIX C

SAMPLE X,Y,Z COORDINATE DATA

Patient	Session
526	12/9/98

R 1 Trace

	X	Y	Z		X	Y	Z
0	-45.0094	-0.90677	52.04731	34	-36.5378	-12.5314	51.76278
1	-45.0668	2.40E-02	52.11445	35	-37.594	-12.8514	52.44136
2	-44.7064	0.902174	52.47974	36	-39.125	-12.8508	53.07804
3	-44.2895	1.784376	52.74735	37	-39.9663	-12.7446	53.36371
4	-43.8007	2.819103	52.96463	38	-40.7633	-12.5326	53.55086
5	-43.2993	3.451306	53.09467	39	-41.973	-12.1121	53.57636
6	-42.754	4.238944	53.13803	40	-42.7922	-11.6876	53.46211
7	-41.2521	4.954761	53.0101	41	-43.3996	-10.7855	53.12243
8	-40.198	5.558731	52.65634	42	-43.5605	-10.1049	52.91435
9	-39.7616	5.62502	52.43871	43	-43.787	-9.16245	52.60212
10	-38.7883	5.656224	51.95731	44	-43.8581	-8.38258	52.56086
11	-37.7743	5.430512	51.26247	45	-43.9282	-7.60176	52.46786
12	-36.9679	5.200114	50.54572	46	-43.9941	-6.14775	52.44227
13	-36.2904	4.65352	49.70297	47	-44.1548	-4.74383	52.3027
14	-35.6987	4.206119	49.01055	48	-44.2819	-4.615	52.21973
15	-34.9208	3.654331	48.38349	49	-44.4528	-3.20756	52.24394
16	-34.4607	3.089546	48.04276	50	-44.5984	-1.39591	52.35454
17	-34.0617	2.199034	47.73819				
18	-33.7063	1.099596	47.57446				
19	-33.2651	-5.81E-02	47.39767				
20	-32.7948	-1.10669	47.28707				
21	-32.5571	-2.11102	47.30141				
22	-32.3637	-3.00995	47.46437				
23	-32.1666	-3.3832	47.67516				
24	-32.2459	-4.49705	47.78918				
25	-32.4778	-5.66344	47.72989				
26	-32.6721	-6.61844	47.84742				
27	-32.8262	-7.78631	48.06571				
28	-33.1785	-8.63357	48.52663				
29	-33.5611	-9.59345	48.99868				
30	-34.1152	-10.5003	49.5611				
31	-34.6488	-11.14	50.02489				
32	-35.2179	-11.7804	50.58967				
33	-35.6646	-12.1557	51.06554				

Units: mm

APPENDIX D

VERTICAL DIMENSION SUMMARIES

Vertical Dimension Summaries

		Z_AV_DIF	Z_AV_DI2	Z_AV_DI3	ZMAXAVDF	ZMINAVDF	MIN_HGHT	MAX_HGHT
1		11.58	134.02	1551.48	11.32	9.29	6.57	14.04
2		10.52	110.62	1163.44	11.92	9.33	6.27	14.99
3		7.31	53.42	390.41	14.11	11.11	8.47	16.75
4		12.32	151.71	1868.71	13.60	11.52	7.57	17.55
5		5.53	30.58	169.13	10.29	6.52	5.21	11.60
6		7.83	61.27	479.58	9.41	6.61	5.19	10.83
7		7.65	58.52	447.71	14.15	11.39	8.77	16.77
8		9.63	92.72	892.80	13.29	10.63	8.09	15.83
9		5.65	31.96	180.68	11.58	8.76	5.85	14.50
10		6.06	36.75	222.77	10.06	6.76	4.46	12.37
11		10.86	118.00	1281.83	14.17	12.02	9.09	17.10
12		11.58	134.20	1554.71	11.22	9.24	7.01	13.45
13		9.64	92.84	894.61	12.87	10.60	8.01	15.47
14		12.78	163.25	2085.82	13.85	11.44	8.39	16.90
15		10.58	112.00	1185.31	12.53	10.72	7.15	16.10
16		11.17	124.79	1394.05	6.79	5.61	4.30	8.11
17		9.45	89.24	843.00	8.02	4.33	3.92	8.43
18		10.78	116.19	1252.45	8.89	7.12	5.27	10.75
19		5.59	31.25	174.67	13.29	11.25	7.90	16.64
20		11.97	143.21	1713.79	14.37	11.31	8.80	16.87
21		6.47	41.84	270.61	14.11	12.14	8.04	18.21
22		7.48	55.89	417.82	10.52	7.03	4.80	12.75
23		11.27	126.90	1429.55	11.86	10.28	6.51	15.62
24		11.32	128.21	1451.66	7.46	5.43	3.79	9.09
25		10.40	108.26	1126.41	12.57	9.61	7.02	15.16
26		10.48	109.92	1152.40	12.28	11.04	7.70	15.62
27		11.67	136.22	1589.88	12.45	8.81	6.83	14.44
28		11.37	129.34	1470.90	13.99	12.09	8.79	17.29
29		7.67	58.89	451.97	11.82	7.70	5.78	13.74
30		11.87	140.95	1673.31	11.97	11.03	7.29	15.71
31		13.30	176.76	2350.05	12.90	11.81	7.01	17.70
32		11.66	135.96	1585.34	10.60	7.38	5.86	12.11
33		12.27	150.48	1845.87	9.26	6.36	4.51	11.11
34		12.92	166.81	2154.49	12.47	11.09	7.58	15.98
35		8.62	74.28	640.20	12.24	9.21	6.43	15.03
36		11.74	137.90	1619.34	11.92	10.84	8.29	14.47
37		10.58	111.97	1184.86	9.41	6.28	4.73	10.97
38		11.55	133.42	1541.17	11.34	8.52	5.96	13.89
39		11.88	141.03	1674.86	11.32	8.33	6.41	13.24
40		8.12	65.87	534.61	8.15	5.96	4.98	9.13
41		7.95	63.18	502.22	8.94	5.58	4.39	10.12
42		8.00	64.03	512.33	13.16	8.09	6.15	15.10
43		9.30	86.47	804.12	14.61	10.92	6.57	18.96
44		6.33	40.08	253.74	7.99	6.00	5.95	8.04
45		6.86	47.10	323.24	12.69	10.45	7.92	15.23
46		13.27	176.04	2335.61	8.43	6.32	4.96	9.79
47		11.82	139.67	1650.74	12.35	10.43	7.42	15.36
48		9.60	92.25	886.09	9.50	6.79	6.32	9.97
49		13.67	186.96	2556.44	12.97	11.29	8.27	15.96
50		10.67	113.80	1214.04	13.46	10.59	8.54	15.51
Total	Mean	9.9716	104.5409	1139.0167	11.5699	9.0591	6.6213	14.0076
	Std. Deviation	2.2830	43.4317	649.4116	2.0653	2.2309	1.4746	2.9122
	Minimum	5.53	30.58	169.13	6.79	4.33	3.79	8.04
	Maximum	13.67	186.96	2556.44	14.61	12.14	9.09	18.96

Units: mm

APPENDIX E

HORIZONTAL DIMENSION SUMMARIES

		LENGTH1	LENGTH2	WIDTH1	WIDTH2
1		21.33	22.23	16.68	15.65
2		19.71	21.86	14.23	12.94
3		18.51	21.08	12.90	9.34
4		19.78	21.74	15.05	14.16
5		19.51	18.21	10.70	9.83
6		21.30	19.22	12.61	11.94
7		17.63	19.86	12.69	11.57
8		17.43	18.89	13.04	12.72
9		16.35	19.70	10.49	10.42
10		20.11	20.72	12.75	12.55
11		20.37	21.24	16.13	15.42
12		21.74	22.44	13.96	13.28
13		19.34	19.64	12.92	12.42
14		20.67	22.03	15.97	15.98
15		19.19	20.47	13.81	14.05
16		18.95	20.19	14.69	13.57
17		17.48	19.85	12.91	14.53
18		21.42	22.47	15.80	15.19
19		21.26	20.68	10.44	10.59
20		19.38	20.93	15.93	15.68
21		17.59	19.55	12.23	11.56
22		20.07	21.94	10.81	12.17
23		19.81	22.42	13.97	13.66
24		20.08	19.87	13.96	13.53
25		20.10	21.53	14.14	14.29
26		21.41	21.08	14.53	14.35
27		21.14	23.65	14.49	14.52
28		22.05	21.16	14.24	13.99
29		20.33	22.23	13.18	12.73
30		21.29	23.77	16.36	16.02
31		22.09	23.09	17.29	17.07
32		21.55	23.32	15.01	14.71
33		21.88	22.03	15.82	16.10
34		22.58	21.29	16.63	15.68
35		19.04	20.31	13.29	12.45
36		22.09	20.59	14.75	14.25
37		24.59	23.66	15.76	15.40
38		23.78	22.29	16.68	16.29
39		20.29	22.77	17.74	17.24
40		19.56	21.97	10.69	10.72
41		20.70	22.73	13.18	14.01
42		16.79	19.71	11.75	11.79
43		19.76	22.58	13.85	15.22
44		17.89	18.73	11.59	11.50
45		18.99	21.81	12.76	11.72
46		23.85	24.52	17.49	16.63
47		22.76	25.45	16.71	14.24
48		21.01	24.26	14.76	14.70
49		21.94	21.66	17.95	17.10
50		21.04	22.37	15.10	13.33
Total	Mean	20.3502	21.5154	14.2080	13.8162
	Std. Deviation	1.8031	1.5834	2.0016	2.0553
	Minimum	16.35	18.21	10.44	9.34
	Maximum	24.59	25.45	17.95	16.63

Units: mm

APPENDIX F

SLOPE SUMMARIES

Slope Summaries

		SLOPE_A	SLOPE_B	SLOPE_AB	SLOPE_C	SLOPE_D	SLOPE_CD	SLOPE_A2	SLOPE_B2	SLOP_AB2	SLOPE_C2	SLOPE_D2	SLOP_CD2
1		.1818	.1870	.1844	.1099	.1593	.1346	.1302	.2856	.2079	.8187	1.0439	.9313
2		.0248	.0581	.0415	.1068	.0515	.0802	.0561	.0888	.0724	.1353	.1078	.1216
3		.0009	.0471	.0240	.0395	.0320	.0357	.0236	.0871	.0553	.0723	.0781	.0752
4		.2956	.1415	.2185	.2533	.1274	.1903	.1956	.1945	.1951	3.1991	2.5581	2.8776
5		.0141	.0119	.0130	.0200	.0164	.0182	.0148	.0314	.0231	.0315	.0333	.0324
6		.1474	.0127	.0800	.0426	.0293	.0360	.3240	.2397	.2819	.0985	.0668	.0827
7		.0123	.0305	.0214	.0334	.0524	.0429	.0408	.0733	.0571	.0659	.1075	.0867
8		.0475	.0006	.0241	.0295	.0381	.0338	.0436	.0334	.0386	.0577	.0508	.0542
9		.0369	.0223	.0296	.0126	.0336	.0231	.1372	.2537	.1954	.4110	.4680	.4395
10		.0189	.0161	.0165	.0233	.0240	.0237	.0218	.0471	.0344	.0380	.0579	.0480
11		.1422	.1717	.1569	.0724	.0336	.0530	.5731	1.4389	1.0060	.1597	.1474	.1536
12		.2321	.2268	.2294	.2183	.2340	.2261	.1293	.2011	.1652	1.7182	1.4967	1.6074
13		.0144	.0476	.0310	.0606	.0688	.0647	.0883	.1037	.0850	.1515	.1431	.1473
14		.0301	.0676	.0488	.0694	.0735	.0714	.0380	.0888	.0534	.0853	.0812	.0732
15		.0430	.0487	.0458	.1148	.0750	.0949	.0590	.1005	.0797	.1307	.1527	.1417
16		.0394	.0135	.0265	.0352	.0405	.0379	.0311	.0343	.0327	.0468	.0448	.0458
17		.0559	.0037	.0298	.0516	.0809	.0663	.0502	.0763	.0632	.0934	.1198	.1066
18		.0456	.9007	.4731	.1533	.0040	.0786	.4110	.5713	.4911	.5336	.3757	.4547
19		.0241	.0229	.0235	.0007	.0008	.0008	.0245	.0147	.0196	.0299	.0232	.0266
20		.0817	.2256	.1537	.0578	.0463	.0520	.8843	1.5086	1.1965	.0985	.1627	.1306
21		.1270	.0812	.1041	.0654	.0751	.0703	.1134	.2130	.1632	.2811	.3841	.3326
22		.0269	.0119	.0194	.0240	.0026	.0133	.0403	.0455	.0429	.0685	.0727	.0706
23		.0246	.0395	.0321	.0586	.0354	.0470	.0177	.0713	.0445	.0681	.0525	.0603
24		.7529	.5109	.7819	.1119	.0875	.0997	.4376	.6881	.5528	.2242	.1905	.2074
25		.0349	.0490	.0419	.0730	.0693	.0712	.0415	.0759	.0587	.0923	.0863	.0893
26		.0855	.1560	.1208	.0660	.0458	.0559	.2916	.4551	.3734	.1354	.1223	.1288
27		.1032	.3512	.2272	.1734	.0597	.1166	.1224	.3591	.2408	.7693	.6367	.7030
28		.0383	.0827	.0605	.1139	.1074	.1107	.0514	.1026	.0770	.1299	.1236	.1268
29		.0081	.0190	.0135	.0105	.0285	.0195	.0371	.0593	.0482	.0814	.0686	.0650
30		.1276	.1018	.1147	.0565	.0435	.0500	.4718	.5802	.5760	.1521	.1259	.1390
31		.0396	.1956	.1176	.0556	.0476	.0516	.2077	.6143	.4110	.0787	.0760	.0774
32		.0348	.0699	.0523	.0757	.1153	.0955	.0361	.0986	.0673	.0878	.1281	.1080
33		.0644	.3005	.1825	.1210	.1433	.1321	.1130	.3121	.2125	1.2385	1.0282	1.1333
34		.0456	.0833	.0644	.1511	.0964	.1238	.0531	.1041	.0786	.1389	.1291	.1340
35		.0024	.0455	.0240	.0263	.0366	.0314	.0272	.0761	.0517	.0757	.0645	.0701
36		.2219	.1744	.1981	.0827	.0753	.0790	.6154	.8313	.7233	.1279	.1565	.1422
37		.2131	.0822	.1476	.3713	.2117	.2915	.1214	.1827	.1521	13.6743	9.9724	11.8234
38		.1847	.2571	.2209	.0762	.0510	.0636	6.1634	7.5637	6.8636	.2071	.1145	.1608
39		.0426	.0572	.0499	.1453	.0467	.0960	.0470	.0879	.0674	.0933	.1299	.1116
40		.0385	.0799	.0592	.0202	.0331	.0266	.2091	.3957	.3024	.1039	.1070	.1054
41		.1013	.4007	.2510	.0962	.0580	.0771	.2466	.3339	.2903	.3051	.3397	.3224
42		.0301	.1076	.0689	.0305	.0271	.0288	.2289	.4214	.3251	.1024	.1088	.1056
43		.3977	.2866	.3421	.1199	.0935	.1067	.2373	.3204	.2789	.4580	.4222	.4391
44		.0212	.0008	.0110	.0233	.0058	.0146	.0262	.0320	.0301	.0453	.0390	.0422
45		.0067	.0863	.0465	.0193	.0217	.0205	.1896	.2919	.2409	.0904	.1029	.0966
46		.0470	.0830	.0650	.1381	.1084	.1232	.0795	.1223	.1009	.1759	.1562	.1676
47		.0282	.1609	.0945	.0437	.0341	.0389	.1681	.6179	.3930	.1182	.1354	.1273
48		.0524	.2331	.1427	.1167	.1005	.1086	.1382	.3229	.2295	1.0950	.9484	1.0217
49		.0335	.0820	.0477	.0906	.0830	.0869	.0542	.0719	.0631	.0979	.1052	.1015
50		.0031	.0775	.0403	.0528	.0568	.0548	.0032	.0910	.0471	.0452	.0895	.0674
Total	Mean	8.85E-02	.138083	.112285	8.234E-02	8.404E-02	7.319E-02	.278691	.425504	.351197	.566330	.470348	.518339
	Std. Deviation	.128622	.177127	.135399	8.819E-02	4.849E-02	5.503E-02	.886349	1.080264	.972176	1.966187	1.441835	1.703361
	Minimum	.0009	.0006	.0110	.0007	.0008	.0008	.0032	.0147	.0196	.0299	.0232	.0266
	Maximum	.7529	.9007	.7819	.3713	.2340	.2915	6.1634	7.5637	6.8636	13.6743	9.9724	11.8234

Units: none

APPENDIX G

VOLUME SUMMARIES

Volume Summaries

		VOLUME1	VOLUME2
1		225.67	451.97
2		204.36	405.78
3		137.55	275.53
4		226.97	419.84
5		68.58	111.73
6		124.42	208.29
7		79.17	242.38
8		126.67	252.85
9		17.89	210.40
10		105.10	238.26
11		212.60	454.37
12		253.55	341.12
13		120.22	368.30
14		396.46	518.34
15		184.41	418.32
16		177.53	249.17
17		108.70	354.23
18		164.08	597.83
19		2.94	111.71
20		195.84	391.81
21		73.28	196.23
22		25.58	212.23
23		208.51	359.67
24		246.31	328.70
25		213.52	379.51
26		238.41	427.61
27		201.90	484.49
28		310.48	446.18
29		87.68	359.49
30		228.39	512.31
31		279.17	500.77
32		288.52	461.62
33		216.78	493.45
34		385.03	506.81
35		141.27	361.82
36		306.77	392.27
37		263.68	431.99
38		257.75	441.62
39		301.21	529.27
40		78.65	278.23
41		125.96	378.43
42		76.63	272.08
43		175.00	461.91
44		50.78	170.39
45		71.52	290.74
46		452.94	918.02
47		195.19	445.98
48		153.76	501.87
49		324.90	481.55
50		297.04	349.40
Total	Mean	188.1865	379.9376
	Std. Deviation	101.3936	139.1924
	Minimum	2.94	111.71
	Maximum	452.94	918.02

Units: mm^3

APPENDIX H

RESULTS OF REGRESSION WITH REJECTED VARIABLES

1. Slope Variables

Slope variables tested for both sexes:

Slope_a	Slope_ab	Slope_c2
Slope_b	Slope_cd	Slope_d2
Slope_c	Slope_a2	Slope_ab2
Slope_d	Slope_b2	Slope_cd2

Slope variables *included* in **female** model:

Slope_a	Slope_a2
Slope_b	Slope_b2
Slope_c	Slope_d2
Slope_d	Slope_cd2

Slope variables *excluded* from **female** model:

Slope_ab
Slope_cd
Slope_c2
Slope_ab2

Model Summary[b]

Model	R	R Square	Adjusted R Square	Std. Error of the Estimate
1	.783[a]	.613	.419	.3085

a. Predictors: (Constant), SLOP_CD2, SLOPE_B2, SLOPE_B, SLOPE_D, SLOPE_A, SLOPE_C, SLOPE_A2, SLOPE_D2

b. SEX = f

Slope variables included in **male** model:

Slope_a	Slope_a2
Slope_b	Slope_b2
Slope_c	Slope_cd2
Slope_d	

Slope variables excluded from **male** model:

Slope_ab
Slope_cd
Slope_c2
Slope_d2
Slope_ab2

Model Summary[b]

Model	R	R Square	Adjusted R Square	Std. Error of the Estimate
1	.845[a]	.714	.596	.2036

a. Predictors: (Constant), SLOP_CD2, SLOPE_B, SLOPE_A2, SLOPE_A, SLOPE_D, SLOPE_C, SLOPE_B2

b. SEX = m

2. Horizontal Dimension Variables

Model Summary

SEX	Model	R	R Square	Adjusted R Square	Std. Error of the Estimate
f	1	.441[a]	.195	.160	.3710
m	1	.775[a]	.600	.583	.2071

a. Predictors: (Constant), LENGTH1

Model Summary

SEX	Model	R	R Square	Adjusted R Square	Std. Error of the Estimate
f	1	.539[a]	.291	.260	.3481
m	1	.588[a]	.346	.318	.2648

a. Predictors: (Constant), LENGTH2

Model Summary

SEX	Model	R	R Square	Adjusted R Square	Std. Error of the Estimate
f	1	.812[a]	.659	.644	.2415
m	1	.743[a]	.552	.532	.2192

a. Predictors: (Constant), WIDTH1

Model Summary

SEX	Model	R	R Square	Adjusted R Square	Std. Error of the Estimate
f	1	.791[a]	.626	.610	.2527
m	1	.749[a]	.561	.542	.2169

a. Predictors: (Constant), WIDTH2